Asymmetry in the lateral line of threespine stickleback, *Gasterosteus aculeatus*: ecology, evolution and behaviour.

by

Nicholas Planidin

B.Sc., University of Victoria, 2018

A Thesis Submitted in Partial Fulfilment of the

Requirements for the Degree of

MASTER OF SCIENCE

in the Department of Biology

Asymmetry in the lateral line of threespine stickleback, *Gasterosteus aculeatus*: ecology, evolution and behaviour.

by

Nicholas Planidin

B.Sc., University of Victoria, 2018

Supervisory Committee

Dr. Thomas Reimchen, Supervisor

Department of Biology

Dr. Francis Juanes, Departmental Member

Department of Biology

Dr. Roswitha Marx, Departmental Member

Department of Biology

Dr. John Taylor, Departmental Member

Department of Biology

Abstract

Behavioural asymmetry (laterality) is widespread among conspicuously bilaterally symmetrical organisms, playing a part in many aspects of life history from reproduction to feeding. Laterality is typically thought to occur due to morphological asymmetry within the brain, in which one hemisphere becomes specialized for a given task. However, the influence of sensory receptor asymmetry on the development of lateralized behaviour has undergone little investigation. The role of inconspicuous receptor asymmetry in behavioural laterality is particularly important, given the ubiquity of small deviations from symmetry.

Here I have investigated morphological asymmetry in the lateral line, a series of mechanoreceptors called neuromasts that comprise one of the major sensory modalities of fishes. I examined a subset of the lateral line of 3,987 threespine stickleback from 64 populations from coastal British Columbia, characterizing neuromast count and asymmetry among habitats. Furthermore, I scored 657 stickleback from four experimental transplant populations relocated from stained lakes to unstained ponds, to determine whether or not neuromast count or asymmetry changes in a novel habitat. Neuromast count did not differ between oceanic and freshwater stickleback, or between sympatric lake-stream pairs but did differ among clarity regimes, ranging from a complete lack of neuromasts to a doubling of neuromasts compared to oceanic stickleback. Loss of neuromasts was associated with reduced light transmission, lower pH and a lack of piscivorous fishes. Stickleback with more lateral plates developed more neuromasts and males bore more neuromasts than females. One transplant pond underwent a 70% increase in neuromast count within just a couple of generations, whereas the other three transplant populations underwent more gradual change, suggesting both phenotypically plastic and genetic mechanisms underlying difference in neuromast counts among populations.

Asymmetry was widespread among individuals, differing by up to seven neuromasts between the two sides on a single bony plate. However, no populations exhibited a strong directional bias. The degree of absolute asymmetry differed among clarity regimes, with stickleback in stained habitats having less asymmetry in their neuromasts counts. Asymmetry did not differ between oceanic and freshwater populations or sympatric lake-stream pairs. Males exhibited greater asymmetry than females, particularly in large-bodied populations. As with neuromast count, neuromast asymmetry quickly changed in some transplant populations and more gradually in others, increasing by up to 14% in just a couple of generations.

To assess the functional consequences of my geographic survey, I experimentally tested 40 stickleback for their response to a simulated predator, localization of vibrations in the dark and rheotaxis. I compared behaviour and laterality to neuromast count and asymmetry measured by fluorescent microscopy. Stickleback with fewer neuromasts were more likely to respond to simulated predator strikes, but other non-lateralized behaviours were independent of neuromast count. The strongest laterality I observed was the 'hugging' of the arena wall with the right side 57% of the time, with laterality being present in other behaviours, albeit weakly. While some behaviours correlated with lateral line asymmetry, there was no consistent association between lateralized behaviour and asymmetry in the lateral line.

I found that ecological factors such as predation landscape and photo-regime shape both mechanoreceptor count and asymmetry in the lateral line, with potential phenotypic plasticity in both traits. The lateral line's role in response to a model predator and lateralized behaviour supports the influence of mechanosensory asymmetry in eco-evolutionary dynamics.

Table of Contents

Supervisory Committee ii

Abstract iii

Table of Contents v

List of Tables ix

List of Figures x

Acknowledgements xiii

Dedication xiv

Chapter 1: General Introduction 1

Chapter 2: Variation in buttressing plate neuromast counts among populations 7

2.1 Abstract 7

2.2 Introduction 8

2.3 Methods 9

2.3.1 Sample and biophysical characteristic collection 9

2.3.2 Lab procedure 14

2.3.3 Statistical analysis 17

2.4 Results 21

2.4.1 Summary of buttressing plate neuromast counts 21

2.4.2 Effect of ecology on buttressing plate neuromast count 26

2.4.3 Buttressing plate neuromast counts in transplant ponds 33

2.5 Discussion 36

Chapter 3: Variation in buttressing plate neuromast count asymmetry among populations 45

3.1 Abstract 45

3.2 Introduction 46

3.3 Methods 47

3.3.1 Metrics of asymmetry 47

3.3.2 Testing for differences among buttressing plate positions 50

3.3.3 Testing the effect of ecology on relative absolute asymmetry 51

3.3.4 Relative absolute asymmetry in transplant ponds 52

3.3.5 Repeatability of counting neuromasts relative to neuromast asymmetry 52

3.4 Results 53

3.4.1 Summary of buttressing plate neuromast asymmetry 53

3.4.2 Differences in relative absolute asymmetry with ecology 61

3.4.3 Relative absolute asymmetry in transplant ponds 66

3.5 Discussion 69

Chapter 4: Testing the role of neuromast count asymmetry in mechanosensory laterality 77

4.1 Abstract 77

4.2 Introduction 77

4.3 Methods 79

4.3.1 Stickleback collection 79

4.3.2 Vibration attraction behaviour experiment 80

4.3.3 Rheotaxis experiment 82

4.3.4 Evasion of a simulated predator attack experiment 83

4.3.5 Counter-balance design and repeat testing 85

4.3.6 Microscopy 87

4.3.7 Video processing 89

4.3.8 Statistical analyses 93

4.4 Results 97

4.4.1 Predator evasion 97

4.4.2 Vibration attraction behaviour 109

4.4.3 Rheotaxis 118

4.4.4 Consistency of behaviour 120

4.5 Discussion 121

Chapter 5: Synthesis 131

References 140

List of Tables

Table 1: Summary of study localities 13

Table 2: Chapter 2 model equations 19

Table 3: Chapter 3 model equations 51

Table 4: Counterbalancing of behavioural experiments 87

Table 5: Chapter 4 model structures 95

Table 6: Chapter 4 model equations 95

Table 7: Individual stitch analysis of the probability of right wall hugs 101

Table 8: Individual stitch analysis of the probability of imitating escape behaviour 103

Table 9: Individual stitch analysis of time to escape 105

Table 10: Individual stitch analysis of max velocity 107

Table 11: Individual stitch analysis of escape angle 109

Table 12: Individual stitch analysis of distance travelled 114

Table 13: Individual stitch analysis of the probability of right wall hugs 116

Table 14: Individual stitch analysis of the probability of right approaches 118

Table 15: Correlation of laterality among behaviours 121

List of Figures

Figure 1: Map of localities sampled..... 11

Figure 2: Diagram and images of buttressing plate neuromasts..... 14

Figure 3: Image of nerves stained by Sudan Black..... 16

Figure 4: Comparison of model structures for chapter 2..... 18

Figure 5: Summary of neuromast presence in all populations..... 22

Figure 6: Summary of neuromast count in all populations..... 24

Figure 7: Neuromast presence and count among buttressing plate positions..... 26

Figure 8: Neuromast presence and count among clarity regimes..... 28

Figure 9: Neuromast presence and count in lake-stream pairs..... 29

Figure 10: Predictors of neuromast presence in lakes..... 31

Figure 11: Predictors of neuromast count in lakes..... 33

Figure 12: Neuromast presence and count in Drizzle Pond..... 34

Figure 13: Neuromast count in transplant ponds from Mayer Lake..... 35

Figure 14: Comparison of model structures for chapter 3..... 49

Figure 15: Summary of absolute asymmetry in all populations..... 54

Figure 16: Summary of signed asymmetry in all populations 56

Figure 17: Summary of relative signed asymmetry in all populations 58

Figure 18: Relative absolute asymmetry among buttressing plate positions 59

Figure 19: Summary of relative absolute asymmetry in all populations 60

Figure 20: Absolute asymmetry among clarity regimes 62

Figure 21: Absolute asymmetry in lake-stream pairs 63

Figure 22: Predictors of absolute asymmetry in lakes 65

Figure 23: Absolute asymmetry in Drizzle Pond 66

Figure 24: Absolute asymmetry in Mayer Lake transplant ponds 68

Figure 25: Eagle's Lake sampling site 80

Figure 26: Schematic of vibration attraction behaviour testing apparatus 81

Figure 27: Schematic of rheotaxis testing apparatus 83

Figure 28: Schematic of predator evasion testing apparatus 84

Figure 29: Example experimental sequence 86

Figure 30: Diagram of lateral line stitches 88

Figure 31: Calculation of predator evasion kinematics 89

Figure 32: Calculation of vibration attraction behaviour kinematics 92

Figure 33: Calculation of rheotaxis kinematics 93

Figure 34: The effect of experimental design on the probability of initiating escape response ... 97

Figure 35: The effect of experimental design on time to escape 98

Figure 36: Max velocity among predator evasion trials 99

Figure 37: Predictors of right wall hugs 100

Figure 38: Predictors of laterality in initiating escape behaviour 102

Figure 39: Laterality in time to escape 104

Figure 40: Predictors of max velocity 106

Figure 41: Predictors of average angle of escape 108

Figure 42: The effect of experimental design on distance travelled 110

Figure 43: The effect of experimental design on number of approaches 111

Figure 44: The effect of experimental design on time spent in the center 111

Figure 45: Predictors of non-lateralized vibration attraction behaviour 113

Figure 46: Predictors of lateralized dark-navigation behaviour 115

Figure 47: Predictors of lateralized rod approaches 117

Figure 48: Changes in rheotaxis behaviour among trials 119

Acknowledgements

Unfortunately, I cannot list everyone at UVic that has played a role in my growth over the last three years but thank you to everyone for making university feel like home and for putting up with all my questions. The guidance and support of my supervisory committee has been invaluable for the completion of this thesis. I could not have done it without them. I started off not understanding the undertaking that was being a TA, but Dr. Neville Winchester, Kieran Cox and Dr. Rossi Marx quickly showed me the ropes, and it has quickly grown into a passion. Thank you, Dr. Steve Perlman, for showing me the world of molecular evolution and your positive disposition. Kenzie Woods and Micah Quindazzi assisted me with fieldwork and frequent discussion; they have both been immensely influential on my academic development.

A lot of generosity supported this project. Ainsley Fraser, Emily May and Dr. Rana El-Sabaawii were greatly helpful in discussing stickleback field work and histology. Statistical discussions with Garth Covernton and Paul van Dam-Bates, and mathematical discussions with JD House were very helpful and much needed. The use of Dr. John Taylor's fluorescent microscope and the assistance of Heather Down in figuring out how it worked made the whole second half of this thesis possible and allowed me to see the lateral line in its full glory. Thank you, Tung, for being the one consistent soul in the basement of Cunningham after dark and always greeting me with a smile. I have always had immense support from family and friends, for which I am truly grateful.

Tom, you have opened my eyes to the beauty of the natural world in a way that I could never have imagined, thank you for taking me under your wing.

Dedication

I would like to dedicate this thesis to my best friend Jason Nguyen, who has been my anchor through all the tumult. Gabe-space forever, bud.

Chapter 1: General Introduction

Preferential use of one side of the body, behavioural laterality, is ubiquitous among bilaterally symmetrical organisms. The most vivid example of behavioural lateralization that one faces in their day-to-day, the preferential use of one hand by humans, has been under investigation since the writings of Thomas Browne (1646). There has since been great effort devoted to understanding the origins and functions of human handedness (Warren 1980). However, this investigation has been plagued by the notion that asymmetric specialization is a uniquely human phenomenon (Levy 1977; Vallortigara et al. 1999). Recently there has been a growing body of evidence suggesting that laterality is widespread, occurring across major families of vertebrates (Bisazza et al. 1998b; Vallortigara et al. 1999) and invertebrates alike (Frasnelli 2013). These behavioural asymmetries are due to differences in brain structure between the two hemispheres, in which one side becomes specialized for a given task (Rogers 2000; Rogers and Andrew 2002). Lateralized specialization incurs many benefits; efficiently using neural tissue in diverse functions (Levy 1977), enabling parallel processing (Rogers et al. 2004), and resolving conflicting sensory information between the two sides (Vallortigara 2000). Furthermore, behavioural lateralization can be advantageous for the ecology of species, improving foraging (Güntürkün et al. 2000), predator evasion (Heuts 1999; Dadda et al. 2010), foraging in the presence of predators (Rogers et al. 2004), tool use (McGrew and Marchant 1999), object manipulation (Magat and Brown 2009) and group coordination behaviours (Bisazza and Dadda 2005). Thus, understanding behavioural laterality and the mechanisms that produce it may allow us to better understand the life history of many species and their interaction with the environment.

While it is clear that central nervous system asymmetry facilitates the development of lateralized behaviour, the influence of sensory receptor asymmetry on lateralized behaviour has undergone little investigation. By necessity, the dominance of one side of the body for a given task results from one hemisphere of the brain being more active than the other (Ridgway 2002; Moorman et al. 2015). Asymmetry in brain activity may be facilitated by genetically or epigenetically determined asymmetry during the brain's ontogeny (Gamse et al. 2003; Halpern et al. 2003; Manns 2006) or due to asymmetric sensory experience in life (Casey and Martino 2000; Anfora et al. 2011). The importance of sensory information in determining laterality then raises the question, to what extent do asymmetries in sensory receptors through which an organism experiences the world influence the laterality of their behaviour? While asymmetry in sensory receptors is taxonomically widespread and occurs in many sensory modalities (Hart et al. 2000; Werner and Seifan 2006; Lychakov et al. 2006, 2008; Krings et al. 2019), tests of the effect of receptor asymmetry on behavioural laterality have been limited to cases of highly asymmetric species or by manipulation of sensory structures in the lab (Anfora et al. 2011; Fernandes et al. 2018). The limited scope of these investigations prevents us from understanding the role of more subtle deviations from symmetry on behaviour and how this may affect the ecology of most species that do not have a conspicuously asymmetric phenotype.

There is a rich history of studies on morphological asymmetries, which have garnered many interpretations for how they arise. There are three major classes of morphological asymmetry that populations can exhibit: directional asymmetry, in which dominance of one side is more frequent than the other; anti-symmetry, in which individuals have a clear dominant side, but the direction is evenly split in the population; and fluctuating asymmetry, in which individuals exhibit deviations from symmetry, but the population is on average and modally

symmetrical. The most common form of asymmetry is fluctuating asymmetry, which is generally subtle compared to the total size of traits. Thoday (1953) suggested that subtle asymmetries may be due to random deviations from the genetically determined symmetrical body plan. As more asymmetric individuals have deviated further from the bilaterally symmetrical body plan, greater asymmetry would indicate a lower quality genotype or a more stressful environment, causing more developmental instability (Soule 1967; Dongen 2006). These asymmetric phenotypes are also linked to lower individual fitness (Møller and Pomiankowski 1993; Gummer and Brigham 1995; Swaddle et al. 1996; Martín and López 2001; Rivera and Neely 2020). However, there is evidence against fluctuating asymmetry as an indicator of fitness (Bjorksten et al. 2000), controversy over its heritability (Markow and Clarke 1997; Møller and Thornhill 1997) and instances of asymmetric individuals with greater fitness than symmetrical ones (Seligmann 1998). The more conspicuous forms of asymmetry, such as the directional asymmetry of flatfishes and anti-symmetry of male fiddler crabs, also provide interesting evidence that asymmetry can be functional. As the ancestral state and start of the ontology of these species are symmetrical, the evolution of conspicuous asymmetry suggests increasingly larger deviations from symmetry can undergo positive selection under the right conditions, one of which possibly being the development of behavioural laterality.

One of the predominant sensory modalities of fishes is the mechanosensory lateral line. The lateral line consists of a series of mechanoreceptors called neuromasts, clusters of hair cells encased in a gelatinous cupula. Neuromasts are spread over the body of fishes and amphibians and are divided into two major submodalities, velocity-sensitive superficial neuromasts and acceleration-sensitive canal neuromasts. Superficial neuromasts occur in rows or ‘stitches’ on the surface of the skin, scales or bony plates, whereas canal neuromasts develop in fluid-filled canals

(Coombs et al. 2014). As neuromasts function by displacement of the cupula from a vertical position, superficial neuromasts are activated while a fish is in a constant flow, but canal neuromasts are sheltered from this stimulus by their canal. However, when the fish experiences accelerating water flow, a difference in pressure between pores connecting lateral line canals to the open water generates flow within the canals, activating canal neuromasts. The hair cells within neuromasts typically orient along a single axis in line with its stitch or canal, containing two opposing sets of hair cells that are maximally sensitive to displacement in opposite directions (Rouse and Pickles 1991; López-Schier et al. 2004). Neuromasts encode the direction of stimuli by rate encoding, meaning that they release spikes of depolarization at a steady rate when unperturbed, further depolarize when hair cells are displaced towards the kinocilium and hyperpolarize when hair cells are displaced away from the kinocilium (Fain 2019). Thus, neuromasts can encode many aspects of mechanosensory stimuli. Mechanosensory information is important for many behaviours such as predator-prey interaction (Coombs and Patton 2009; Junges et al. 2010; Schwalbe et al. 2012), rheotaxis (Baker and Montgomery 1999; Suli et al. 2012; Brown and Simmons 2016; Jiang et al. 2017), schooling (Middlemiss et al. 2017; Mekdara et al. 2018) and conspecific interaction (Butler and Maruska 2016). In addition to functional diversity, lateral line morphology is also highly variable among (Coombs et al. 2014) and within species (Fischer et al. 2013).

The threespine stickleback, *Gasterosteus aculeatus* (Linnaeus, 1758), is a model species of fish found circumglobally in temperate waters (Wootton 1976). Stickleback are ancestrally marine, with some anadromous populations (Bell and Foster 1994). However, stickleback that enter freshwater streams to reproduce sometimes remain in a lake or stream throughout their life history, forming new freshwater populations (Hagen 1967). These populations are of particular

interest because they have adapted to a diversity of ecological regimes during multiple independent colonization events, allowing investigation of ecology's role in evolution (McPhail 1969; Moodie and Reimchen 1976). The radiation of stickleback in the freshwater environment has led to a wide degree of adaptations such as changes in numbers of bony lateral plates (Heuts 1947; Colosimo et al. 2005), spine length (Marchinko 2009), pigmentation (Reimchen 1989; Greenwood et al. 2011), visual opsins (Marques et al. 2017), number of gill rakers (Gross and Anderson 1984) and aspects of behaviour (Dingemanse et al. 2007; Barrett et al. 2009; Wund et al. 2015). One of the hotspots for studying adaptation to a diverse set of ecological regimes are the stickleback of Haida Gwaii and coastal British Columbia, as a diversity of stickleback ecomorphs have evolved in this region (Reimchen et al. 2013) since the retreat of the Cordilleran ice sheet approximately 17,000 years ago (Darvill et al. 2018). Of particular interest to this investigation is the variation in asymmetry of the pelvic girdle (Reimchen 1980, 1997; Bell et al. 1985; Reimchen and Nosil 2001a) and lateral plates (Bergstrom and Reimchen 2000, 2003, 2005; Reimchen and Nosil 2001b; Reimchen and Bergstrom 2009) among ecological regimes. Thus, stickleback are an ideal model for assessing how ecology can shape asymmetry in morphology and behaviour.

This thesis aims to investigate the interplay between behavioural lateralization and morphological asymmetry in the lateral line system of threespine stickleback and its role in adaptation to divergent ecological regimes. I have examined changes in the number of neuromasts present on the fourth through eighth lateral plates among 3,897 stickleback from 64 ecologically diverse localities in coastal British Columbia, correlating differences in habitat with differences in neuromast count. I also examined four experimental transplant populations moved from lakes to ponds, examining inter-generational changes in neuromast count for populations in

a novel habitat for as many as twelve generations. I then repeated this analysis, looking at differences in asymmetry of neuromast counts among ecological regimes and changes in transplant populations. Lastly, to determine if sensory receptor asymmetry influences behavioural laterality, I tested 40 stickleback for lateralization in predator avoidance, prey localization and rheotaxis behaviour and compared it to neuromast count and asymmetry.

Chapter 2: Variation in buttressing plate neuromast counts among populations

Part of this chapter has been published as:

Planidin NP, Reimchen TE (2019) Spatial, sexual, and rapid temporal differentiation in neuromast expression on lateral plates of Haida Gwaii threespine stickleback (*Gasterosteus aculeatus*). Can J Zool 97:988–996

2.1 Abstract

The lateral line exhibits a diversity of morphologies among species of divergent life history. There are also differences in the number of neuromasts that populations of single species express among ecological regimes, suggesting that changes in ecology influence diversity in the structure and function of the lateral line. However, limited investigation has gone into the ecological characteristics that lead to increases and decreases in numbers of neuromasts. Here I have investigated 3,897 stickleback from 64 ecologically diverse localities in coastal British Columbia, comparing changes in buttressing plate neuromast count to habitat and morphological characteristics. I found that pH, predation regime and number of lateral plates were the best predictors of buttressing plate neuromast count, explaining differences between the neuromast counts of oceanic and freshwater stickleback. Populations in a more acidic environments developed fewer neuromasts than those in basic environments ($p < 0.001$), stickleback exposed to piscivorous fishes have significantly more neuromasts than those that were not ($p = 0.028$) and stickleback with more lateral plates developed more neuromasts per lateral plate ($p < 0.001$). Buttressing plate neuromast counts were also sexually dimorphic, with males developing more neuromasts than females on average ($p < 0.001$), with greater sexual dimorphism in longer stickleback ($p < 0.001$) and those with few lateral plates ($p < 0.001$). I also compared 657

stickleback across multiple generations in four experimental transplant populations to their source populations. In one transplant, buttressing plate neuromast counts increased by 70% within just a couple generations suggesting phenotypic plasticity; however, in other transplants that underwent a different transition in ecology, change was more gradual.

2.2 Introduction

Among fishes and amphibians, the lateral line has evolved a variety of morphologies and functions. Some species are highly specialized, such as striped panchax, *Aplocheilus lineatus* (Valenciennes, 1846), which have guiding ridges around neuromast on the top of their head, allowing them to locate prey stuck due to surface tension (Schwarz et al. 2011). Another example of specialization is blind Mexican cavefish, *Astyanax mexicanus* (De Filippi, 1853), which have a high density of superficial neuromasts on their cheekbones for foraging in complete darkness (Lloyd et al. 2018). These two examples represent the functional specificity possible in the lateral line, as its morphology has been tuned to a precise kind of stimuli. There are also broader organizational trends that reflect the hydrodynamic stimuli a species experiences, such as developing additional dorsal trunk lines on benthic species or ventral trunk lines on neuston (Webb 1989). Even closely related species can differ in their lateral line morphology due to divergence in their life histories (Edgley and Genner 2019).

Diversification of lateral line structure can occur among populations of a single species in divergent habitats. Populations with different prey (Spiller et al. 2017), predators (Fischer et al. 2013), and flow regimes (Rudolfsen et al. 2018) can all exhibit changes in lateral line morphology. Threespine stickleback, a species that lacks canal neuromasts, undergoes changes in lateral line morphology when colonizing freshwater habitats, developing more superficial

neuromasts (Wark and Peichel 2010; Ahnelt et al. 2021). While the number of neuromasts that threespine stickleback develop is highly adaptable to environmental stimuli, the specific environmental factors that have shaped changes in this species' lateral line has yet to be determined.

Here I have examined the buttressing plate neuromasts of 64 populations of threespine stickleback from a diversity of habitats from across coastal British Columbia, comparing habitat and morphological characteristics to neuromast counts on the buttressing lateral plates, to determine what factors are shaping the lateral line of threespine stickleback. I have compared lake, stream and oceanic populations, as well as major clarity regimes, followed by a more detailed analysis of a subset of lakes for which pH, area and predation regime information were available. Furthermore, to assess the rate at which buttressing plate neuromast counts change in a new environment, two sympatric lake-stream pairs and multiple generations from four transplant pond populations were examined for their lateral line structure and compared to their source populations.

2.3 Methods

2.3.1 Sample and biophysical characteristic collection

Threespine stickleback and biophysical measurements from 64 localities were previously collected as part of continuing research on the Haida Gwaii archipelago (n = 53), Dewdney-Banks archipelago (n = 9) and Vancouver Island (n = 2) (review in Reimchen 1989; Reimchen and Nosil 2006; Reimchen et al. 2013; Table 1; Fig. 1). Threespine stickleback were captured using minnow traps baited with aged cheddar cheese and euthanized with MS222 or clove oil. Specimens were fixed and stored in formalin until 1985, when all samples were transferred to

70% ethanol. All specimens collected after 1985 were fixed and stored in 70% ethanol. Localities were selected by T.E. Reimchen to encompass the breadth of biodiversity found on the Haida-Gwaii archipelago and the Dewdney-Banks archipelago, as well as oceanic reference populations and reference populations on Vancouver Island. All localities were classified as lake (n = 51), stream (n = 10) or oceanic (n = 3) and categorized as stained (n = 19), partially-stained (n = 12) or clear water (n = 33), from spectrophotometer readings or observation of a Secchi disk at 1 m (Reimchen 1989). I have also used biophysical information that was collected for a subset of lakes (n = 43). pH was measured with a Multi-parameter PCSTestr 35; lake area was determined either from Canadian government ordinate survey maps or with Google Earth, and the presence/absence of stickleback predator species was noted during stickleback sample collection. The types of predators were then condensed into three predation regime categories; invertebrate and avian (IA), cutthroat trout and avian (CT) and rainbow trout and avian (RT) (Reimchen 1994). For Dewdney-Banks populations**,** predation regime was inferred from the defense morphology of the stickleback collected, as they are closely correlated (Reimchen and Nosil 2006). Eagle's Lake, Vancouver Island, was sampled for behavioural analysis and underwent a different sampling and lab procedure than other populations (see Chapter 4); in short, neuromasts were counted on live fish using fluorescent microscopy.

I examined samples from four transplant populations. Drizzle Pond was established in 1997 by 16 adult stickleback from Drizzle Lake. I scored samples from generations three, four, nine and twelve in Drizzle Pond and fish sampled in 1979, 1981, 1983, 1987, 1988, 1989 and 2015 from Drizzle Lake. Roadside Pond, Bevans Pond and Mayer Pond Two were established in 1993, 1993 and 2011 by 100, approximately 100 and 41 stickleback from Mayer Lake, respectively (Leaver and Reimchen 2009). For Roadside Pond, I scored generations two, six and

twelve; for Bevan's Pond, I scored generations one and ten, and for Mayer Pond Two, I scored generation three. I scored fish sampled from Mayer Lake in 1982, 1997, 2002 and 2003. Drizzle Lake and Mayer Lake stickleback are of the giant ecomorph (Moodie 1972; Moodie and Reimchen 1976).

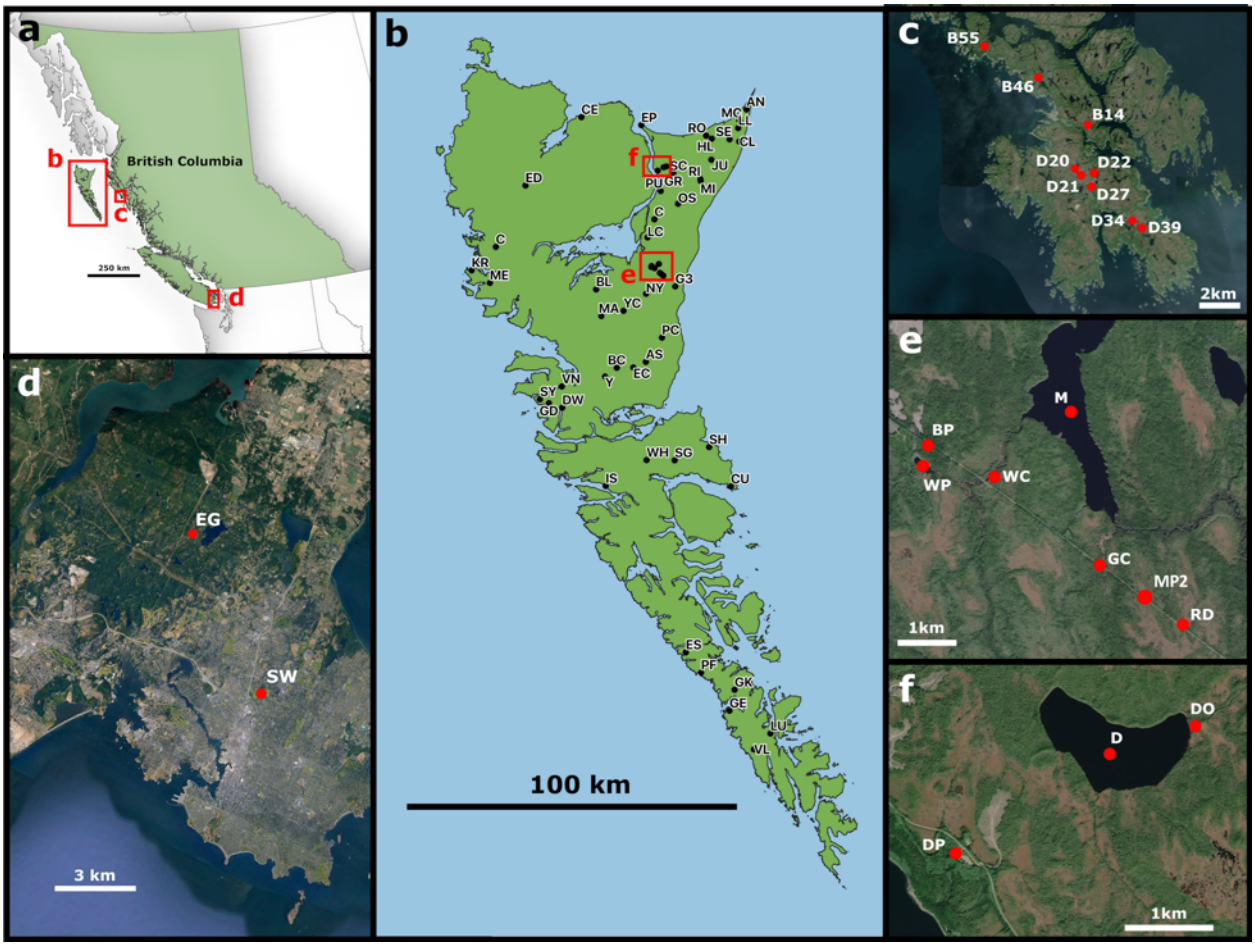

Figure 1. Summary of study localities. (*a*) Map of regions sampled. (*b*) Haida Gwaii, (*c*) Dewdney-Banks, (*d*) Vancouver Island. (*e*) Mayer Lake and Gold Creek lake-stream pair, with Roadside Pond Bevan's Pond and Mayer Pond Two transplant populations and other nearby localities. (*f*) Drizzle Lake and Drizzle Outlet lake-stream pair, with Drizzle Pond transplant population. See Table 1 for a summary of population characteristics.

Table 1. Summary of sample localities. Abrev. indicates abbreviations in Fig. 1. Females and Males columns are sample sizes for each sex, Plates is the average number of buttressing plates on both sides and Plate pairs is the average number of buttressing plate positions with lateral plates present on both sides. Localities with pH, area and predator data were those used in the lake-specific habitat analyses. IA = invertebrate / avian, CT = cutthroat trout / avian, RT = rainbow trout / avian.

Locality	Abrev.	Females	Males	Plates	Plate pairs	Region	Habitat	Clarity	pH	Area (h)	Predators
Anderson South	AS	20	20	8.5	4.2	Haida Gwaii	Lake	Clear	7.1	14	CT
Anser	AN	45	35	7.8	3.7	Haida Gwaii	Lake	Stained	5.3	18	CT
B46	B46	20	20	8.1	3.9	Dewdney-Banks	Lake	Clear	5.7	2.9	IA
B55	B55	20	20	7.9	3.8	Dewdney-Banks	Lake	Clear	5.9	7.9	CT
BA14	B14	20	20	8.1	3.9	Dewdney-Banks	Lake	Clear	5	4.6	CT
Boulton	B	22	55	6.2	1.8	Haida Gwaii	Lake	Partial-Stain	4.9	15	IA
Brent Creek	BC	37	17	9.2	3.8	Haida Gwaii	Stream	Partial-Stain	-	-	-
Blackwater Creek	BL	20	9	9.9	8.3	Haida Gwaii	Stream	Clear	-	-	-
Cedar	CE	25	15	8.1	3.9	Haida Gwaii	Lake	Stained	4.05	3.7	CT
Clearwater	CL	11	30	6.5	2.9	Haida Gwaii	Lake	Partial-Stain	-	-	-
Coates	C	27	23	10	5	Haida Gwaii	Lake	Clear	6	90	RT
Cumshewa	CU	36	10	8.6	4.2	Haida Gwaii	Lake	Stained	-	-	-
D20	D20	20	20	8	3.9	Dewdney-Banks	Lake	Clear	-	-	-
D21	D21	20	20	7.8	3.7	Dewdney-Banks	Lake	Clear	5.2	0.6	CT
D22	D22	20	20	6.4	3	Dewdney-Banks	Lake	Clear	5.7	1.6	CT
D27	D27	20	20	8.5	4.2	Dewdney-Banks	Lake	Partial-Stain	6	6.6	RT
D34	D34	20	20	7.6	3.6	Dewdney-Banks	Lake	Clear	5.2	10.7	IA
D39	D39	20	20	4.5	1.7	Dewdney-Banks	Lake	Clear	5.3	0.8	IA
Dawson	DW	19	19	9.5	4.6	Haida Gwaii	Lake	Clear	-	-	-
Drizzle	D	628	361	8.3	3.9	Haida Gwaii	Lake	Stained	5.1	97	CT
Drizzle Outlet	DO	22	21	8.4	4.1	Haida Gwaii	Stream	Stained	-	-	-
Eagle's	EG	25	15	10	5	Vancouver Island	Lake	Clear	10	0.8	CT
Eden	ED	20	20	9.8	4.8	Haida Gwaii	Lake	Clear	6.8	513	RT
Elk Creek	EC	46	10	9.5	4.6	Haida Gwaii	Stream	Partial-Stain	-	-	-
Entry Point	EP	13	8	10	5	Haida Gwaii	Oceanic	Clear	-	-	-
Escarpment	ES	42	49	9.4	4.6	Haida Gwaii	Lake	Clear	6.3	97	RT
Geikie	GE	19	15	7.4	3.4	Haida Gwaii	Stream	Stained	-	-	-
Gold Creek	GC	20	20	8.5	4.1	Haida Gwaii	Stream	Stained	-	-	-
Goski	GK	22	18	9.5	4.7	Haida Gwaii	Lake	Clear	7.25	10	RT
Gowgaia East	GE	19	19	10	5	Haida Gwaii	Lake	Partial-Stain	-	-	-
Gros	GR	11	9	5.8	2.5	Haida Gwaii	Lake	Partial-Stain	-	-	-
Gudal	GD	20	19	9.3	4.5	Haida Gwaii	Lake	Clear	7.4	25	RT
Harelda Lower	HL	21	44	3.5	1.5	Haida Gwaii	Lake	Stained	4.3	5	CT
Inskip Lagoon	IS	28	21	10	5	Haida Gwaii	Oceanic	Clear	-	-	-
Juno	JU	20	8	1.1	0.3	Haida Gwaii	Lake	Stained	4.38	8	IA
Krajina	KR	20	20	9.4	4.6	Haida Gwaii	Lake	Clear	6	16	RT
Loonk Creek	LC	35	21	6.9	3.1	Haida Gwaii	Stream	Stained	-	-	-
Lummi	LL	20	20	6.2	2.9	Haida Gwaii	Lake	Stained	4.65	39	IA
Lutea	LU	36	14	9.4	4.7	Haida Gwaii	Lake	Clear	6.8	3	RT
Marie	MA	20	15	9	4.3	Haida Gwaii	Lake	Clear	7	36	CT
Mayer	M	118	170	9.6	4.7	Haida Gwaii	Lake	Stained	4.9	373	CT
Mercer	ME	24	16	9.5	4.6	Haida Gwaii	Lake	Clear	-	-	-
Mica	MC	20	20	8.1	3.9	Haida Gwaii	Lake	Stained	4.1	11	CT
Middle	MI	23	12	2.3	0.8	Haida Gwaii	Lake	Stained	4.7	1	IA
New Year	NY	20	20	5.8	2.6	Haida Gwaii	Lake	Partial-Stain	4.7	6.9	CT
Otter South	OS	18	21	9	4.5	Haida Gwaii	Lake	Stained	4.6	36	CT
Pontoon	PC	20	20	8.3	4	Haida Gwaii	Lake	Partial-Stain	6.7	1	IA
Puffin	PF	20	20	10	5	Haida Gwaii	Lake	Clear	-	-	-
Pure	PU	20	18	8.2	4	Haida Gwaii	Lake	Partial-Stain	4.45	34	CT
Richter	RI	25	5	5.7	2.7	Haida Gwaii	Lake	Stained	4.25	12	IA
Rouge	RO	43	68	2.4	0.8	Haida Gwaii	Lake	Partial-Stain	4.2	2	IA
Serendipity	SE	5	5	0	0	Haida Gwaii	Lake	Partial-Stain	4.1	3	IA
Sheldon	SH	16	16	10	5	Haida Gwaii	Oceanic	Clear	-	-	-
Skidegate	SG	20	2	9.7	4.8	Haida Gwaii	Lake	Clear	7.3	734	CT
Skonun Creek	SC	5	16	2.8	1.1	Haida Gwaii	Stream	Partial-Stain	-	-	-
Stiu	SY	36	17	10	5	Haida Gwaii	Lake	Clear	7.15	24	RT
Swan	SW	20	19	8.9	4.3	Vancouver Island	Lake	Clear	8.8	8.3	IA
Van Inlet	VN	16	16	9.7	4.7	Haida Gwaii	Lake	Clear	7.15	23	RT
Victoria Lower	VL	20	18	10	5	Haida Gwaii	Lake	Clear	6.95	149	RT
White Swan	WH	17	20	8.8	4.3	Haida Gwaii	Lake	Clear	6.85	0.6	CT
Woodpile Creek	WC	20	20	8.6	4.1	Haida Gwaii	Stream	Stained	-	-	-
Woodpile	WP	20	20	8.3	4.2	Haida Gwaii	Lake	Stained	4.85	4	CT
Yakourn Lake	Y	20	20	9.2	4.5	Haida Gwaii	Lake	Clear	6.3	790	CT
Yakoun River	YC	34	9	9.3	4.6	Haida Gwaii	Stream	Clear	-	-	-
Drizzle Pond	DP	180	141	8.1	3.5	Haida Gwaii	Transplant	Partial-Stain	6.5	0.1	IA
Roadside Pond	RD	131	101	9.7	4.7	Haida Gwaii	Transplant	Partial-Stain	5.7	0.2	IA
Bevan's Pond	BP	40	40	8.8	4.3	Haida Gwaii	Transplant	Partial-Stain	6.4	0.1	IA
Mayer Pond Two	MP2	19	3	8.8	4.2	Haida Gwaii	Transplant	Stained	5.5	0.1	IA

2.3.2 Lab procedure

I scored the number of neuromasts and neuromast pores on the fourth through eighth (buttressing) lateral plates on both sides of the trunk (Fig. 2) under a dissecting microscope. These plates were chosen as they are the most conserved among populations with few lateral plates and because the plates protect neuromast cupulae from abrasion that commonly affects superficial neuromasts on the naked trunk, both during the lifetime of the fish and while preserved. Pores and neuromast cupula on the lateral plates are readily identifiable by their shape, contrasting sheen, texture, and colour from the rest of the lateral plate (Fig. 2b-d). Occasionally, neuromasts within a pore were separated by a calcified wall, and I treated them as separate pores (Fig. 2d). I also determined sex, standard length, and lateral plate counts on both sides for all individuals. Fish with a standard length much less than 40 mm were not measured, as their lateral plates were often not fully developed.

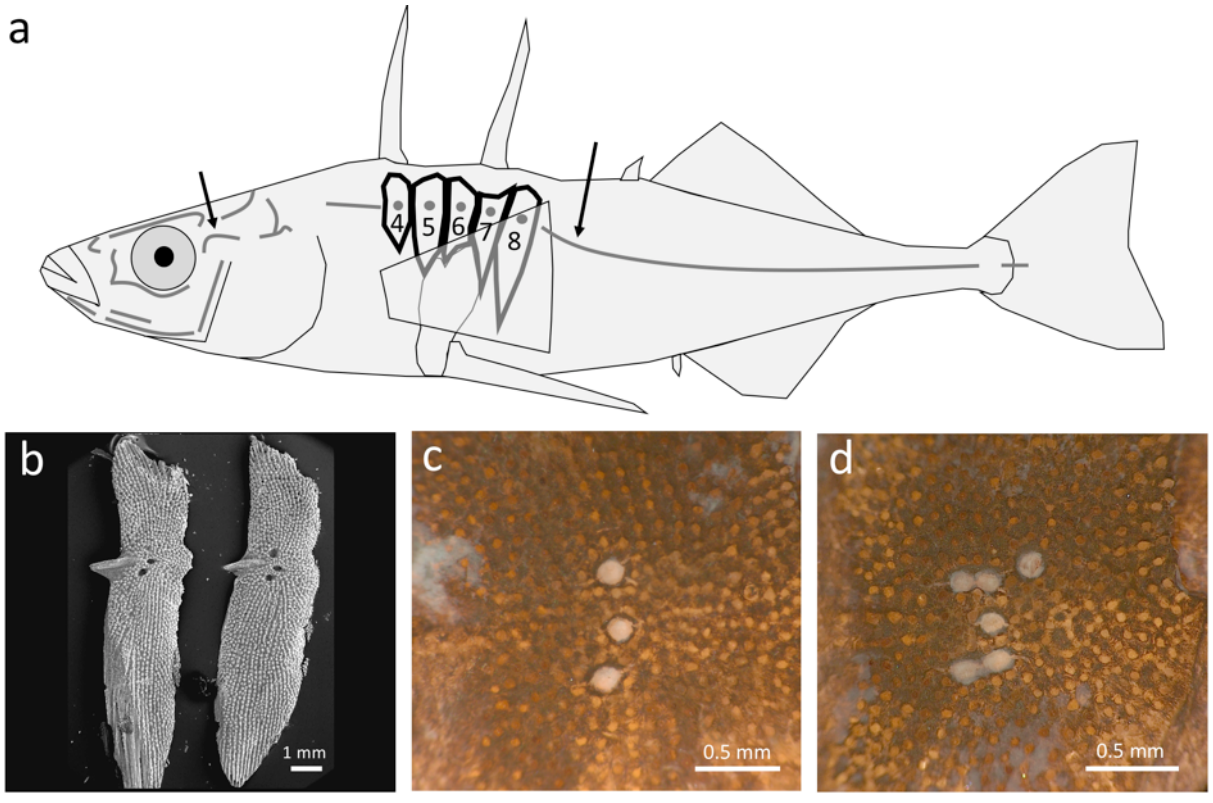

Figure 2. Depiction of neuromasts on the buttressing plates of threespine stickleback (*Gasterosteus aculeatus*). (*a*) Sketch of the lateral line of threespine stickleback with buttressing region of lateral plates emphasized. Arrows indicate regions of superficial neuromasts as denoted in Wark and Peichel (2010). (*b*) Scanning electron micrograph of the seventh and eighth left lateral plates, with two and three neuromast pores, respectively. Image provided by J. A. Buckland-Nicks. (*c*) Light micrograph of neuromasts on the fifth left lateral plate, with three neuromasts innervating three separate pores. (*d*) Light micrograph of neuromasts on the fourth left lateral plate, with two oblong pores containing two neuromasts each and two pores containing single neuromasts.

I tested repeatability in seven populations, Drizzle Lake, Drizzle Pond, Mayer Lake, Roadside Pond, Gudal Lake, Swan Lake and Lake D21. These were selected to span the breadth of morphologies observed in the study. Repeat scoring of neuromasts was done in the reverse sequence (right side first) relative to the initial scoring (left side first) to ensure that the order of scoring did not impart any bias in results. Neuromast counts were highly repeatable, with an average absolute difference of 0.15 neuromasts per plate between measurements, equating to less than one neuromast differing every six plates counted.

I cleared and stained a small subset of samples with Sudan Black to confirm neurological tissue presence (Fig. 3). I attempted multiple staining methods (Taylor 1967; Filipski and Wilson 1984; Nishikawa 1987); however, stain uptake and complete clearing of the samples was sporadic and inhibited further investigation into afferent nerve structure. While previous methods state that Sudan Black readily stains specimens preserved in ethanol, Filipski and Wilson (1984) used freshly preserved specimens and state that methyl-alcohol-free ethanol must be used, Nishikawa's (1987) specimens were fixed in formaldehyde and Taylor (1967) mentions that

staining and clearing regularly destroyed older specimens and those fixed in ethanol. Thus, I suspect that the fatty tissue of stickleback that were fixed in formaldehyde at least 30 years ago had degraded more than previously tested specimens, stickleback fixed with ethanol could not be properly cleared due to their lack of integrity and staining of stickleback fixed by both methods was complicated due to contamination by methyl alcohol.

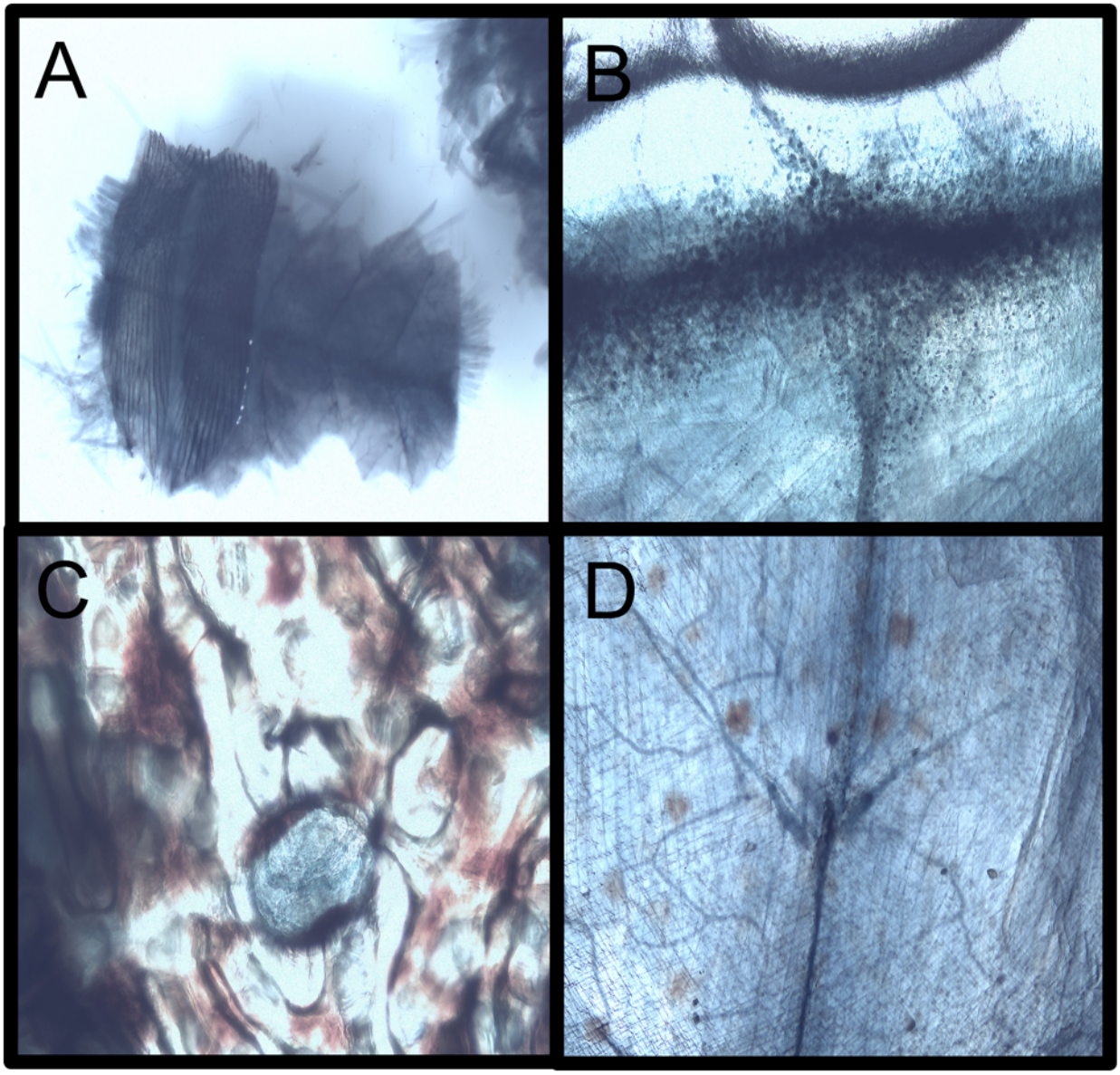

Figure 3. Histological stains using Sudan Black, following the procedure of Filipski & Wilson (1984). (*a*) 7th and 8th lateral plates and skin from body segments 9-11. (*b*) A myomere without a lateral plate present. (*c*) Individual plate pore, (*d*) Close up of naked trunk segment.

2.3.3 Statistical analysis

I used a generalized Poisson hurdle model with a mixed-effects structure to predict neuromast counts per plate. This complex error structure is warranted, as simpler structures produce unrealistic predictions of the dataset. A Gaussian error distribution predicts non-count values (KS test: $p < 0.001$; Outlier test: $p < 0.001$; Fig. 4a), Poisson predicts neuromast counts far greater than those observed and too many zeros (KS test: $p < 0.001$; Outlier test: $p < 0.001$; Fig. 4b) and generalized Poisson predicts neuromast counts greater than those observed and too few zeros (KS test: $p < 0.001$; Outlier test: $p = 0.012$; Fig. 4c). The general Poisson hurdle model still produces outliers and deviance, likely due to the high number of plates with three neuromasts relative to all other counts (KS test: $p < 0.001$; Outlier test: $p = 0.20$; Fig. 4d), but the range of neuromast counts that it predicts is within biological reason, and a more complex model structure is beyond the scope of this work. I fit the hurdle models in two stages. First, I modeled neuromast presence/absence (NP) on each plate using a binomial generalized linear mixed effect model ($GLMM_b$) with a logit link. Second, I modeled neuromast count (NC) on each plate with at least one neuromast present using a truncated (excluding zero values) generalized Poisson generalized linear mixed-effects model ($GLMM_{tgp}$) with a log link. Fitting the model in two stages allows separate predictors of NP and NC to be tested. In cases where all or nearly all stickleback had neuromasts on every plate, I used a generalized Poisson generalized linear mixed-effects model ($GLMM_{gp}$) in place of the $GLMM_{tgp}$.

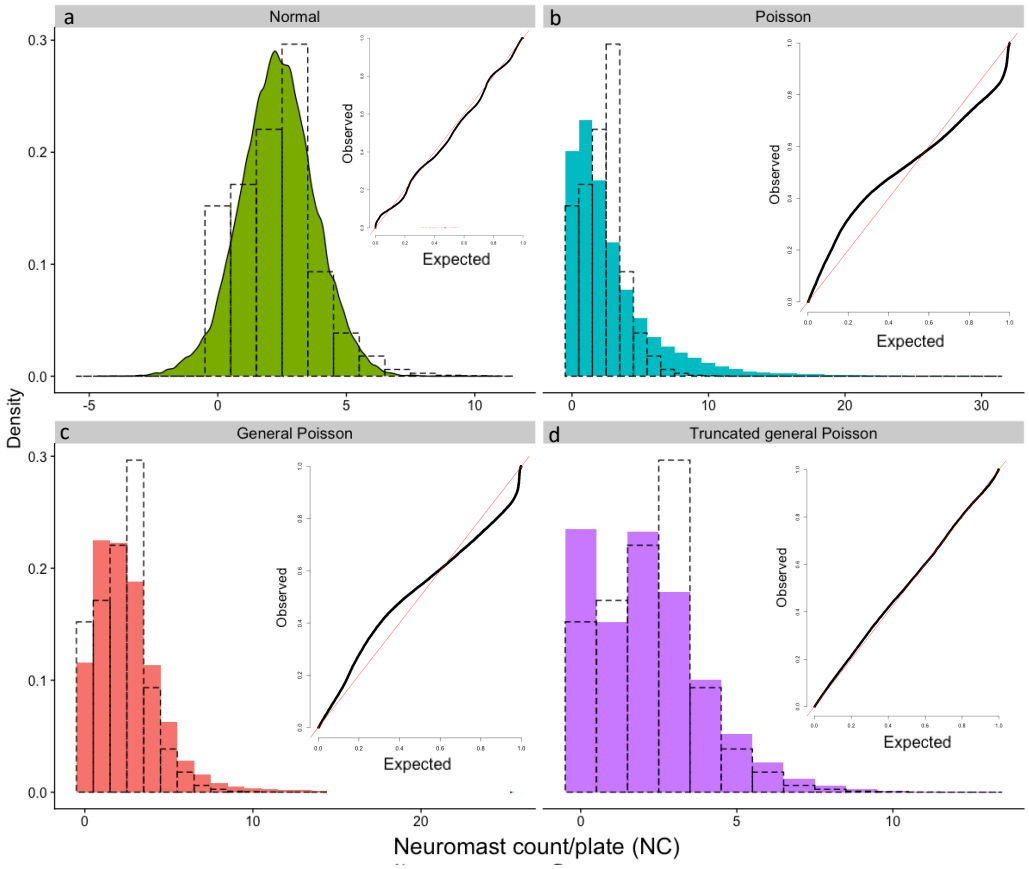

Figure 4. Diagnostics for modelling lateral plate neuromasts with equation 1 (Table 2). Dotted bars are the raw data, coloured bars are counts generated by model simulation (histograms are counts, and density plot is continuous). Inset figures are *DHARMa* Q-Q plots for each model.

The ontogeny of trunk neuromasts and their afferent neuron structure also provides justification for dividing NP and NC. The trunk lateral line first develops as a series of primary neuromasts, deposited on separate myomeres from a primordium that travel rostro-caudally down the flank before hatching (Ledent 2002). Following hatching, secondary neuromasts form on myomeres between primary neuromasts from a second primordium propagating rostro-caudally (Ledent 2002), and accessory neuromasts form adjacent to these primary and secondary neuromasts by budding (Ledent 2002; Wada et al. 2010). Early forming afferent neurons

connected to these primary neuromasts have a high resistance to stimuli and mediate larval escape behaviour, whereas later forming afferent neurons are more sensitive (Liao and Haehnel 2012). Single afferent neurons also innervate hair cells of a single polarity across multiple adjacent neuromasts (Faucherre et al. 2009; Haehnel et al. 2012), suggesting that these groups are the smallest functional unit of processing in the hindbrain. Therefore, I can differentiate between the presence and absence of early primary neuromasts and afferent neuron units with NP and the subsequent proliferation of accessory neuromasts and afferent neuron signal-to-noise ratio with NC. While the ontogeny of stickleback trunk neuromasts has yet to be examined, this general developmental pattern is likely deeply conserved among fishes.

I determined if there were differences in NP and NC among plate positions and between the sexes, using equation 1 (64 populations; 3,802 individuals; 31,661 plates; Table 2). I performed backward stepwise model selection on all models, using Wald's χ^2 tests at $\alpha = 0.05$, a conservative estimate of model complexity relative to other methods such as AIC; however, this technique is subject to selection bias (Zucchini 2000; Murtaugh 2009).

Table 2. Model equations before backward stepwise selection. (*) denotes an interaction between factors in addition to their primary effects. Brackets encompass the random effects structure, (1) denotes random intercepts and (/) denotes a nested random effects structure with the rightmost term nested within the leftmost term. Italicized text indicates categorial factors. SL = standard length, LP = lateral plate count.

Equation #	Full model structure
1	Y = *sex* * *position* + (1 | *population* / *individual ID*)
2	Y = *sex* * (*habitat* + *clarity* + *region*) + *position* + (1 | *population* / *individual ID*)
3	Y = *sex* * (pH + log(area) + *predation regime* + SL + log(LP)) + position + (1 | *population* / *individual ID*)
4	Y = *sex* * (pH + log(area) + *predation regime* + SL + log(LP)) + position + (0 + SL + log(LP) | *population*) + (1 | *population* / *individual ID*)
5	Y = *sex* * SL + *position* + (1 | *sample date* / *individual ID*)
6	Y = *sex* * *population* + *position* + (1 | *sample date* / *individual ID*)
7	Y = *sex* * generation + *position* + (1 | *individual ID*)

I tested the effect of broad ecological regime on NP and NC with equation 2 (64 populations; 3,802 individuals; 31,661 plates; Table 2). I included interactions between sex and environmental factors to test for the effect of habitat on sexual dimorphism, as environment influences sexual dimorphism in other traits of threespine stickleback (Reimchen and Nosil 2004). As the three clarity categories are associated with changes in many biophysical and morphological characteristics, I further tested a subset of lakes for the effects of pH, lake area, predation regime, standard length and lateral plate count on NP and NC (Table 1). I used equation 3 to model NP, as random slopes of standard length and log(lateral plate count) converged to zero, and I used equation 4 to model NC (42 populations; 2,981 individuals; 24,484 plates; Table 2). I also tested intrapopulation effects of standard length on NP and NC in Drizzle Lake (988 individuals; 8,242 plates) and NC in Mayer Lake (284 individuals; 2,732 plates), with equation 5 (Table 2). I did not assess changes in NP within Mayer Lake, and I used a $GLMM_{gp}$ in place of a $GLMM_{tgp}$ for the NC test, as only 0.5% of buttressing plates lacked neuromasts in this population.

Using equation 6 (Table 2), I tested differences in NP and NC between lake-stream pairs; Drizzle Lake and Drizzle Outlet (43 individuals; 330 plates), Mayer Lake and Gold Creek (40 individuals; 350 plates) and between the transplant ponds and their source populations; Drizzle Pond (321 individuals; 2,616 plates) from Drizzle Lake, and Roadside Pond (234 individuals; 2,253 plates), Bevan's Pond (80 individuals; 706 plates) and Mayer Pond Two (22 individuals; 193 plates) from Mayer Lake. As with the standard length analysis, fish derived from Mayer Lake rarely had lateral plates without neuromasts, so I only tested NC and used a $GLMM_{gp}$. I assessed incremental change in NP and NC within ponds using equation 7 and compared

observed changes in NP and NC to model predictions from equations 3 and 4 after model selection (Table 2).

I did all the analysis in R 3.6.3. I fit all models using the *glmmTMB* library (Brooks et al. 2017), validated models by visually inspecting plots produced by *DHARMa* (Hartig 2019), and calculated estimated marginal means with *emmeans* (Lenth 2019). All continuous predictors were rescaled prior to model fitting. Any non-significant p values presented were calculated by adding the non-significant predictor back into the final model. Post-hoc pairwise comparisons are estimated marginal means contrasts, Tukey adjusted for multiple comparisons.

2.4 Results

2.4.1 Summary of buttressing plate neuromast counts

Neuromasts on the buttressing lateral plates are highly variable in occurrence and abundance among Haida Gwaii and Dewdney-Banks populations. Roughly a third of populations display a gradient from a complete lack of buttressing plate neuromasts to a consistent presence on every plate, whereas the rest have neuromasts present on all buttressing plates more than 85% of the time (Fig. 5). Buttressing plates neuromast counts are also highly variable, ranging from zero to more than six per plate on average (Fig. 6). Serendipity Lake completely lacked lateral plates and thus lacked buttressing plate neuromasts.

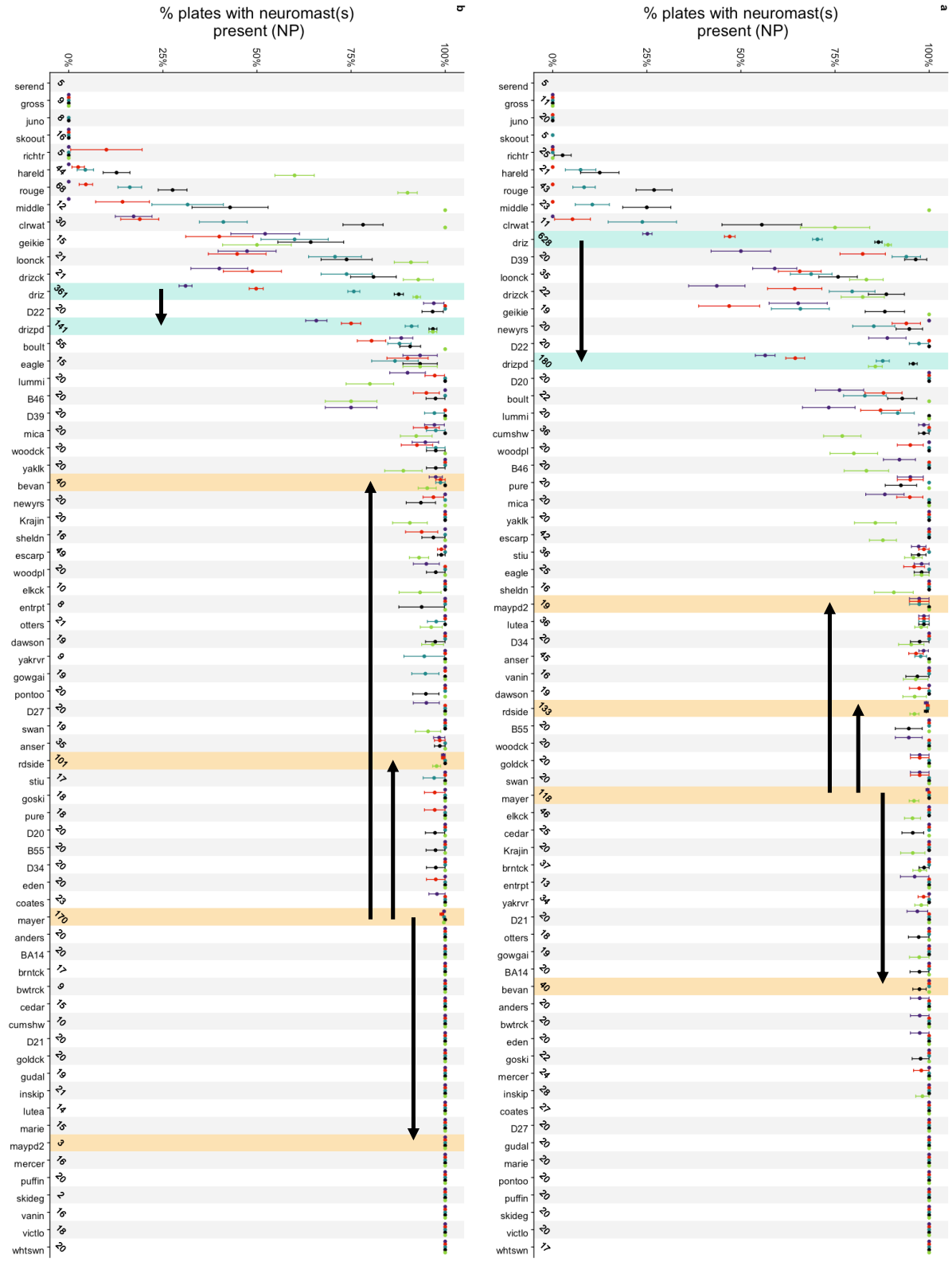
% plates with neuromast(s) present (NP)
0%
25%
50%
75%
100%
b
serend 5
gross 9
juno 8
skoout 16
richtr 5
hareld 34
rouge 68
middle 12
clrwat 30
geikie 16
loonck 27
drizck 21
driz 361
D22 20
drizpd 141
boult 35
eagle 15
lummi 20
B46 20
D39 20
mica 20
woodck 20
yaklk 20
bevan 40
newyrs 20
Krajin 20
sheldn 16
escarp 49
woodpl 20
elkck 10
entrpt 8
otters 27
dawson 19
yakrvr 9
gowgai 19
pontoo 20
D27 20
swan 19
anser 35
rdside 101
stiu 17
goski 18
pure 18
D20 20
B55 20
D34 20
eden 20
coates 23
mayer 170
anders 20
BA14 20
brntck 17
bwtrck 9
cedar 15
cumshw 10
D21 20
goldck 20
gudal 19
inskip 27
lutea 14
marie 15
maypd2 3
mercer 16
puffin 20
skideg 2
vanin 16
victlo 18
whtswn 20
% plates with neuromast(s) present (NP)
0%
25%
50%
75%
100%
a
serend 5
gross 17
juno 20
skoout 5
richtr 23
hareld 21
rouge 43
middle 23
clrwat 17
driz 628
D39 20
loonck 23
drizck 20
geikie 19
newyrs 20
D22 20
drizpd 180
D20 20
boult 22
lummi 20
cumshw 38
woodpl 20
B46 20
pure 20
mica 20
yaklk 20
escarp 45
stiu 38
eagle 23
sheldn 16
maypd2 19
lutea 38
D34 20
anser 45
vanin 16
dawson 19
rdside 133
B55 20
woodck 20
goldck 20
swan 20
mayer 178
elkck 48
cedar 23
Krajin 20
brntck 37
entrpt 13
yakrvr 4
D21 20
otters 18
gowgai 19
BA14 20
bevan 40
anders 20
bwtrck 20
eden 20
goski 22
mercer 24
inskip 23
coates 22
D27 20
gudal 20
marie 20
pontoo 20
puffin 20
skideg 20
victlo 20
whtswn 17

Figure 5. Interpopulation variation of neuromast presence (NP) on buttressing plates (in order: four = purple, five = red, six = blue, seven = black, eight = green), among (*a*) females and (*b*) males of 64 threespine stickleback populations from coastal British Columbia and four experimental transplant ponds. Each point is a population average for a given plate position, and error bars denote binomial 95% CIs for the mean. Populations are ordered by increasing NP. The number of fish of a given sex scored for each population is listed at the bottom. Highlighted populations are source populations and their transplants, with arrows indicating the change in population rank from source to transplant populations.

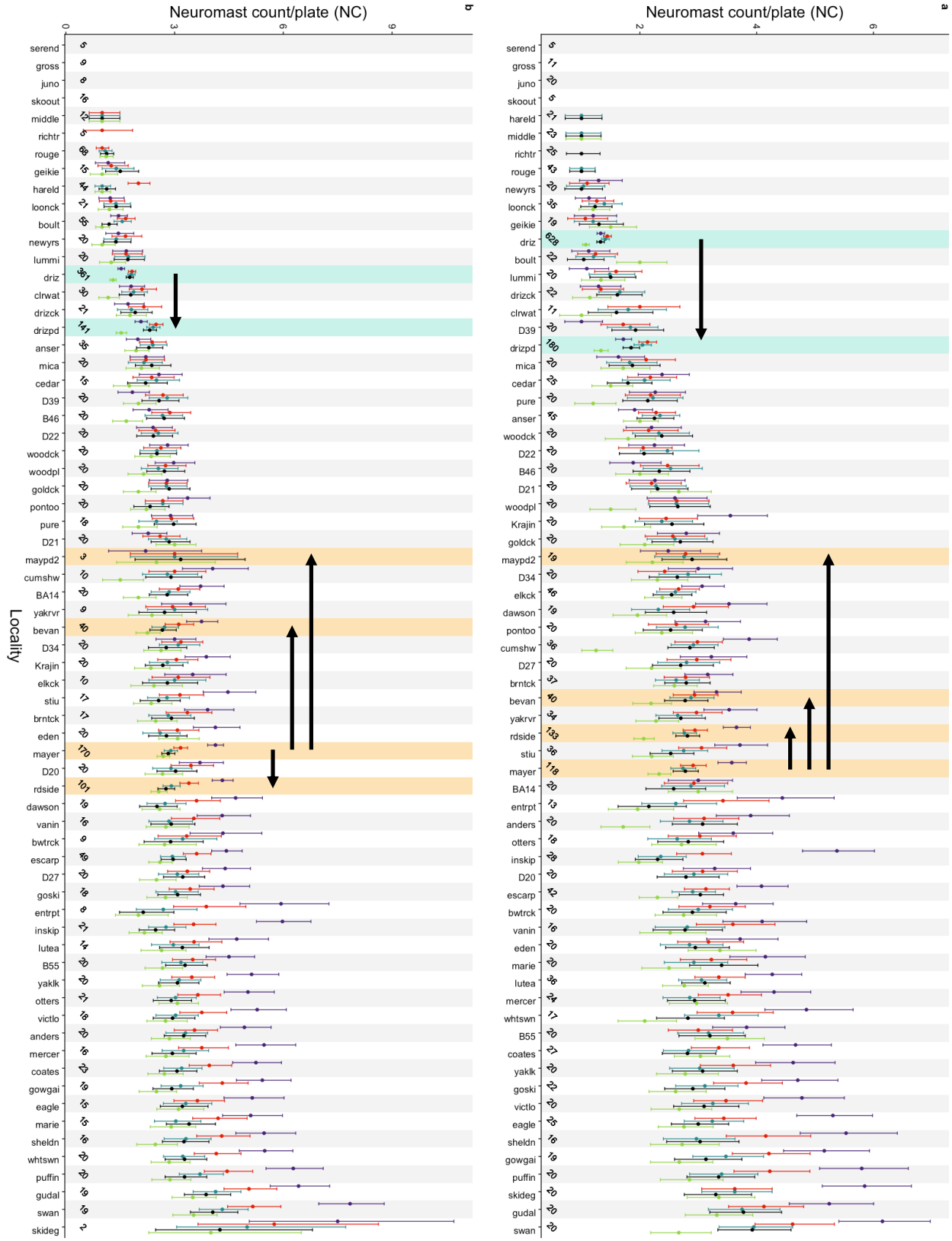
Neuromast count/plate (NC)
b
Locality
serend
gross
juno
skoout
middle
richtr
rouge
geikie
hareld
loonck
boult
newyrs
lummi
driz
clrwat
drizck
drizpd
anser
mica
cedar
D39
B46
D22
woodck
woodpl
goldck
pontoo
pure
D21
maypd2
cumshw
BA14
yakrvr
bevan
D34
Krajin
elkck
stiu
brntck
eden
mayer
D20
rdside
dawson
vanin
bwtrck
escarp
D27
goski
entrpt
inskip
lutea
B55
yaklk
otters
victlo
anders
mercer
coates
gowgai
eagle
marie
sheldn
whtswn
puffin
gudal
swan
skideg
Neuromast count/plate (NC)
a
serend
gross
juno
skoout
hareld
middle
richtr
rouge
newyrs
loonck
geikie
driz
boult
lummi
drizck
clrwat
D39
drizpd
mica
cedar
pure
anser
woodck
D22
B46
D21
woodpl
Krajin
goldck
maypd2
D34
elkck
dawson
pontoo
cumshw
D27
brntck
bevan
yakrvr
rdside
stiu
mayer
BA14
entrpt
anders
otters
inskip
D20
escarp
bwtrck
vanin
eden
marie
lutea
mercer
whtswn
B55
coates
yaklk
goski
victlo
eagle
sheldn
gowgai
puffin
skideg
gudal
swan

Figure 6. Interpopulation variation of neuromast count (NC) on buttressing plates (in order: four = purple, five = red, six = blue, seven = black, eight = green), among (*a*) females and (*b*) males of 64 threespine stickleback populations from coastal British Columbia and four experimental transplant ponds. Each point is a population average for a given plate position, and error bars denote Poisson 95% CIs for the mean. Populations are ordered by increasing NC. Number of fish of a given sex scored for each population is displayed at the bottom. Highlighted populations are source populations and their transplants, with arrows indicating the change in population rank from source to transplant populations.

NP and NC differ among buttressing plate positions and between the sexes. Anterior plates are more likely to lack neuromasts but develop more neuromasts on average ($GLMM_b$: position: $\chi^2_4 = 1075$, $p < 0.001$; $GLMM_{tgp}$: position: $\chi^2_4 = 3320$, $p < 0.001$; Fig. 7). Males are more likely to develop neuromasts on their buttressing plates than females, and males develop more buttressing plate neuromasts on average ($GLMM_b$: sex: $\chi^2_1 = 14.5$, $p < 0.001$; $GLMM_{tgp}$: sex: $\chi^2_1 = 249$, $p < 0.001$; Fig. 7). Sexual dimorphism in NP and NC is greatest on the anterior plates ($GLMM_b$: position × sex: $\chi^2_4 = 20.0$, $p < 0.001$; $GLMM_{tgp}$: position × sex: $\chi^2_4 = 22.4$, $p < 0.001$; Fig. 7).

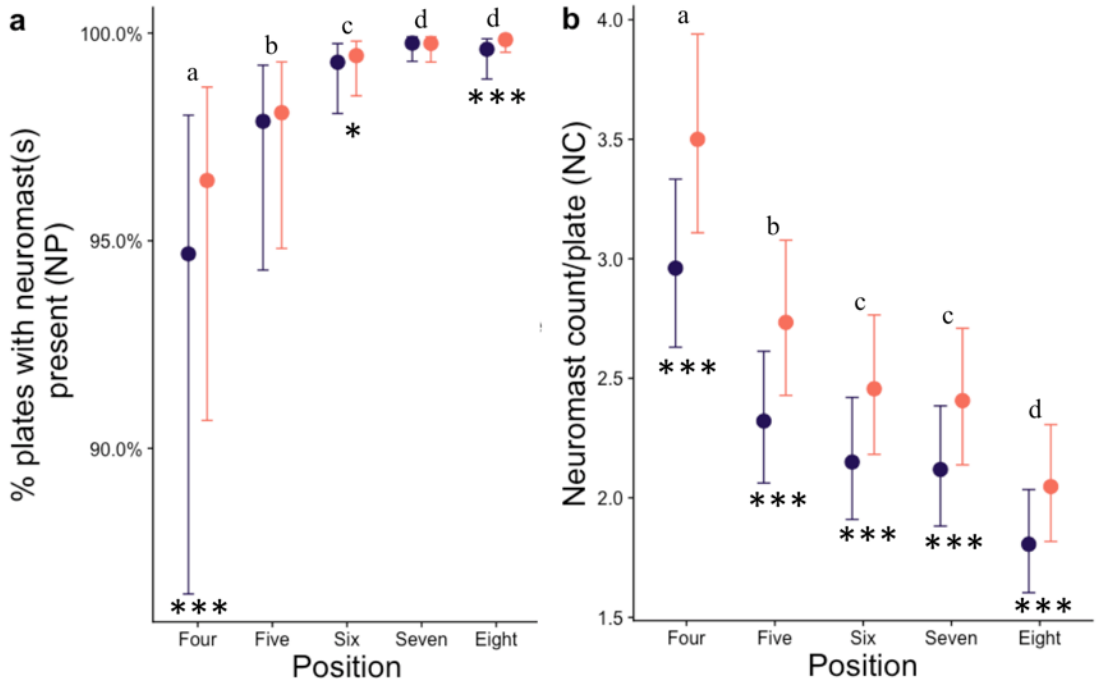

Figure 7. Sexual dimorphism in (*a*) neuromast presence (NP) and (*b*) neuromast count (NC) on buttressing plates. Points are estimated marginal means (EMMs) for females (purple) and males (pink) from a (*a*) $GLMM_b$ or (*b*) $GLMM_{tgp}$ model. Error bars are 95% CIs for EMMs. Stars denote significance of sexual dimorphism for a given lateral plate position (* < 0.05; ** < 0.01; *** < 0.001) and letters denote paired differences among plate positions, averaged over sex. Post-hoc tests have been Tukey adjusted for multiple comparisons.

2.4.2 Effect of ecology on buttressing plate neuromast counts

NP differs among clarity regimes and sexual dimorphism in NP differs among habitat types. The probability of buttressing plate neuromasts developing remains the same across habitat types ($GLMM_b$: habitat: $\chi^2_3 = 0.4$, $p = 0.80$). However, lake males have more NP than lake females (female – male: log-odds ± se = -0.42 ± 0.09, $t_{31643} = 4.7$, $p < 0.001$), stream males tend to have lower NP than stream females (female – male: log-odds ± se = 0.43 ± 0.24; $t_{31643} = 1.8$,

$p = 0.076$) and oceanic males and females have similar NP (female – male: log-odds ± se = -0.14 ± 0.8; $t_{31643} = 0.2$, $p = 0.86$; $GLMM_b$: sex × habitat: $\chi^2_3 = 11.4$, $p = 0.003$). Additionally, stained and partially stained populations were more likely to have buttressing plates lacking neuromasts than clear water populations ($GLMM_b$: clarity: $\chi^2_2 = 26.6$, $p < 0.001$; Fig. 8a). Geographic region did not significantly affect NP ($GLMM_b$: region: $\chi^2_2 = 0.9$, $p = 0.65$) and neither region or clarity regime had a significant effect on sexual dimorphism of NP ($GLMM_b$: sex × region: $\chi^2_2 = 4.7$, $p = 0.097$; $GLMM_b$: sex × clarity: $\chi^2_2 = 1.2$, $p = 0.56$).

NC is variable among clarity regimes and sexual dimorphism in NC differs among habitats and clarity regimes. Stickleback from stained and partially stained localities have fewer buttressing plate neuromasts than clear water localities ($GLMM_{tgp}$: clarity: $\chi^2_2 = 42.7$, $p < 0.001$; Fig. 8b). Furthermore, sexual dimorphism in NC is greater in stained (log(female - male) ± se = -0.18 ± 0.02; $t_{26828} = 9.1$, $p < 0.001$) than partially-stained (-0.15 ± 0.03; $t_{26828} = 5.4$, $p < 0.001$) and clear water populations (-0.07 ± 0.02; $t_{26828} = 4.1$, $p < 0.001$; $GLMM_{tgp}$: sex × clarity: $\chi^2_2 = 38.9$, $p < 0.001$). NC is consistent across habitat types ($GLMM_{tgp}$: habitat: $\chi^2_2 = 0.6$, $p = 0.76$); however, sexual dimorphism in NC is greater in lakes (-0.16 ± 0.01; $t_{26828} = 14.8$, $p < 0.001$) and oceanic localities (-0.16 ± 0.04; $t_{26828} = 3.7$, $p < 0.001$) than streams (-0.09 ± 0.03; $t_{26828} = 3.6$, $p < 0.001$; $GLMM_{tgp}$: sex × habitat: $\chi^2_2 = 6.2$, $p = 0.046$). Geographic region did not significantly affect NC or sexual dimorphism in NC ($GLMM_{tgp}$: region: $\chi^2_2 = 2.3$, $p = 0.32$; $GLMM_{tgp}$: sex × region: $\chi^2_2 = 3.4$, $p = 0.18$).

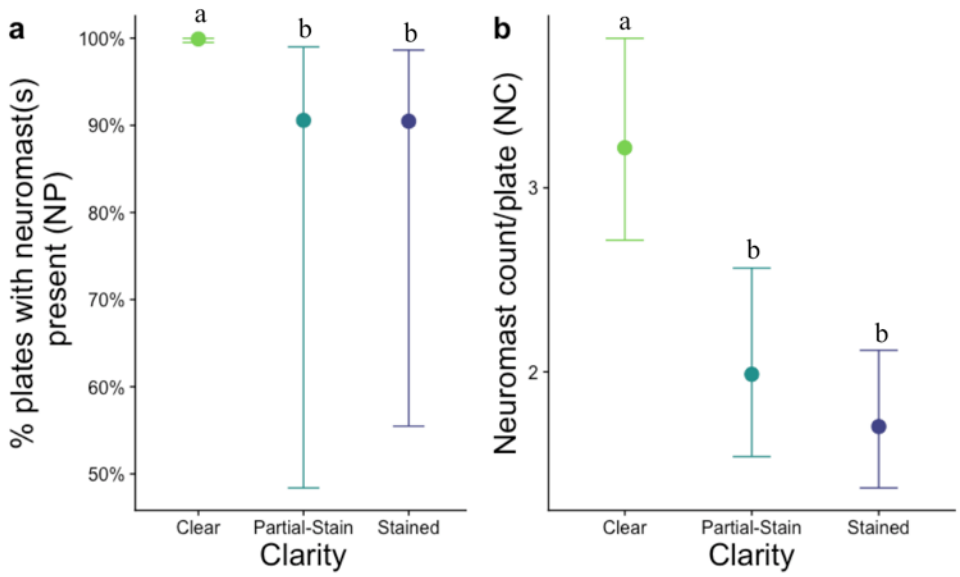

Figure 8. Differences in (*a*) neuromast presence (NP) and (*b*) neuromast count (NC) among clarity regimes. Each point is the estimated marginal mean from a (*a*) $GLMM_b$ or (*b*) $GLMM_{tgp}$ model. Error bars are 95% CIs for estimated marginal means averaged over all other model parameters. Letters denote paired differences among clarity regimes, Tukey adjusted for multiple comparisons.

The two lake-stream pairs examined differ in their relationship. Drizzle Outlet stickleback tended to have greater NP and NC than Drizzle Lake fish ($GLMM_b$: locality: $\chi^2_1 = 3.1$, $p = 0.077$; $GLMM_{tgp}$: locality: $\chi^2_1 = 3.0$, $p = 0.085$; Fig. 9a-b), whereas stickleback in Gold Creek have lower NC than Mayer Lake fish ($GLMM_{gp}$: locality: $\chi^2_1 = 10.1$, $p = 0.002$; Fig. 9c). Sexual dimorphism in NP is reversed between Drizzle Lake and Drizzle outlet, although this difference is not statistically significant ($GLMM_b$: $\chi^2_1 = 2.77$, $p = 0.096$). Sexual dimorphism in NC did not differ between either lake-stream pair ($GLMM_{tgp,gp}$: all $\chi^2_1 \leq 0.77$, $p \geq 0.38$).

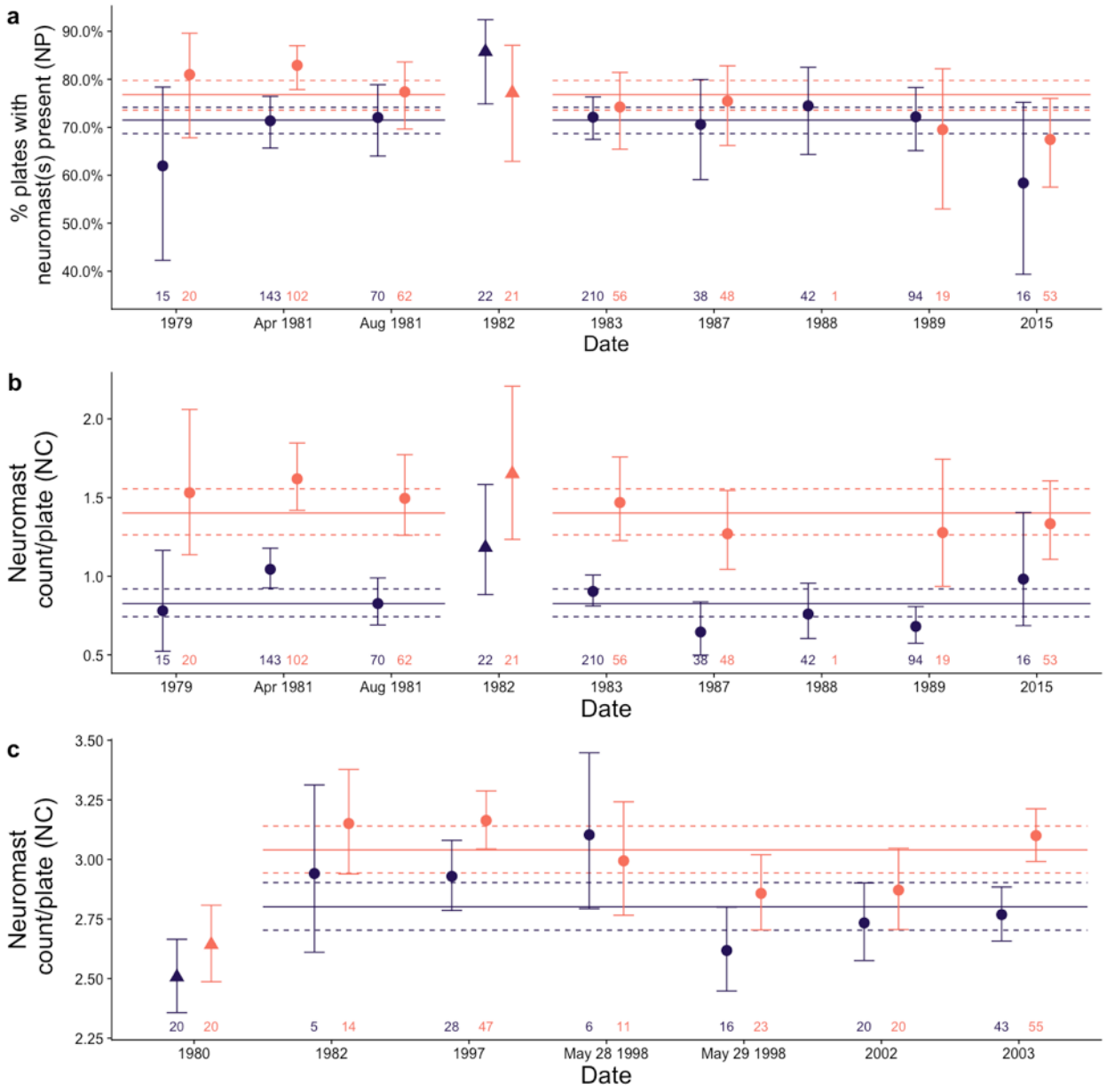

Figure 9. The difference in (*a*) neuromast presence (NP) and (*b,c*) neuromast count (NC) between (*a,b*) Drizzle lake (circles) and Drizzle Outlet (triangles) and (*c*) Mayer Lake (circles) and Gold Creek (triangles). Females are shown in purple, and males and shown in pink. Points are estimated marginal mean (EMMs) from a (*a*) $GLMM_b$, (*b*) $GLMM_{tgp}$ or (*c*) $GLMM_{gp}$ model. Error bars are 95% CIs for EMMs. Solid and dashed horizontal lines represent the population

average for a given sex and its 95% CI, respectively. Sample sizes for each sex on each date, are given at the bottom.

Among lakes, the best predictors of NP are pH, predation regime and standard length. NP increases with pH, and sexual dimorphism in NP decreases with pH ($GLMM_b$: pH: $\chi^2_1 = 12.9$, $p < 0.001$; $GLMM_b$: pH × sex: $\chi^2_1 = 6.9$, $p = 0.009$; Fig. 10a). Populations exposed to cutthroat trout have the greatest NP, followed by rainbow trout and invertebrate exposed populations ($GLMM_b$: predation: χ^2_2=13.4, $p = 0.001$; Fig. 10b). For ~40 mm fish, males have greater NP than females, but larger males and females are similar ($GLMM_b$: standard length × sex: $\chi^2_1 = 5.8$, $p = 0.016$; Fig. 10c). The same trend occurred within Drizzle Lake; longer males have less NP whereas longer females greater NP (male log-odds = -0.46±0.22; female log-odds = 0.12±0.15; $GLMM_b$: sex × standard length: $\chi^2_1 = 4.7$, $p = 0.030$). Lake area and lateral plate count did not affect NP ($GLMM_b$: log(area): $\chi^2_1 = 0.3$, $p = 0.56$; $GLMM_b$: log(lateral plates): $\chi^2_1 = 0.6$, $p = 0.42$) and all habitat and morphological characteristics other than pH and standard length had no significant effect on sexual dimorphism in NP ($GLMM_b$: all × sex: $\chi^2_{1\text{-}2} \leq 0.2$, $p \geq 0.70$).

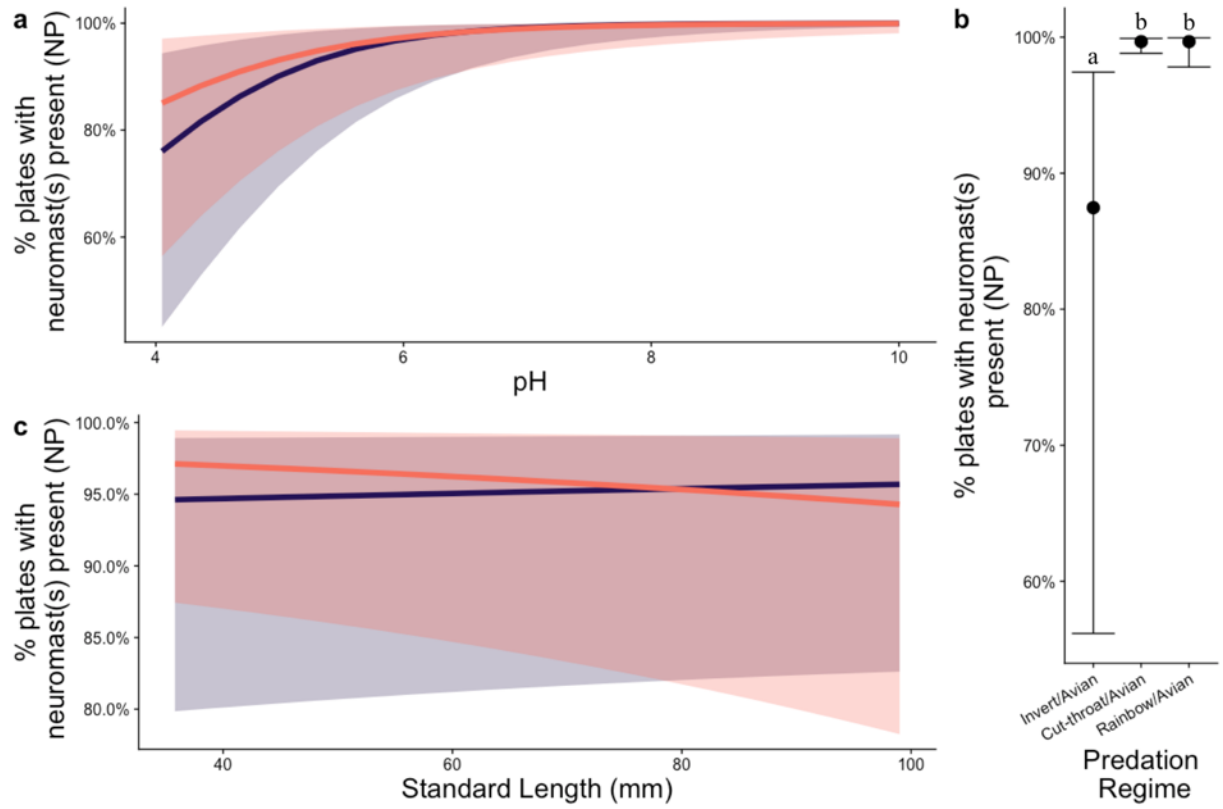

Figure 10. Influence of pH (*a*), predation regime (*b*) and standard length (*c*) on neuromast presence (NP) in 42 lake populations of threespine stickleback from coastal British Columbia. (*a,c*) Lines denote estimated marginal means (EMMs) of a $GLMM_b$, and shaded regions denote 95% CIs for the mean, for females (purple) and males (pink). (*b*) Points and error bars are EMMs and their 95% CI, respectively; letters denote paired differences among clarity regimes, Tukey adjusted for multiple comparisons. EMMs are averaged over all model parameters other than those being visualized.

The best predictors of NC among lakes were pH, predation regime, lateral plate count and standard length. The number of neuromasts that develop on a single buttressing plate increases with pH, and populations with invertebrate predators have lower NC than populations with cutthroat trout and rainbow trout predators ($GLMM_{tgp}$: pH: $\chi^2_1 = 28.1$, $p < 0.001$; $GLMM_{tgp}$:

predation regime: $\chi^2_2 = 7.2$, $p = 0.028$; Fig. 11a-b). NC increases with the number of lateral plates more strongly for females than males, whereas NC increases more strongly with standard length for males than females ($GLMM_{tgp}$: log(lateral plates): $\chi^2_1 = 19.1$, $p < 0.001$; log(lateral plates) × sex: $\chi^2_1 = 28.0$, $p < 0.001$; $GLMM_{tgp}$: SL: $\chi^2_1 = 0.4$, $p = 0.52$; $GLMM_{tgp}$: standard length × sex: $\chi^2_1 = 25.4$, $p = < 0.001$; Fig. 11c-d). Correlation between standard length and NC within populations varies; in Drizzle lake neuromast count does not change with standard length ($GLMM_{tgp}$: standard length: $\chi^2_1 = 0.04$, $p = 0.84$; $GLMM_{tgp}$: sex × standard length: $\chi^2_1 = 0.2$, $p = 0.64$), but in Mayer Lake longer individuals of both sexes have more neuromasts (scaled log-odds = 0.08 ± 0.02; $GLMM_{gp}$: standard length: $\chi^2_1 = 12.3$, $p < 0.001$; $GLMM_{gp}$: sex × standard length: $\chi^2_1 = 0.1$, $p = 0.71$).

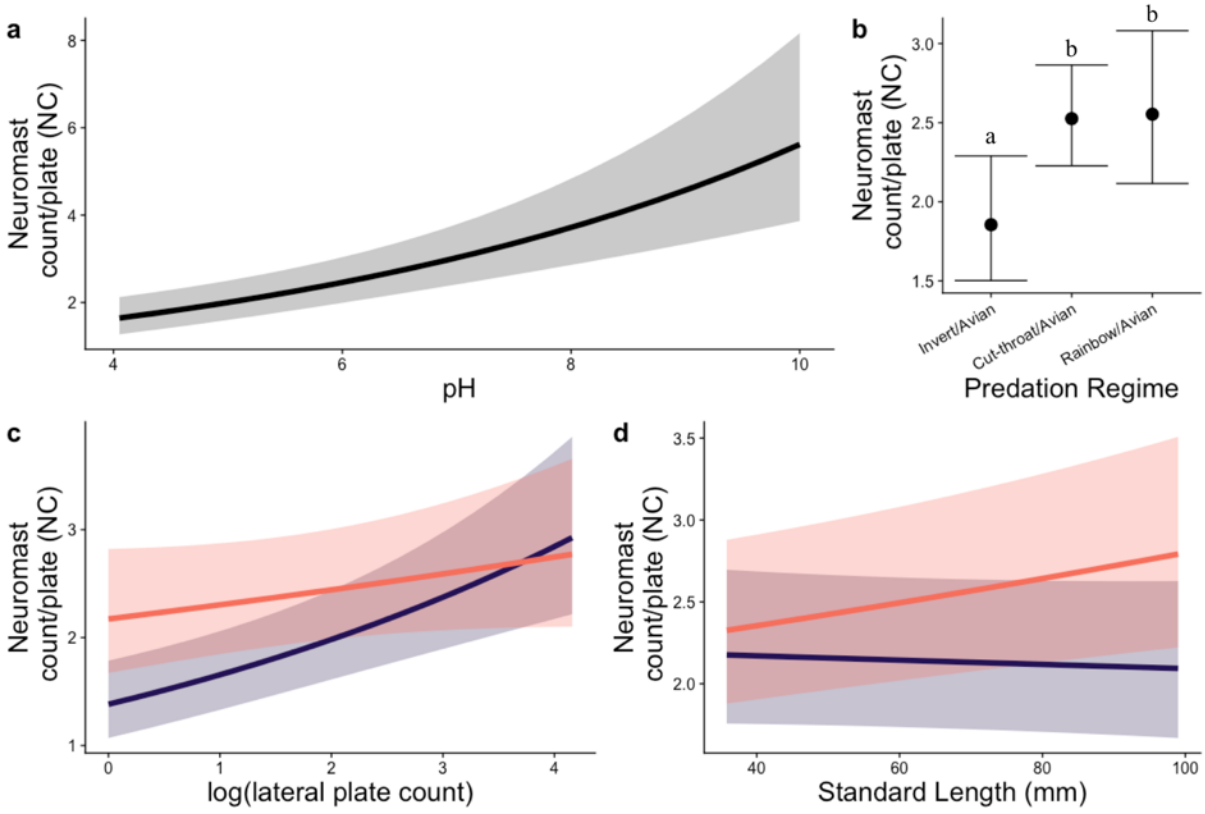

Figure 11. Influence of (*a*) pH, (*b*) predation regime, (*c*) lateral plate count and (*d*) standard length on neuromast count (NC), in 42 lake populations of threespine stickleback from coastal British Columbia. (*a,c,d*) Lines denote estimated marginal means (EMMs) of a $GLMM_{tgp}$ and shaded regions denote 95% CIs for the mean. (*b*) Points and error bars are EMMs and their 95% CI respectively; letters denote paired differences among predation regimes, Tukey adjusted for multiple comparisons. (*c,d*) females are shown in purple and males are shown in pink. EMMs are averaged over all model parameters other than those being visualized.

2.4.3 Buttressing plate neuromast counts in transplant ponds

Drizzle Pond rapidly developed more buttressing plate neuromasts than Drizzle Lake. NP and NC are greater in Drizzle Pond ($GLMM_b$: $\chi^2_1 = 176$, $p < 0.001$; $GLMM_{tgp}$: $\chi^2_1 = 96.9$, $p < 0.001$), falling within the expected NP and NC given the change in environment (Fig. 12a-b). NC sexual dimorphism decreased in Drizzle Pond relative to Drizzle Lake $GLMM_{tgp}$: $\chi^2_1 = 13.1$, $p < 0.001$; Fig. 12b), but sexual dimorphism in NP remained the same ($GLMM_b$: $\chi^2_1 = 2.0$, $p = 0.16$). There was no difference in NP or NC among generations of Drizzle Pond stickleback ($GLMM_b$: $\chi^2_1 = 1.9$, $p = 0.17$; $GLMM_{tgp}$: $\chi^2_1 = 0.9$, $p = 0.34$).

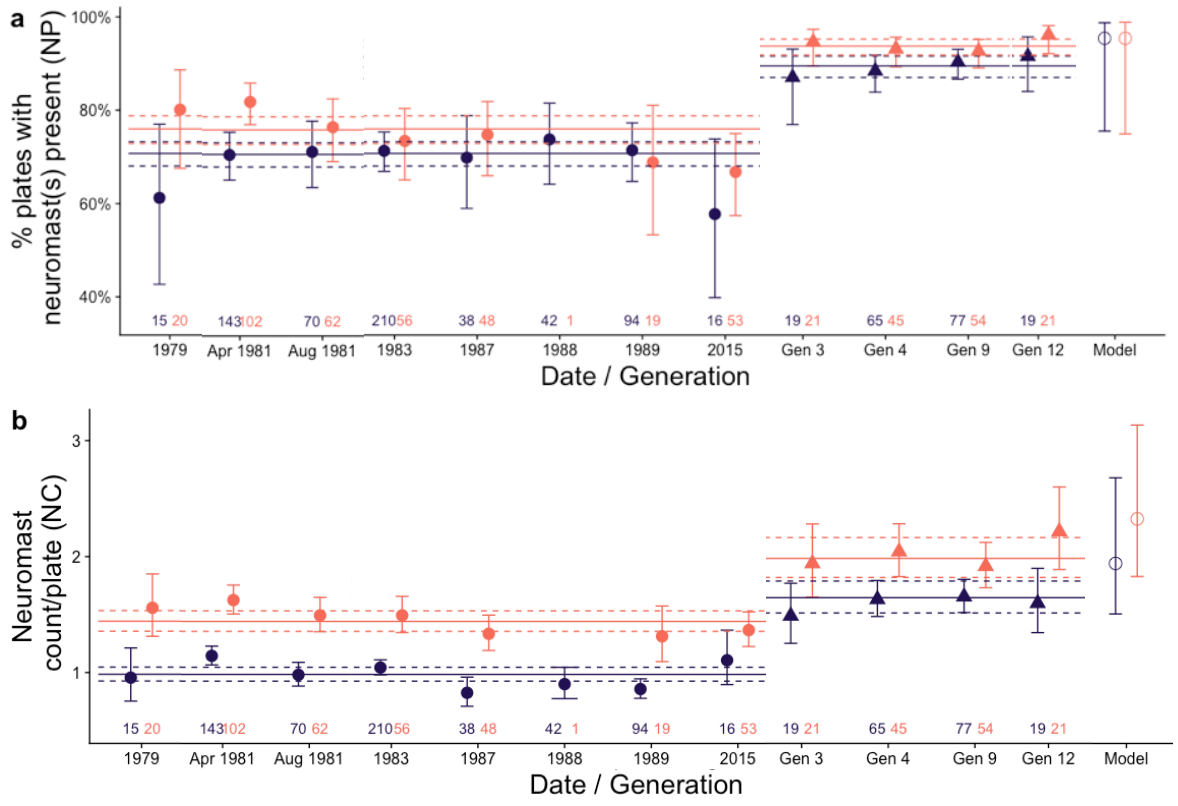

Figure 12. Change in (*a*) neuromast presence (NP) and (*b*) neuromast count (NC) of threespine stickleback transplanted from Drizzle Lake (circles) to Drizzle Pond (triangles). Points are estimated marginal means (EMMs) from a (*a*) $GLMM_b$ (*b*) or $GLMM_{tgp}$ with error bars denoting the mean 95% CI. Purple (females) and pink (males) horizontal lines represent the population average for a given sex (solid) and their 95% CIs (dashed). Hollow 'model' points are the predicted NP and NC values for Drizzle Pond from the environmental model ((*a*) equation 3, (*b*) equation 4), error bars are 95% CI of this model estimate.

There was no change in NC between Mayer Lake and Roadside Pond ($GLMM_{gp}$: $\chi^2_1 = 0.1$, $p = 0.77$; Fig. 13a), Mayer Lake and Bevan's Pond ($GLMM_{gp}$: $\chi^2_1 = 1.1$, $p = 0.30$; Fig. 13b) or Mayer Lake and Mayer Pond Two ($GLMM_{gp}$: $\chi^2_1 = 1.4$, $p = 0.24$; Fig. 13c); however, all transplant ponds tended towards the expected NC

given the change in environment (Fig. 13a-c). Sexual dimorphism in NC is the same as Mayer Lake in all transplant ponds ($GLMM_{gp}$: all $\chi^2_1 \leq 1.4$, $p \geq 0.24$; Fig. 13a-c). Roadside Pond stickleback have significantly declined in NC over 12 generations ($GLMM_{gp}$: $\chi^2_1 = 51.2$, $p < 0.001$; Fig. 13a).

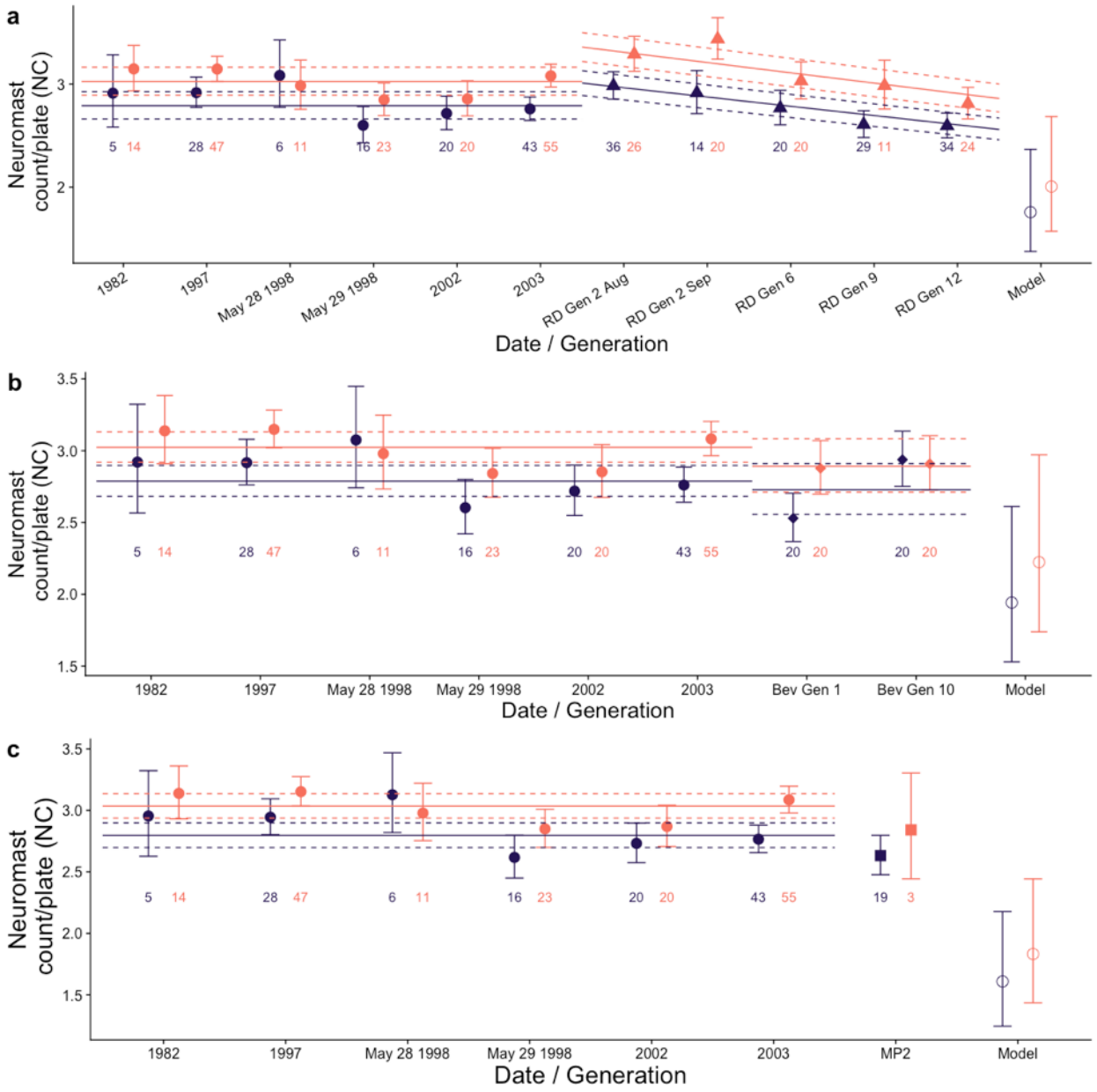

Figure 13. Change in neuromast count (NC) of threespine stickleback transplanted from Mayer Lake (circles) to (*a*) Roadside Pond (triangles), (*b*) Bevan's Pond (diamonds) and (*c*) Mayer Pond Two (squares). Points are estimated marginal means (EMMs) from a $GLMM_{gp}$, with error bars denoting the mean 95% CI. Purple (females) and pink (males) horizontal lines represent the population average for a given sex (solid) and its 95% CI (dashed). Hollow 'model' points are the predicted NC for each transplant pond from the environmental model (equation 4), error bars are 95% CI on this model estimate.

2.5 Discussion

Buttressing plate neuromast presence (NP) and buttressing plate neuromast count (NC) are highly variable among threespine stickleback populations on the coast of British Columbia. Among the three regions examined, stickleback populations ranged from completely lacking buttressing plate neuromasts to having upwards of six neuromasts per buttressing plate. These large differences in NP and NC can mainly be attributed to facets of ecology rather than major habitat types and do not differ among geographic regions. Stained water systems have less NP and lower NC, whereas neuromasts are abundant on the buttressing plates in clear water localities. The four primary habitat characteristics that differ between these major habitat types are water spectra, pH, predation landscape and lake size. Stickleback in low pH and invertebrate/avian predation landscapes often lack neuromasts on their buttressing plates and have low NC, whereas stickleback in habitats with high pH and salmonid predators rarely lack neuromasts on their buttressing plates and have high NC. While lakes and streams generally did not differ in NP or NC, streams were less sexually dimorphic in NC and Gold Creek had lower NC than Mayer Lake. NC increases with the number of lateral plates and NC sexual dimorphism is greatest in long stickleback but reduced in stickleback with many lateral plates. Lastly,

stickleback transplanted from a stained lake to an unstained pond can undergo stark changes in NP and NC within just a couple of generations, as seen in Drizzle Pond. While the Mayer Lake transplants showed no significant change in NC from Mayer Lake, Roadside Pond did undergo gradual loss of neuromasts over 12 generations, and all transplants tended towards their expected NC given the shift in habitat.

My findings suggest that differences in neuromast count among habitats are due to changes in water chemistry and predation landscape. Wark and Peichel (2010) found that freshwater lake and stream stickleback in British Columbia had more neuromasts than oceanic stickleback across their lateral line system and Ahnelt et al. (2021) found that freshwater stickleback had more facial neuromasts than marine and anadromous stickleback in Denmark. In contrast, I found no difference in NC between freshwater and oceanic populations, with some freshwater populations having greater NC and some having fewer NC than the ancestral morphology. It is unlikely that the difference observed between studies is due to the specific subset of the lateral line examined, as the same general trend occurs across lateral line stitches in both studies and the Mp stitch, of which the buttressing plates are a subset, shows some of the most prominent changes with habitat (Wark and Peichel 2010; Ahnelt et al. 2021). The freshwater habitats examined in these studies were likely not stained and potentially eutrophic. As such, an increase in neuromasts in these populations relative to oceanic stickleback is consistent with my findings for clear water populations, especially if light limitation due to eutrophication promotes greater NC. The similarity in NC between lakes and streams is in accordance with previous work (Wark and Peichel 2010; Jiang et al. 2017); however, differences in NC between Mayer Lake and Gold Creek suggests that ecological characteristics other than flow regime may differ between a lake and its tributary stream, causing changes in NC. Reduced

sexual dimorphism in streams may be due to reduced niche space for the sexes to diverge within, such as along the benthic-limnetic axis commonly seen in lakes (Nosil and Reimchen 2005; Kitano et al. 2012; Scharnweber et al. 2013).

Clarity regime is associated with a suite of ecological characteristics that influence many aspects of stickleback morphology. Stained lakes are typically smaller, have reduced transmission of light, lower pH, and support invertebrate and avian predators rather than piscivorous fish species (Reimchen 1994). Differences in the spectral regime of stained lakes have led to a redshift adaptation in the *SWS2* opsin (Marques et al. 2017), small lakes have less diversity in feeding morphology (Nosil and Reimchen 2005), and changes in lateral plate and spine morphology are affected by predation landscape (Reimchen et al. 2013). Thus, it is not unexpected that NP and NC change over this ecological gradient and covaries with other morphological traits.

Predation pressure by puncturing predators and developmental constraints imposed by pH exert opposing selective pressures on NC. Stickleback exposed to puncturing predators have greater NP and NC compared to populations lacking puncturing predators. While the role of the lateral line in predator evasion (York and Bartol 2014; Stewart et al. 2014) makes differences in NP and NC among predation regimes expected, it is not immediately clear why the lateral line is important in the detection of puncturing predators but not compression predators. It may be that puncturing predators such as cutthroat trout feed on earlier life history stages of stickleback compared to avian piscivores and invertebrates (Reimchen 1990, 1995). Thus, they assert stronger selective pressure at earlier life history stages, when the lateral line's functional range, which is on the order of centimeters, is much larger relative to the stickleback's body size. It is also worth noting that most studies of predator evasion by lateral line mechanosensation have

been on larval fish (Blaxter and Fuiman 1990; McHenry et al. 2009; Stewart and McHenry 2010; Stewart et al. 2014), further suggesting that the lateral line is vital in early life history predator-prey interactions. While I could not disentangle the effects of pH and water spectra in the analysis due to their close correlation, given the trend observed the effects of acidity are likely stronger than those of spectra. There is usually an excess development of superficial neuromasts under limited light conditions, as seen in the blind Mexican cavefish (Yoshizawa et al. 2010; Lloyd et al. 2018) and deep sea fishes (Marshall 1996; Marranzino and Webb 2018). Conversely, low pHs that occur naturally in stained localities inhibit the development of larval zebrafish neuromasts (Lin et al. 2019). Thus, given that low transmission / low pH populations have few neuromasts, the additional physiological cost that acidity imposes on the development of the lateral line has outweighed the benefits of superficial neuromast proliferation in these low light environments.

Some population differ from the general trend among lakes, which may further elucidate the mechanisms driving changes in NP and NC. Mayer Lake, Gold Creek and Otter Lake all have high numbers of neuromasts relative to other stained populations. All three of these populations have cutthroat trout present, and Mayer Lake has a particularly large population of this predator (Moodie 1972). In contrast, Drizzle Lake and Geikie Creek have the 'typical' number of neuromasts for stained populations, despite the presence of cutthroat trout. The difference in NP and NC among these populations suggests that the presence of predators can induce the development of high numbers of buttressing plate neuromasts despite low pH; however, taxa-specific predation pressure rather than the presence or absence of a given predator is likely more important in influencing NP and NC.

Another example that goes against the general trend is Swan Lake, a eutrophic lake that completely lacks predatory fishes yet has the highest NC observed. The only other species of fish in this lake are pumpkinseeds (*Lepomis gibbosus*) (personal observation and communication with Emily May), which are unlikely to predate on stickleback directly (García-Berthou and Moreno-Amich 2000). Therefore, neuromasts are likely serving a function other than the evasion of puncturing predators in this population. As eutrophication limits light availability without imposing the physiological cost of tannin staining, the proliferation of neuromasts may indicate adaptation to a low light environment (Marshall 1996; Yoshizawa et al. 2010; Marranzino and Webb 2018; Lloyd et al. 2018). Stickleback were also often caught in a boom or bust cycle at this locality (personal observation), suggesting that they are schooling, which would support greater energetic investment in the lateral line (Partridge and Pitcher 1980; Larsson 2009; Mekdara et al. 2018). If schooling promotes the development of neuromasts in Swan Lake, it contrasts limnetic and schooling females in Drizzle Lake (Reimchen et al. 2016), which have lower NP and NC than benthic males. However, the schooling behaviour of female stickleback in Drizzle Lake may be adapted to be less mechanosensation dependent, due to the physiological cost imposed by high acidity. Swan Lake also has a rich community of piscivorous birds, *e.g.* egrets, cormorants and mergansers (personal observation), which likely predate on stickleback. If predation pressure, rather than predatory taxa, is the primary determinant in producing greater NC, avian predators at Swan Lake may be exerting selective pressure comparable to salmonids in other localities.

Ecologically dependent sexual dimorphism in the lateral line of stickleback is consistent with other traits. Male stickleback have more neuromasts than females on their buttressing plates (this study) and facial neuromasts (Ahnelt et al. 2021), with increased dimorphism in lake fish

relative to oceanic populations (Ahnelt et al. 2021; this study). Changes in NC sexual dimorphism with standard length may be due to the increased expression of sexual dimorphism observed across traits in reproductively mature stickleback (Kitano et al. 2007); however, the lateral line is likely fully developed prior to the minimum standard length observed in this study. Mortality of males with few neuromasts but not females with few neuromasts would also increase NC sexual dimorphism over time. Given the energy investment of nesting behaviour by males (Pressley 1981) and their increased mortality at sexual maturity (Golovin et al. 2019), this mechanism seems more likely. However, sexual dimorphism in neuromast count did not change with standard length in Mayer Lake; one of the most sexually dimorphic populations, the population with the widest range of standard lengths in this study and a lake with an active predatory fish community. While predation regime affects sexual dimorphism in lateral plate counts (Reimchen et al. 2016), it does not influence sexual dimorphism in NC. It is possible that sexual dimorphism in lateral plate counts and NC are both being acted upon by predation landscape, but as lateral plate count is a more proximal cause of NC, it has precluded the effect of predation regime within my model. The increase in sexual dimorphism of NP at low pHs may be due to differences in metabolic gene expression between the sexes during early stages of life history (Velando et al. 2017). Early life history is when stickleback would be most vulnerable to pH and when primary neuromasts would be developing, potentially explaining why pH only affects sexual dimorphism in NP and not NC. While there are many possible mechanisms for how ecology shapes sexual dimorphism in NP and NC, all effects appear to be small and operating along the same stained-clear axis of lake ecology.

The association between NC and lateral plate count is likely due to their genetic and developmental linkage. The ectodysplasin (*Eda)* gene controls the differentiation between fully

and low plated stickleback, and influences neuromast count and patterning on the posterior trunk, including myomeres lacking lateral plates (Wark et al. 2012; Mills et al. 2014; Archambeault et al. 2020). However, changes in *Eda* haplotype are associated with the transition from fully to low plated morphs, which do not differ in NC (Planidin and Reimchen 2019). Rather, most of the reduction in NC occurs in fish ranging from low plated to fully naked, suggesting that other loci may play a role in reducing neuromast development and the association between lateral plate count and NC.

The rapid increase in NP and NC in Drizzle Pond following transplant from Drizzle Lake suggests that lateral line morphology is phenotypically plastic. Stickleback in Drizzle Pond underwent an increase in NP and NC to the expected 'ideal' pond phenotype by the second generation. This rapid change must either be due to an extremely steep selection gradient or phenotypic plasticity. As subsequent generations of Drizzle Pond fish retained the same NP and NC, phenotypic plasticity is the most likely mechanism. Phenotypic plasticity of the lateral line has been associated with changes in flow regime (Shields and Underhill 1993) and predation regime (Fischer et al. 2013). However, neuromast counts in Drizzle Pond increased, whereas guppies moved from a high-predation to a low-predation environment lost neuromasts (Fischer et al. 2013), suggesting that the shift from Drizzle Lake to Drizzle Pond is not indicative of a loss of predation pressure, or at least, increases in NC due to changes in pH have exerted a stronger selective effect than changes due to predation. While sampling effects may have artificially increased the degree of change within Drizzle Pond, it is highly improbable that all differences are due to sampling effects, given the extent of change and its correspondence with the environmental model predictions.

There were no significant changes in NC between Mayer Lake and its transplant ponds, but all transplants tended towards a loss of buttressing plate neuromasts. Given that predation landscape and pH are strong influencers of NC and the stark shift in both of these habitat characteristics between Mayer Lake and its transplant ponds, the lack of change is unexpected. Mayer Lake stickleback have atypically high NC for a stained water population, making them much more 'pond-like' than Drizzle Lake stickleback and likely caused less selective pressure to lose neuromasts in the Mayer Lake transplants. Differences in the rate of change of stickleback transplanted from Mayer Lake and Drizzle Lake may also suggest genetic or epigenetic differences between these two populations. The gradual changes in NC within Roadside Pond suggest that there has been genetic selection on NC whereas the rapid change in Drizzle Pond may be due to changes in epigenetic modification. While twelve generations may not have been enough time for divergence in NC between Mayer Lake and Roadside Pond to become statistically significant, stark changes have occurred in other traits (Leaver and Reimchen 2012; Marques et al. 2018), including lateral plates and *Eda*; therefore, loci other than those linked to *Eda* may have caused the high NC in Mayer Lake. As Mayer Pond Two is stained, whereas Roadside Pond and Bevan's Pond are not stained, and all three localities have undergone a similar reduction in NC, changes in predation landscape rather than pH are a more likely cause for the slightly decreased NC observed in these ponds.

The buttressing plates of threespine stickleback have undergone consistent changes in neuromast count in association with ecological landscape, among natural populations and experimental transplant ponds. Physiological stress, spectral regime and predation pressure interact to determine the optimal neuromast phenotype of stickleback and phenotypic plasticity allows stickleback to adapt to these new habitats quickly. Complex ecosystem dynamics are

shaping sexual dimorphism in mechanosensation and interactions between lateral plate phenotype and *Eda*, with the potential for phenotypic plasticity and many loci acting on the lateral line. Adaptation in the lateral line of threespine stickleback helps elucidate the mechanisms under which the lateral line system's morphology may have diversified among species and how ecological context can modulate those outcomes.

Chapter 3: Variation in buttressing plate neuromast count asymmetry among populations

Part of this chapter is in the process of publication:

Planidin NP, Reimchen TE (2021) Ecological predictors of lateral line asymmetry in stickleback (*Gasterosteus aculeatus*). Evol Ecol *In Press*

3.1 Abstract

Stickleback exhibit differences in defence morphology asymmetry among ecological landscapes, suggesting that asymmetry plays a role in the functional ecology of the species. However, the role of asymmetry in sensory modalities such as the lateral line has yet to be investigated. Here I have evaluated the extent of deviation from bilateral symmetry of 3,897 fish in 64 natural and four transplant populations of threespine stickleback from lakes, streams and oceanic habitats of coastal British Columbia, predicting that neuromasts would be largely bilaterally symmetrical for optimal detection of external stimuli. In contrast, I found asymmetry in all populations, the greatest amount occurring on the anterior buttressing lateral plates and in populations with the fewest neuromasts. I found no consistent trends of signed (directional) asymmetry (SA) among the populations, while relative absolute asymmetry (RAA) is lower in dystrophic (stained) habitats than in clearwater habitats ($p < 0.001$), except for fish with few neuromasts. Sexual dimorphism in RAA is also greater in stained habitats ($p < 0.001$). Transplants from stained lakes to unstained ponds resulted in a 0.1% to 14% difference in RAA from the source population in less than 12 generations but varied in direction among experiments. These data suggest a widespread tendency for populations exposed to reduced photic information to exhibit reduced asymmetry in their lateral line system, changing rapidly in response to a new environment.

3.2 Introduction

Asymmetry is prevalent in stickleback morphology. The bony lateral plates of threespine stickleback range from covering the entire flank (fully plated), to low-plated (3-8 plates), to 'naked' fish among freshwater habitats (Reimchen et al. 2013). Lateral plates also exhibit widespread changes in their bilateral asymmetry dependent on ecological context and life history (Moodie and Reimchen 1976; Bergstrom and Reimchen 2000). Fish with asymmetries of lateral plates are less common in populations that are exposed to puncturing predators (Moodie and Reimchen 1976), exhibit increased parasite load (Reimchen and Nosil 2001b; Bergstrom and Reimchen 2005) and have better young survival (Moodie and Moodie 1996). Furthermore, within a population, left-biased plate asymmetry increases from littoral to limnetic habitats, but also the frequencies vary with respect to collecting conditions such as temperature and wind speed (Reimchen and Bergstrom 2009).

Threespine stickleback morphology can change quickly in response to a new environment. After being transplanted from a large stained lake to an unstained pond, stickleback have undergone changes in many traits over just eight generations, representing one-third of the difference observed between stickleback in natural lakes and ponds (Spoljaric and Reimchen 2007; Leaver and Reimchen 2012). This transplant population has also undergone genome-wide changes of a similar degree, particularly in regions associated with phenotypic traits (Marques et al. 2018). The number of neuromasts on the buttressing plates has also increased or decreased in two transplant pond experiments, depending on the source population phenotype (Chapter 2).

To determine whether asymmetry occurs in the lateral line of threespine stickleback and if so, to what extent it is affected by ecology, I scored the number of neuromasts occurring on the

left and right buttressing plates of threespine stickleback from 64 localities from the coast of British Columbia, Canada. These populations spanned major habitat types such as oceanic, lake and stream as well as ecological landscapes from clear, partially-stained and deeply stained clarity regimes. I explored associations between neuromast count asymmetry and habitat characteristics. I further tested a subset of 43 lakes for which pH, area and predation regime data were available for the influence of biophysical and life history traits on neuromast asymmetry, as well as two lake-stream pairs. I also examined the extent of asymmetry in four transplant populations in relation to their source populations. While non-directional asymmetries of the lateral line have been previously assessed as a component of multi-metric studies of fluctuating asymmetry in several fish species, including ninespine stickleback, *Pungitius pungitius* (Almeida et al. 2008; Trokovic et al. 2012), here I present a direct investigation of lateral line asymmetry among a diversity of ecological contexts and its potential rate of change.

3.3 Methods

3.3.1 Metrics of asymmetry

The following analysis uses the same biophysical dataset and examination of stickleback in the lab as Chapter 2. I calculated four metrics of asymmetry from neuromast counts of buttressing plate positions with plates present on both sides (for average number of plate pairs per population see Table 1). R is the number of neuromasts on the right side, and L is the number of neuromasts on the left side of a plate pair for a given position. Initially, I compared signed asymmetry (SA = R-L) and absolute asymmetry (AA = |R-L|) among all populations. Models assuming normality of SA (KS test: $p < 0.001$; Outlier test $p < 0.001$; Fig. 14a) and a Poisson error distribution of AA (KS test: $p < 0.001$; Outlier test $p = 0.83$; Fig. 14b) generated impossible

predictions, *e.g.* non-integer neuromast asymmetry in the case of SA and non-zero asymmetry for plates lacking neuromasts for both SA and AA; because of this, I used the corrected metrics relative signed asymmetry (RSA = $\frac{R}{R+L}$) and relative absolute asymmetry (RAA = $\frac{|R-L|}{R+L}$) for subsequent analysis. RSA (KS test: $p < 0.001$; Outlier test $p < 0.001$; Fig. 14c) and RAA (KS test: $p < 0.001$; Outlier test $p = 0.06$; Fig. 14d) are not without limitation, as they both exhibit overdispersion and RAA makes some impossible predictions, such as a plate pair with one neuromast being symmetrical. Note that RAA can be converted to the commonly used metric for fluctuating asymmetry $\frac{|R-L|}{\frac{(R+L)}{2}}$ by multiplying it by two (Palmer and Strobeck 1986).

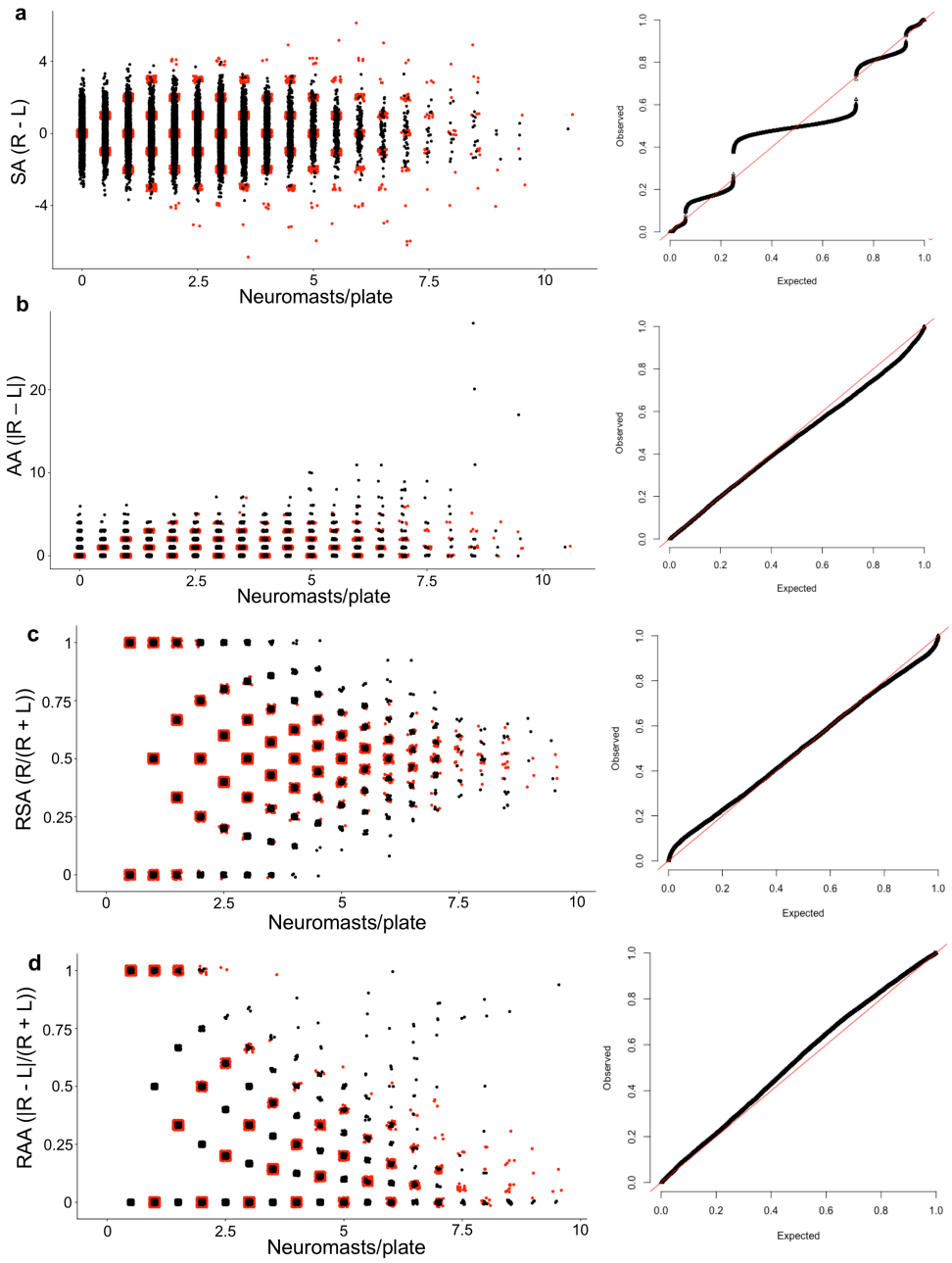

Figure 14. Comparison of raw data to model simulations predicting (*a*) signed asymmetry (SA), (*b*) absolute asymmetry (AA), (*c*) relative signed asymmetry (RSA) and (*d*) relative absolute asymmetry (RAA), from equation 1 (Table 3). Red points are raw data, black points are simulated from models and all points are jittered for visibility. Q-Q plots on the right are from *DHARMa*.

3.3.2 Testing for differences among buttressing plate positions

I modeled both RSA and RAA using a binomial GLMM with a logit link, with the total number of neuromasts on each plate pair (R + L) included as weights (number of binomial trials). For initial testing of the presence of RSA and RAA equation 1 was used (Table 3). Interaction effects between sex, plate position and neuromasts per plate (NPP) are justified as NPP varies with sex and plate position and since asymmetry in other traits also exhibit sexual dimorphism in threespine stickleback (Reimchen et al. 2008, 2016; Reimchen and Bergstrom 2009; Planidin and Reimchen 2019). This model and all subsequent models underwent backward stepwise model selection using $\alpha = 0.05$ as in Chapter 2. Since it is unclear whether AA or RAA is more important in determining the functional consequences of asymmetry in buttressing plate neuromasts, I have converted model predictions of RAA to AA by multiplying RAA by the total number of neuromasts on both plates $|R\text{-}L| = \frac{|R\text{-}L|}{R+L} * R+L$ and presented RAA and AA in Fig. 20-24.

I did all statistical analyses in R 3.6.3, fit models with *lme4* (Bates et al. 2015, p. 4), performed model diagnostics with *DHARMa* (Hartig 2019) and generated estimated marginal means using *emmeans* (Lenth 2019). I rescaled all continuous predictors prior to model fitting. I calculated all non-significant test statistics presented by adding the predictor back into the final selected model. As I found that only RAA differed among populations, I dropped RSA from subsequent analyses.

Table 3. Model equations for binomial GLMMs used throughout analyses. Eq. = equation number, NPP = neuromasts per plate, LP = lateral plate count, SL = standard length. Italicized words indicate categorical factors, whereas other predictors are continuous. Squaring indicates

all two-way interactions, (|) indicates random effects with a 1 on the left being random intercepts and a continuous predictor on the left *e.g.* NPP being random slopes, (:) indicates an interaction, (||) are random slopes that have been assumed to lack covariance and (/) is a nested random effects structure.

Eq.	Model structure
1	$\text{RSA or RAA} = (\text{NPP} + \textit{sex} + \textit{position})^2 + (\text{NPP} \mid \textit{local}) + (1 \mid \textit{local} : \textit{individual ID})$
2	$\text{RAA} = (\text{NPP} + \textit{sex}) * (\textit{position} + \textit{region} + \textit{habitat} + \textit{clarity}) + (\text{NPP} \mid \textit{local}) + (1 \mid \textit{local} : \textit{individual ID})$
3	$\text{RAA} = (\text{NPP} + \textit{sex}) * (\textit{position} + \log(\text{LP}) + \text{SL} + \text{LP}_{\lvert\text{R-L}\rvert} + \text{pH} + \log(\text{area}) + \textit{predators}) + (\text{NPP} + \log(\text{LP}) + \text{LP}_{\lvert\text{R-L}\rvert} \parallel \textit{local}) + (1 \mid \textit{local} : \textit{individual ID})$
4	$\text{RAA} = (\text{NPP} + \textit{sex}) * (\textit{position} + \text{SL}) + (1 \mid \textit{date} / \textit{individual ID})$
5	$\text{RAA} = (\text{NPP} + \textit{sex}) * (\textit{position} + \textit{population}) + (1 \mid \textit{date} / \textit{individual ID})$
6	$\text{RAA} = (\text{NPP} + \textit{sex}) * (\textit{position} + \text{generation}) + (1 \mid \textit{individual ID})$

3.3.3 Testing the effect of ecology on relative absolute asymmetry

I assessed the differences in RAA among major geographic regions (Haida Gwaii and Dewdney-Banks), habitat types (oceanic, lake and stream) and regimes of water clarity (stained, partially stained, clear) among 61 populations (3,788 fish; 18,940 plate pairs). I tested these habitat characteristics with equation 2, with two-way interactions between habitat characteristics, NPP and sex, to determine sex specific effects and to account for potential covariation between NPP and ecological factors (Engqvist 2005; Table 3).

To further understand why RAA differed among clarity regimes I tested a subset of 43 lakes (2,845 fish; 11,298 plate pairs) for which more complete environmental data were available (Table 1), for additional habitat and morphological predictors of asymmetry, as well as two parapatric lake-stream pairs. Clarity code correlates with tannin concentration, predation regime and lake area (Reimchen 1989). Therefore, I tested pH, log(lake area) (hectares) and predation

regime (invertebrate/avian, cutthroat/avian, rainbow trout/avian) as predictors of differences in RAA among lakes, as well as standard length (mm), log(lateral plate count) and absolute lateral plate asymmetry (|R-L|), using equation 3 (Table 3). I included random slopes by population for each morphological trait and removed covariance between random slopes for model convergence (Harrison et al. 2018; Table 3). Covariation between RSA and lateral plate count is of interest due to the association between NPP and lateral plate count (Planidin and Reimchen 2019), as well as the common genetic loci controlling lateral plate and neuromast development (Wark et al. 2012). The effects of lateral plate asymmetry on RAA are of interest given the contentions around correlations in asymmetry among different traits (Leung et al. 2000). Lateral plate asymmetry is not dependent on lateral plate count ($\chi^2_1 = 0.282$, $p = 0.596$). I tested intrapopulation effects of standard length on RAA in the two populations that were sampled across multiple years, Drizzle Lake (989 individuals; 2,908 plate pairs) and Mayer Lake (288 individuals; 1,342 plate pairs), using equation 4 (Table 3). Lake-stream pairs, Drizzle Lake and Drizzle Outlet (43 individuals; 143 plate pairs) and Mayer Lake and Gold Creek (40 individuals; 165 plate pairs) were analyzed using equation 5 (Table 3).

3.3.4 Relative absolute asymmetry in transplant ponds

I tested four experimental transplant ponds; Drizzle Pond (321 individuals; 1,133 plate pairs) from Drizzle Lake, and Roadside Pond (234 individuals; 1,026 plate pairs), Bevan's Pond (80 individuals; 346 plate pairs) and Mayer Pond Two (22 individuals; 92 plate pairs) from Mayer Lake and, for differences in RAA relative to their source populations, using equation 5 (Table 3). I then tested for intergenerational change in RAA using equation 6 (Table 3). RAA in all ponds was plotted against the expected value given the final reduced model from equation 3 (Table 3).

3.3.5 Repeatability of counting neuromasts relative to neuromast asymmetry

Measurements were highly repeatable. Replicate and side had no significant effect on number of neuromasts observed, with a 95% CI on directional measurement error of 6.8% of the standard deviation of average neuromast SA, ± 0.04 versus ± 0.55 (replicate: $\chi^2_1 = 0.05$, $p = 0.818$; side: $\chi^2_1 = 1.19$, $p = 0.276$). Furthermore, the relative rate of measurement error does not increase with the number of neuromasts and the 95th quantile of relative measurement error is only 5.1% of the average RAA, 0.02 versus 0.39 ($\chi^2_1 = 1.47$, $p = 0.225$).

3.4 Results

3.4.1 Summary of buttressing plate neuromast asymmetry

Asymmetry in lateral plate neuromast counts is ubiquitous. Left and right plates at the same position differ in the number of neuromasts they express 71.2%, 60.7%, 53.4%, 51.2% and 49.0% of the time, for positions four through eight, respectively. Thus, 93.4% of fish are asymmetric in neuromast count at one plate position or more. AA is variable among individuals, ranging from 0 to 7, and among populations (Fig. 15). SA is also variable among individuals, ranging from -7 to 6, and among populations, with 22 left-biased populations and 35 right-biased populations (Fig. 16).


AA (|R-L|)
0
2
4
6
b
serend 5
gross 9
juno 8
skoout 16
richtr 5
hareld 44
middle 12
clrwat 30
lummi 20
rouge 68
woodpl 20
boult 55
newyrs 20
maypd2 3
cumshw 10
goldck 20
elkck 10
geikie 15
anders 20
mayer 170
brntck 17
yakrvr 9
woodck 20
victlo 18
loonck 21
rdside 101
driz 387
inskip 21
anser 35
D27 20
gowgai 19
bwtrck 9
vanin 16
D34 20
pure 18
puffin 20
B46 20
drizck 21
cedar 15
Krajin 20
mica 20
goski 18
yaklk 20
drizpd 141
coates 23
pontoo 20
entrpt 8
D21 20
bevan 40
eden 20
D39 20
lutea 14
mercer 16
dawson 19
D20 20
escarp 49
stiu 17
BA14 20
eagle 15
otters 21
skideg 2
gudal 19
whtswn 20
sheldn 16
D22 20
B55 20
marie 15
swan 19
AA (|R-L|)
0
2
4
6
a
serend 5
gross 11
juno 20
skoout 5
richtr 25
rouge 43
hareld 27
middle 23
geikie 19
newyrs 20
clrwat 11
loonck 35
boult 20
driz 628
drizck 22
rdside 133
anser 46
bwtrck 20
goldck 20
mayer 118
maypd2 19
cumshw 36
otters 18
marie 20
elkck 46
D20 20
woodck 20
lummi 20
vanin 16
eden 20
cedar 25
woodpl 20
Krajin 20
pontoo 20
bevan 40
inskip 28
coates 21
pure 20
brntck 37
drizpd 180
entrpt 13
mica 20
puffin 20
yaklk 20
D34 20
stiu 36
gowgai 19
anders 20
D21 20
skideg 20
D39 20
lutea 36
yakrvr 34
dawson 19
whtswn 17
escarp 40
mercer 24
B46 20
goski 22
gudal 20
victlo 20
D27 20
sheldn 16
BA14 20
swan 20
D22 20
eagle 25
B55 20

Figure 15. Interpopulation variation of absolute asymmetry (AA) on the buttressing plates (in order: four = purple; five = red; six = blue; seven = black; eight = green), among (*a*) female and (*b*) male threespine stickleback from 64 populations across coastal British Columbia. Each point is a population average for a given plate position, and error bars denote Poisson 95% CIs for the mean estimate. Populations are ordered by increasing percentage of neuromast presence. The number of fish of a given sex scored for each population is displayed at the bottom. Highlighted populations are source populations and their transplants, with arrows indicating the change in population rank from source to transplant populations.

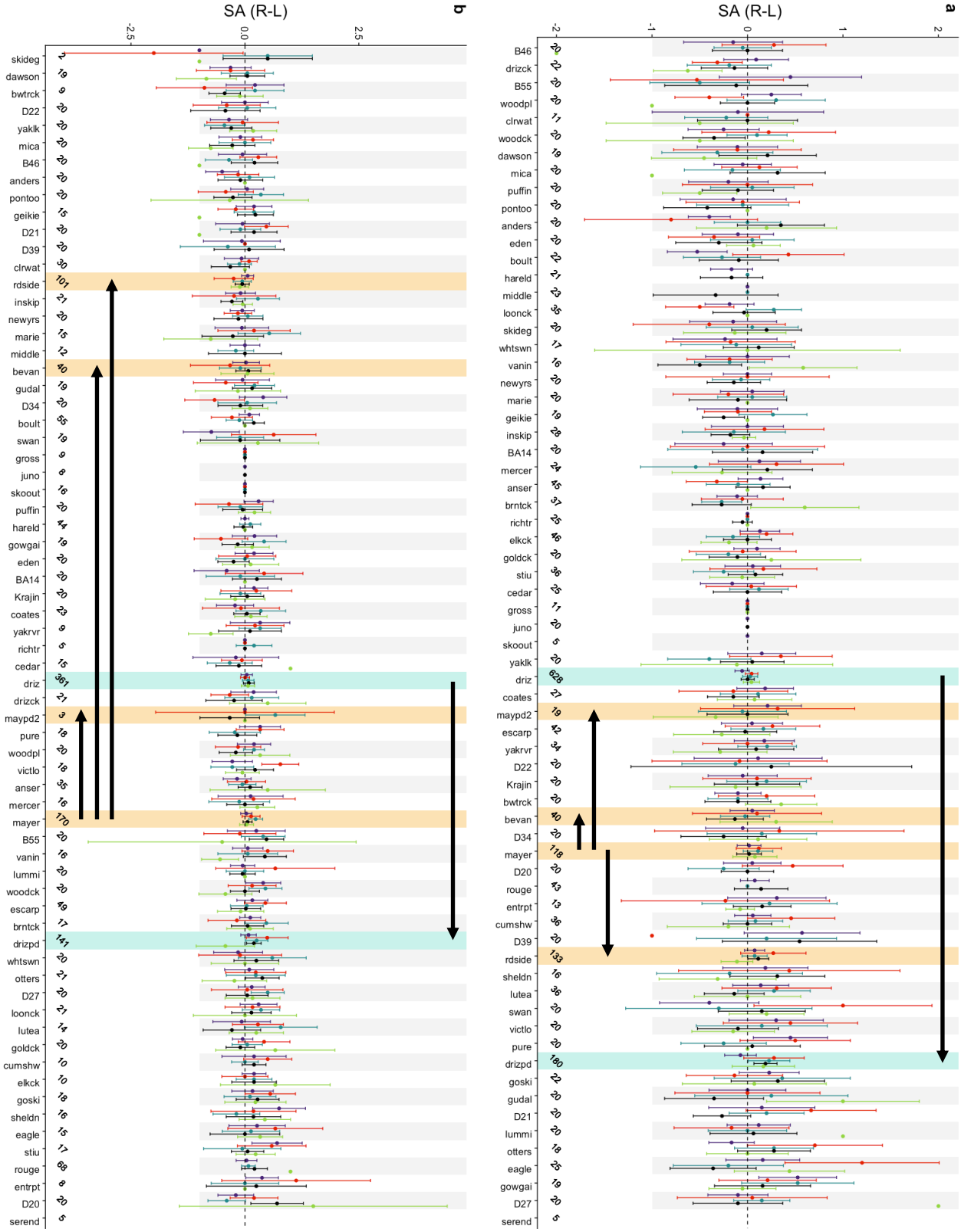
SA (R-L)
b
-2.5
0.0
2.5
skideg 2
dawson 19
bwtrck 9
D22 20
yaklk 20
mica 20
B46 20
anders 20
pontoo 20
geikie 15
D21 20
D39 20
clrwat 30
rdside 101
inskip 21
newyrs 20
marie 15
middle 12
bevan 40
gudal 19
D34 20
boult 55
swan 19
gross 9
juno 8
skoout 16
puffin 20
hareld 44
gowgai 19
eden 20
BA14 20
Krajin 20
coates 29
yakrvr 9
richtr 5
cedar 15
driz 361
drizck 21
maypd2 3
pure 18
woodpl 20
victlo 18
anser 35
mercer 16
mayer 170
B55 20
vanin 16
lummi 20
woodck 20
escarp 49
brntck 17
drizpd 141
whtswn 20
otters 21
D27 20
loonck 21
lutea 14
goldck 20
cumshw 10
elkck 10
goski 18
sheldn 16
eagle 15
stiu 17
rouge 68
entrpt 8
D20 20
serend 5
SA (R-L)
a
-2
-1
0
1
2
B46 20
drizck 22
B55 20
woodpl 20
clrwat 11
woodck 20
dawson 19
mica 20
puffin 20
pontoo 20
anders 20
eden 20
boult 22
hareld 21
middle 23
loonck 35
skideg 20
whtswn 17
vanin 16
newyrs 20
marie 20
geikie 19
inskip 28
BA14 20
mercer 24
anser 45
brntck 37
richtr 25
elkck 46
goldck 20
stiu 36
cedar 25
gross 17
juno 20
skoout 5
yaklk 20
driz 628
coates 27
maypd2 19
escarp 42
yakrvr 34
D22 20
Krajin 20
bwtrck 20
bevan 40
D34 20
mayer 118
D20 20
rouge 43
entrpt 13
cumshw 38
D39 20
rdside 133
sheldn 16
lutea 38
swan 20
victlo 20
pure 20
drizpd 180
goski 22
gudal 20
D21 20
lummi 20
otters 19
eagle 25
gowgai 19
D27 20
serend 5

Figure 16. Interpopulation variation of signed asymmetry (SA) on the buttressing plates (in order: four = purple; five = red; six = blue; seven = black; eight = green), among (*a*) female and (*b*) male threespine stickleback from 64 populations across coastal British Columbia. Each point is a population average for a given plate position, and error bars denote Gaussian 95% CIs for the mean estimate. Populations are ordered by increasing percentage of neuromast presence. The number of fish of a given sex scored for each population is displayed at the bottom. Highlighted populations are source populations and their transplants, with arrows indicating the change in population rank from source to transplant populations.

RAA differs among populations, sexes, among buttressing plate positions and with NPP, whereas RSA does not. RAA significantly varies among populations ($\chi^2_{59} = 2393$, $p < 0.001$; Fig. 17). Anterior positions exhibit greater RAA than posterior positions, and males have significantly greater RAA than females on all plate positions other than the fourth (sex: $\chi^2_1 = 38.7$, $p < 0.001$; position: $\chi^2_4 = 259$, $p < 0.001$; sex × position: $\chi^2_4 = 10.5$, $p = 0.033$; Fig. 18). RAA declines with neuromast count, with the most rapid decline occurring on the sixth plate and a steeper decline in males than females (NPP: $\chi^2_1 = 96.0$, $p < 0.001$; NPP × position: $\chi^2_4 = 71.3$, $p < 0.001$; NPP × sex: $\chi^2_1 = 7.5$, $p = 0.006$; Fig. 18). RSA does not significantly vary among populations ($\chi^2_{59} = 20.7$, $p = 1.00$; Fig. 19), between sexes, among buttressing plate positions or with neuromast count, including two-way interactions (all trait effects: $\chi^2_{1\text{-}4} \leq 1.6$, $p \geq 0.29$).

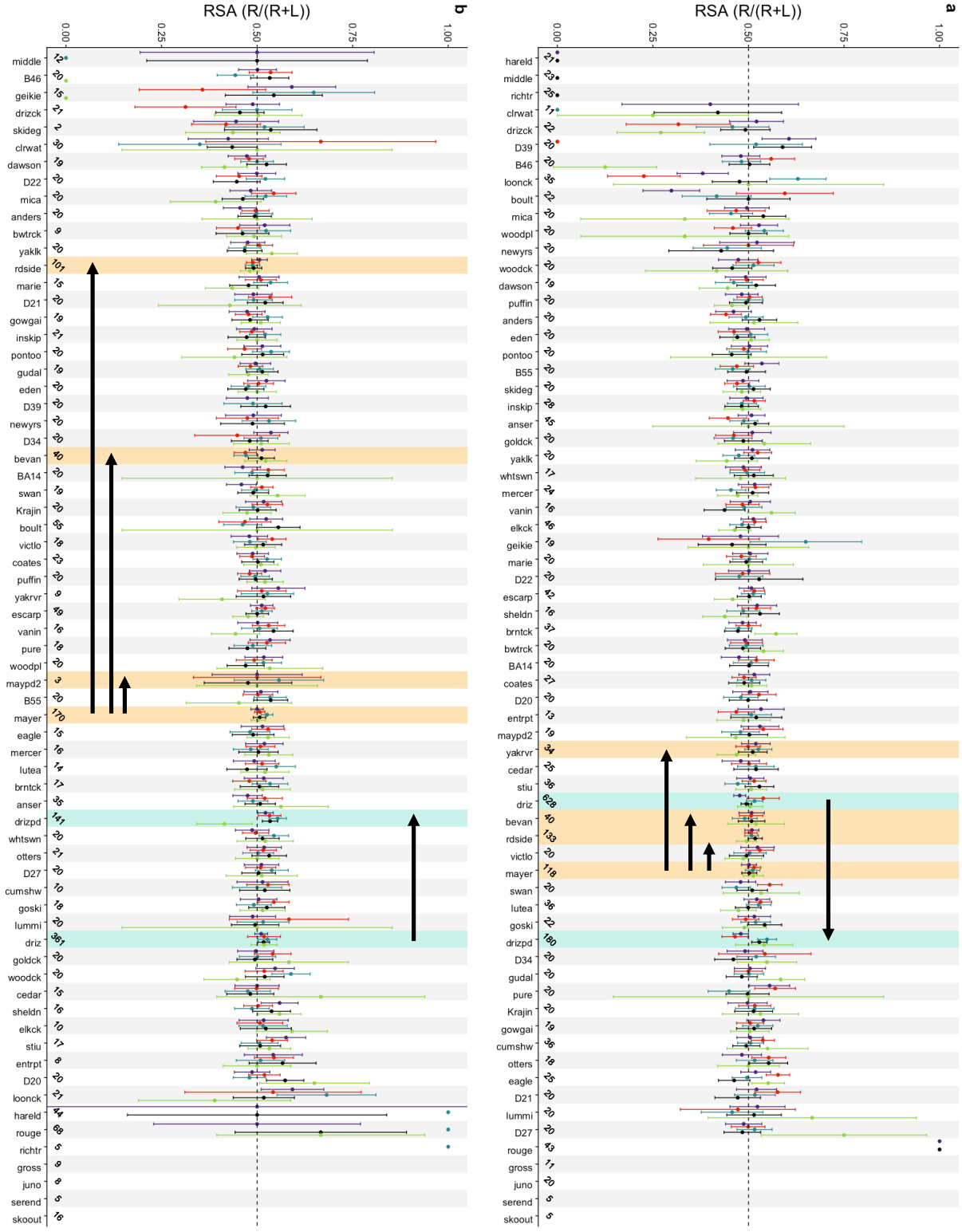
RSA (R/(R+L))
b
0.00
0.25
0.50
0.75
1.00
middle
B46
geikie
drizck
skideg
clrwat
dawson
D22
mica
anders
bwtrck
yaklk
rdside
marie
D21
gowgai
inskip
pontoo
gudal
eden
D39
newyrs
D34
bevan
BA14
swan
Krajin
boult
victlo
coates
puffin
yakrvr
escarp
vanin
pure
woodpl
maypd2
B55
mayer
eagle
mercer
lutea
brntck
anser
drizpd
whtswn
otters
D27
cumshw
goski
lummi
driz
goldck
woodck
cedar
sheldn
elkck
stiu
entrpt
D20
loonck
hareld
rouge
richtr
gross
juno
serend
skoout
RSA (R/(R+L))
a
0.00
0.25
0.50
0.75
1.00
hareld
middle
richtr
clrwat
drizck
D39
B46
loonck
boult
mica
woodpl
newyrs
woodck
dawson
puffin
anders
eden
pontoo
B55
skideg
inskip
anser
goldck
yaklk
whtswn
mercer
vanin
elkck
geikie
marie
D22
escarp
sheldn
brntck
bwtrck
BA14
coates
D20
entrpt
maypd2
yakrvr
cedar
stiu
driz
bevan
rdside
victlo
mayer
swan
lutea
goski
drizpd
D34
gudal
pure
Krajin
gowgai
cumshw
otters
eagle
D21
lummi
D27
rouge
gross
juno
serend
skoout

Figure 17. Interpopulation variation of relative signed asymmetry (RSA) on the buttressing plates (in order: four = purple; five = red; six = blue; seven = black; eight = green), among (*a*) female and (*b*) male threespine stickleback from 64 populations across coastal British Columbia. Each point is a population average for a given plate position, and error bars denote binomial 95% CIs for the mean estimate. Populations are ordered by increasing percentage of neuromast presence. The number of fish of a given sex scored for each population is displayed at the bottom. Highlighted populations are source populations and their transplants, with arrows indicating the change in population rank from source to transplant populations.

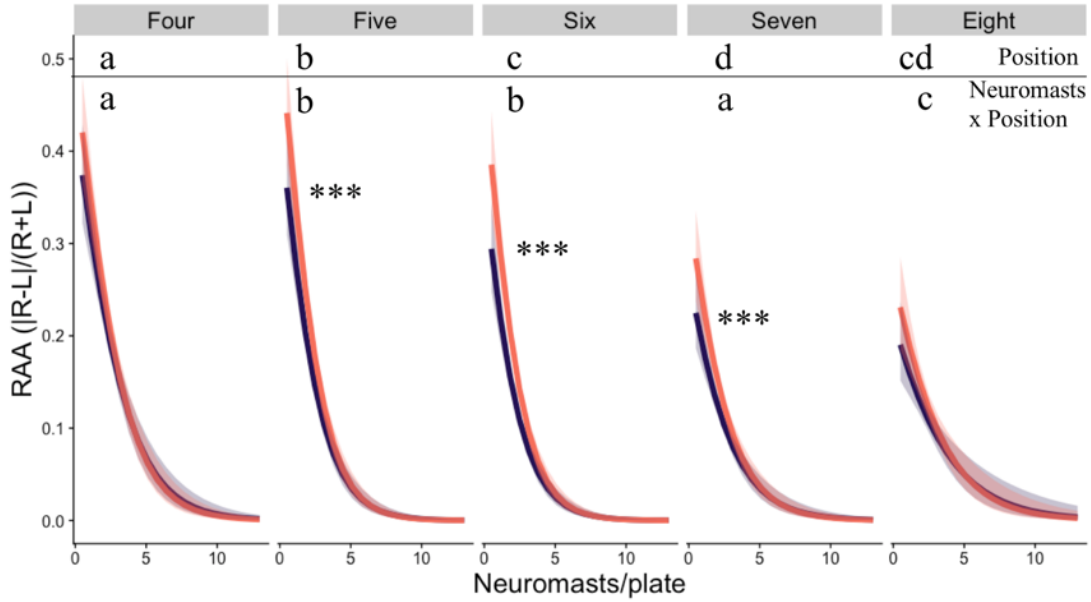

Figure 18. Changes in relative absolute asymmetry (RAA) in females (purple) and males (pink), among buttressing plate positions and with neuromasts per plate (NPP). Lines are estimated marginal means, and shaded regions are 95% CIs. Letters at the top denote differences in pairwise comparisons of mean RAA among plate positions (above the line) and between the effect of NPP on RAA among plate positions (below the line). Stars indicate significant sexual dimorphism (* < 0.05; ** < 0.01; *** < 0.001).

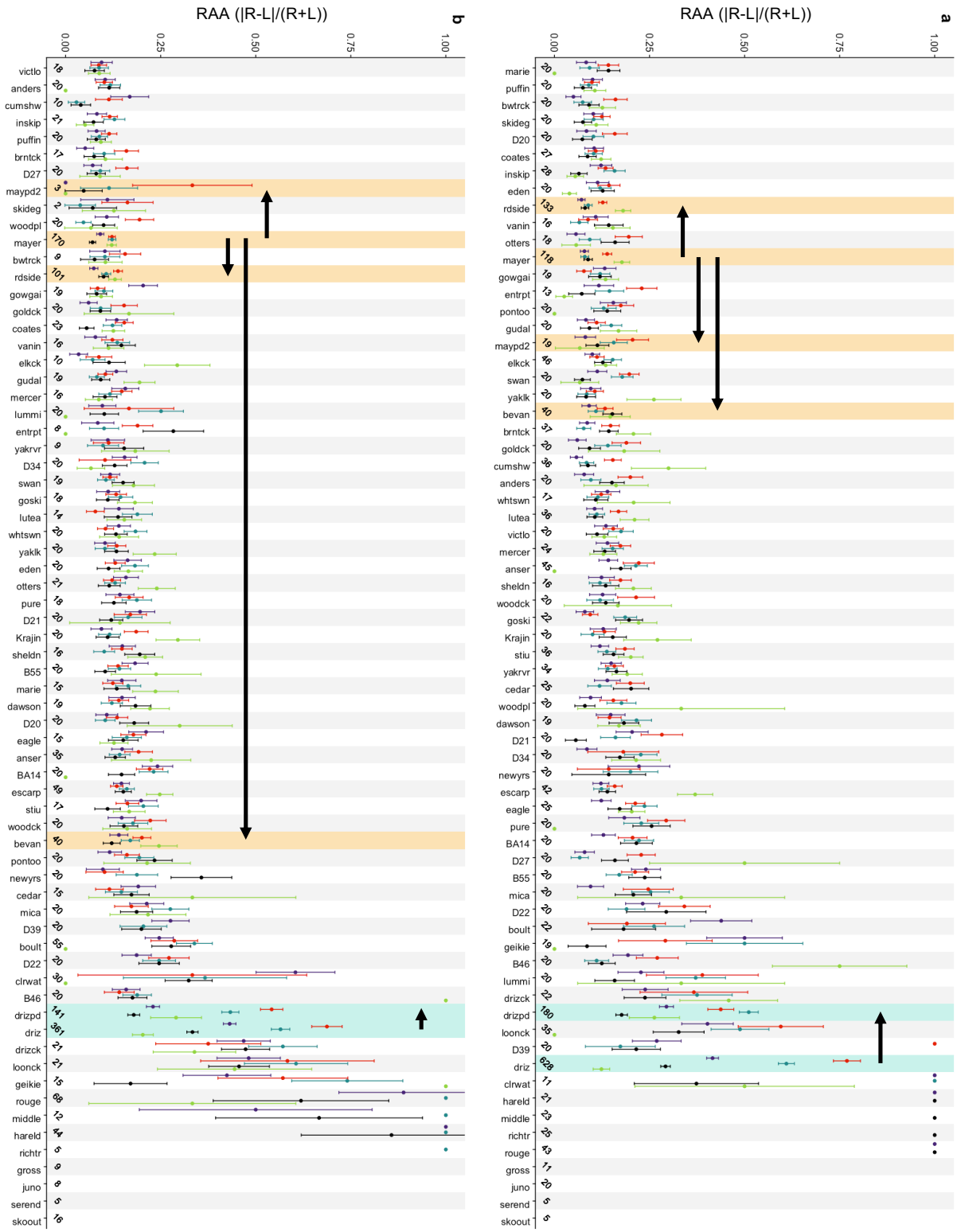
RAA (|R-L|/(R+L))
a
0.00
0.25
0.50
0.75
1.00
marie 20
puffin 20
bwtrck 20
skideg 20
D20 20
coates 21
inskip 28
eden 20
rdside 133
vanin 16
otters 18
mayer 118
gowgai 19
entrpt 13
pontoo 20
gudal 20
maypd2 19
elkck 46
swan 20
yaklk 20
bevan 40
brntck 37
goldck 20
cumshw 38
anders 20
whtswn 17
lutea 36
victlo 20
mercer 24
anser 45
sheldn 16
woodck 20
goski 22
Krajin 20
stiu 36
yakrvr 34
cedar 25
woodpl 20
dawson 19
D21 20
D34 20
newyrs 20
escarp 42
eagle 26
pure 20
BA14 20
D27 20
B55 20
mica 20
D22 20
boult 22
geikie 19
B46 20
lummi 20
drizck 22
drizpd 180
loonck 35
D39 20
driz 628
clrwat 11
hareld 21
middle 23
richtr 25
rouge 43
gross 11
juno 20
serend 5
skoout 5
RAA (|R-L|/(R+L))
b
0.00
0.25
0.50
0.75
1.00
victlo 18
anders 20
cumshw 10
inskip 27
puffin 20
brntck 11
D27 20
maypd2 3
skideg 2
woodpl 20
mayer 170
bwtrck 9
rdside 101
gowgai 19
goldck 20
coates 23
vanin 16
elkck 10
gudal 19
mercer 16
lummi 20
entrpt 8
yakrvr 9
D34 20
swan 19
goski 18
lutea 14
whtswn 20
yaklk 20
eden 20
otters 21
pure 18
D21 20
Krajin 20
sheldn 16
B55 20
marie 15
dawson 19
D20 20
eagle 15
anser 35
BA14 20
escarp 49
stiu 17
woodck 20
bevan 40
pontoo 20
newyrs 20
cedar 15
mica 20
D39 20
boult 55
D22 20
clrwat 30
B46 20
drizpd 141
driz 361
drizck 27
loonck 27
geikie 15
rouge 68
middle 12
hareld 14
richtr 5
gross 9
juno 9
serend 5
skoout 16

Figure 19. Interpopulation variation of relative absolute asymmetry (RAA) on the buttressing plates (in order: four = purple; five = red; six = blue; seven = black; eight = green), among (*a*) female and (*b*) male threespine stickleback from 64 populations across coastal British Columbia. Each point is a population average for a given plate position, and error bars denote binomial 95% CIs for the mean estimate. Populations are ordered by increasing percentage of neuromast presence. The number of fish of a given sex scored for each population is displayed at the bottom. Highlighted populations are source populations and their transplants, with arrows indicating the change in population rank from source to transplant populations.

3.4.2 Differences in relative absolute asymmetry with ecology

RAA differs among geographic regions and clarity regimes but not habitat types. Haida Gwaii stickleback have less RAA than Dewdney-Banks and Vancouver Island stickleback (Haida Gwaii emm [95% CI] = 0.118 [0.110, 0.126]; Dewdney-Banks emm [95% CI] = 0.140 [0.122, 0.160]; Vancouver Island emm [95% CI] = 0.148 [0.114, 0.190]; region: $\chi^2_2 = 8.0$, $p = 0.019$), but sexual dimorphism in RAA and the relationship between NPP and RAA do not differ between regions (all $\chi^2_2 \leq 0.9$, $p \geq 0.64$). Stained localities exhibit reduced RAA for fish with many neuromasts, but fish with few neuromasts have comparable RAA among all clarity regimes (clarity: $\chi^2_2 = 23.9$, $p < 0.001$; NPP × clarity: $\chi^2_2 = 26.2$, $p < 0.001$; Fig. 20). Sexual dimorphism in RAA differs among clarity regimes, with the greatest sexual dimorphism occurring in stained localities (sex × clarity: $\chi^2_2 = 24.8$, $p < 0.001$; Fig. 20). There is no significant difference in RAA, sexual dimorphism in RAA or the relationship between NPP and RAA among habitat types (all $\chi^2_3 \leq 3.6$, $p \geq 0.17$). RAA did not differ between either lake-stream

pair (Drizzle Lake-Drizzle Outlet: $\chi^2_1 = 0.3$, p = 0.583; Mayer Lake-Gold Creek: $\chi^2_1 = 1.32$, p = 0.251; Fig. 21).

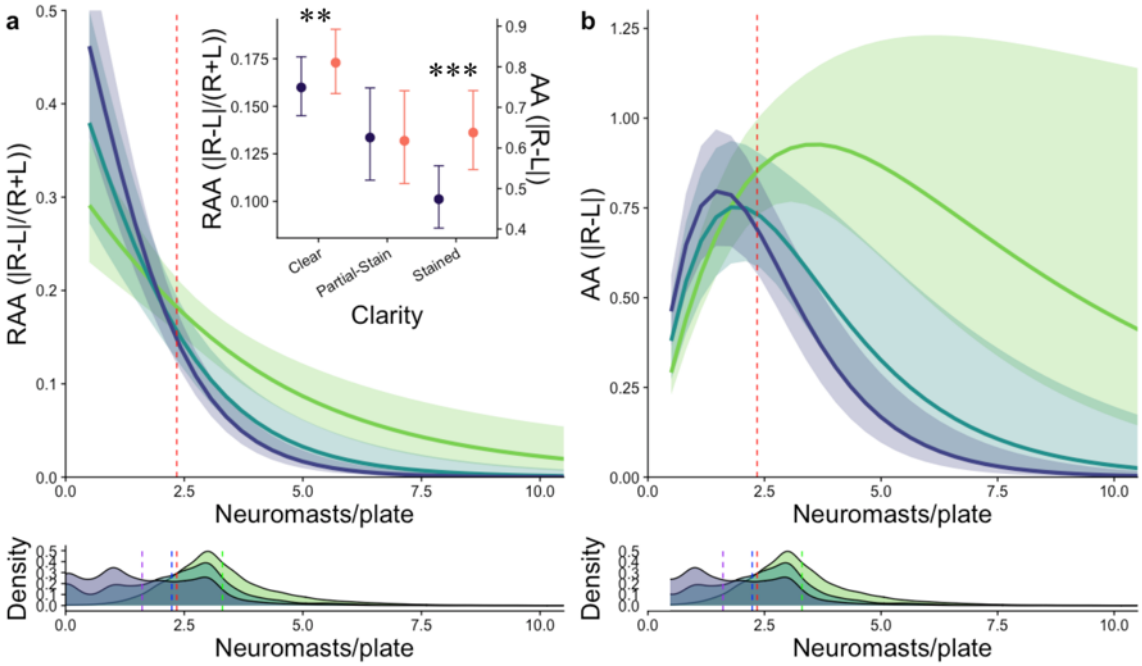

Figure 20. Differences in (*a*) relative absolute asymmetry (RAA) and (b) absolute asymmetry (AA), of buttressing plate neuromasts in stained (purple), partially stained (blue) and clear water (green) populations. Trend lines are marginal means (EMMs), and shaded regions are a 95% CI. Inset figure in (*a*) displays RAA/AA of females (purple) and males (pink) at the average neuromast count, marked by the red vertical dashed line. Points in the inset are EMMs with 95% CI error bars. Significance level of marginal mean contrast of $p < 0.001$ ***, $p < 0.01$ **. Density plots show the distribution of neuromasts per plate (NPP) among each clarity regime, with dashed vertical lines indicating the mean. EMMs are averaged over all predictors other than those being visualized.

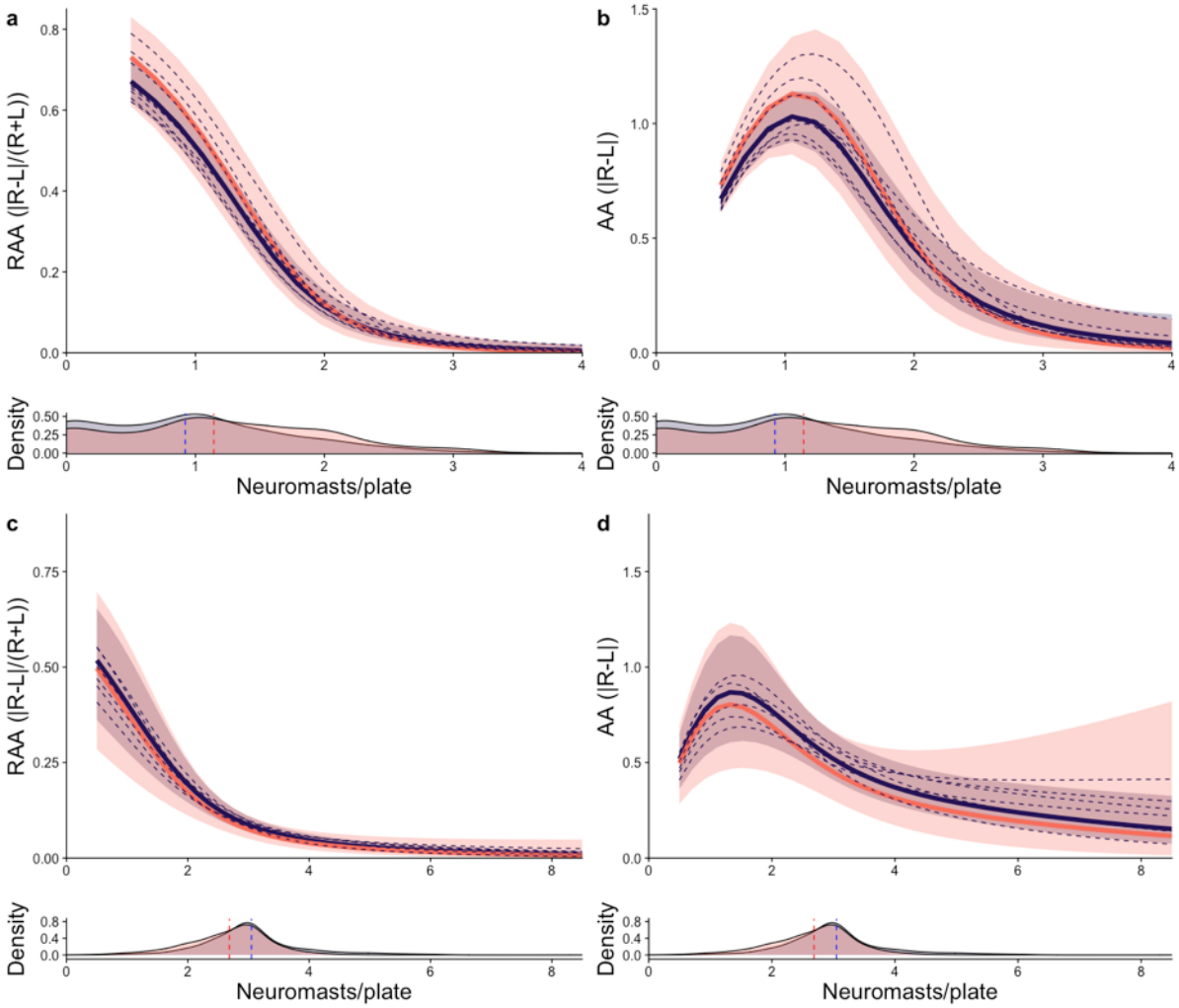

Figure 21. (*a*) Relative absolute asymmetry (RAA) and (*b*) absolute asymmetry (AA) of Drizzle Lake (purple) and Drizzle Outlet (pink). (*c*) RAA and (*d*) AA of Mayer Lake (purple) and Gold Creek (pink). Solid lines are estimated marginal means (EMMs), shaded regions are a 95% CI. Dotted lines in the main figures are model estimates for different sample dates. Density plots show the distribution of neuromasts per plate in each population, with dashed vertical lines on the density plot indicating population means. EMMs are averaged over all predictors other than those being visualized.

pH, standard length and lateral plate count are the best predictors of RAA among lake populations. The influence of NPP on RAA is greater at lower pHs (NPP × pH: $\chi^2_1 = 9.5$, $p = 0.002$; Fig. 22), RAA sexual dimorphism is greater in longer stickleback (sex × standard length: $\chi^2_1 = 11.2$, $p < 0.001$; Fig. 22a), and stickleback with more lateral plates have lower RAA (log(lateral plate count): $\chi^2_1 = 4.1$, $p = 0.042$; Fig. 22b). Population random slopes for standard length converged to zero, standard length did not affect RAA within Drizzle Lake, including NPP and sex interaction (all $\chi^2_1 \leq 1.0$, $p \geq 0.32$) and the decline in RAA with NPP is greater for longer fish in Mayer Lake (log-odds = 0.96 ± 0.41, $\chi^2_1 = 5.5$, $p = 0.019$). However, sexual dimorphism in RAA does not change with standard length within Mayer Lake ($\chi^2_1 = 0.1$, $p = 0.79$). All other ecological characteristics, *i.e.* predation regime and area, as well as lateral plate asymmetry, did not significantly affect RAA, including sex and NPP interactions (all $\chi^2_{1\text{-}2} \leq 3.8$, $p \geq 0.13$).

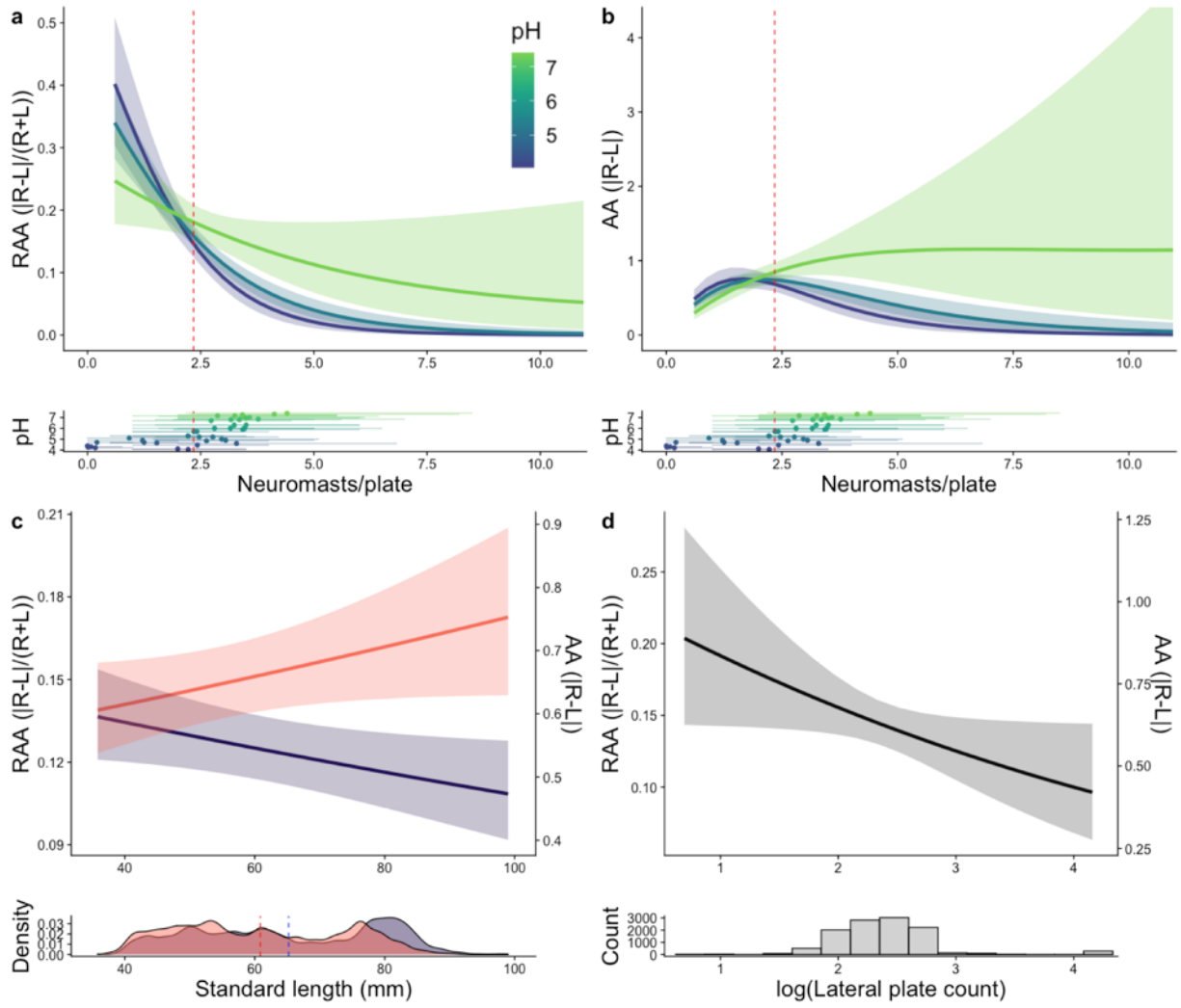

Figure 22. Relationship between (*a*) relative absolute asymmetry (RAA) and (*b*) absolute asymmetry (AA) of buttressing plate neuromasts with pH. (*c*) Changes in RAA/AA of females (purple) and males (pink) with standard length. (*d*) Reduction in RAA/AA with log(lateral plate count). Trend lines are estimated marginal means (EMMs). (*a,b*) Populations with the minimum, maximum and median pH are shown to indicate the range of variation observed. (*c,d*) Trends are for fish with an average neuromast count, indicated by the vertical dotted line in *a* and *b*. Scatter plots show the distribution of population average neuromast counts with pH, error bars span between 2.5th and 97.5th quantiles for a given population. Vertical dotted lines on density plot (*c*)

indicates the mean standard length for a given sex. All EMMs are averaged over all predictors not being visualized.

3.4.3 Relative absolute asymmetry in transplant ponds

The transplant from Drizzle lake to Drizzle pond follows the expected change in RAA, but not sexual dimorphism in RAA. Following transplant from Drizzle lake to Drizzle pond, there was a significant increase in RAA but no changes to sexual dimorphism or the relationship between neuromast count and RAA (population: $\chi^2_1 = 17.5$, $p < 0.001$; sex × population: $\chi^2_1 = 2.2$, $p = 0.13$; NPP × population: $\chi^2_1 = 0.3$, $p = 0.58$; Fig. 23). There was no significant intergenerational change in RAA in Drizzle Pond ($\chi^2_1 = 0.49$, $p = 0.48$).

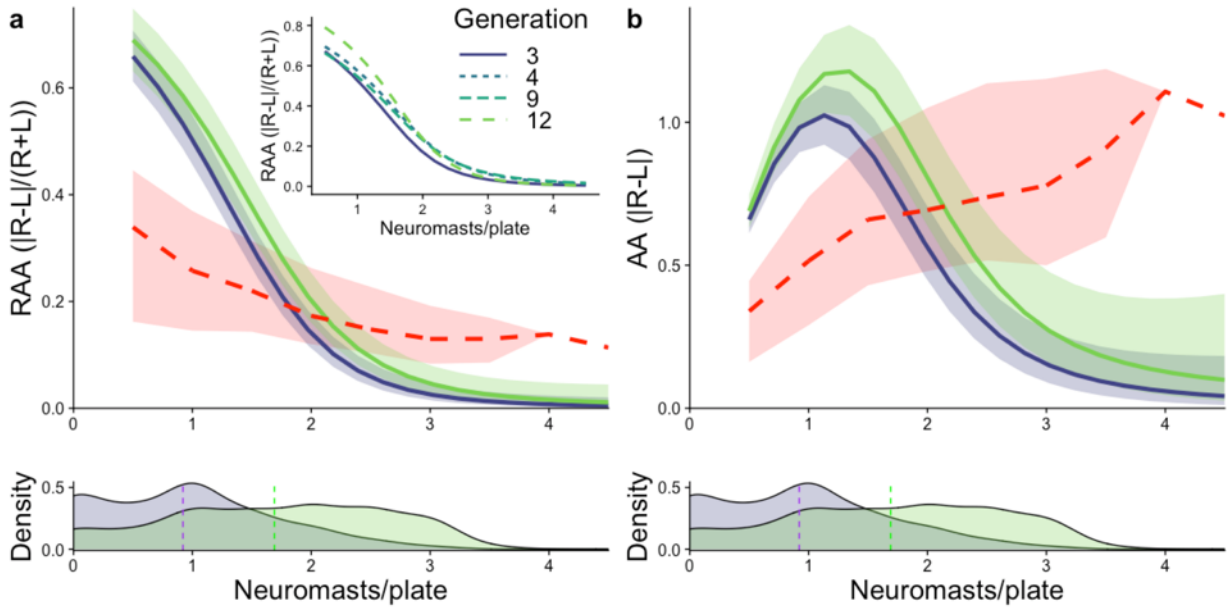

Figure 23. Changes in (*a*) relative absolute asymmetry (RAA) and (*b*) absolute asymmetry (AA) following transplant from Drizzle lake (purple) to Drizzle Pond (green). Trend lines estimated marginal means (EMMs) and shaded regions are their 95% CI. The dotted red line is the RAA/AA for a Drizzle Pond predicted by the reduced equation 4, given its environmental and

morphological characteristics. Stochasticity in expected RAA is due to differences in average standard length for a given neuromast count within pond samples, and the red shaded region spans the 2.5th and 97.5th quantiles of the model estimates. Inset figures indicate intergeneration change within pond Drizzle Pond. Density plots show the distribution of neuromasts per plate in both populations, with vertical dashed lines indicating the population means. All EMMs are averaged over all predictors not being visualized.

RAA changed in two of three populations transplanted from Mayer Lake. RAA in fish with few neuromasts decreased from Mayer Lake to Roadside Pond, but fish with many neuromasts are similar between the two populations (NPP × population: $\chi^2_1 = 9.5$, $p = 0.002$; population: $\chi^2_1 = 0.1$, $p = 0.82$; Fig. 24a,b), and there was no change in sexual dimorphism in RAA (sex × population: $\chi^2_1 = 1.1$, $p = 0.29$;). This trend also grows stronger in subsequent generations of Roadside Pond (NPP × generation: $\chi^2_1 = 26.6$, $p < 0.001$; Fig. 24a). RAA increased from Mayer Lake to Bevan's Pond, but the influence of sex and NPP did not differ (population: $\chi^2_1 = 4.7$, $p = 0.030$; neuromast count × population: $\chi^2_1 = 1.3$, $p = 0.25$; sex × population: $\chi^2_1 = 1.8$, $p = 0.17$; Fig. 24c,d). RAA increased in subsequent generations of Bevan's pond, further diverging from Mayer Lake (generation: $\chi^2_1 = 8.3$, $p = 0.004$; Fig. 24c). RAA did not change between Mayer Lake and Mayer Pond Two, including sex and NPP interactions (all $\chi^2_{1\text{-}2} \leq 2.8$, $p \geq 0.25$; Fig. 24e,f).

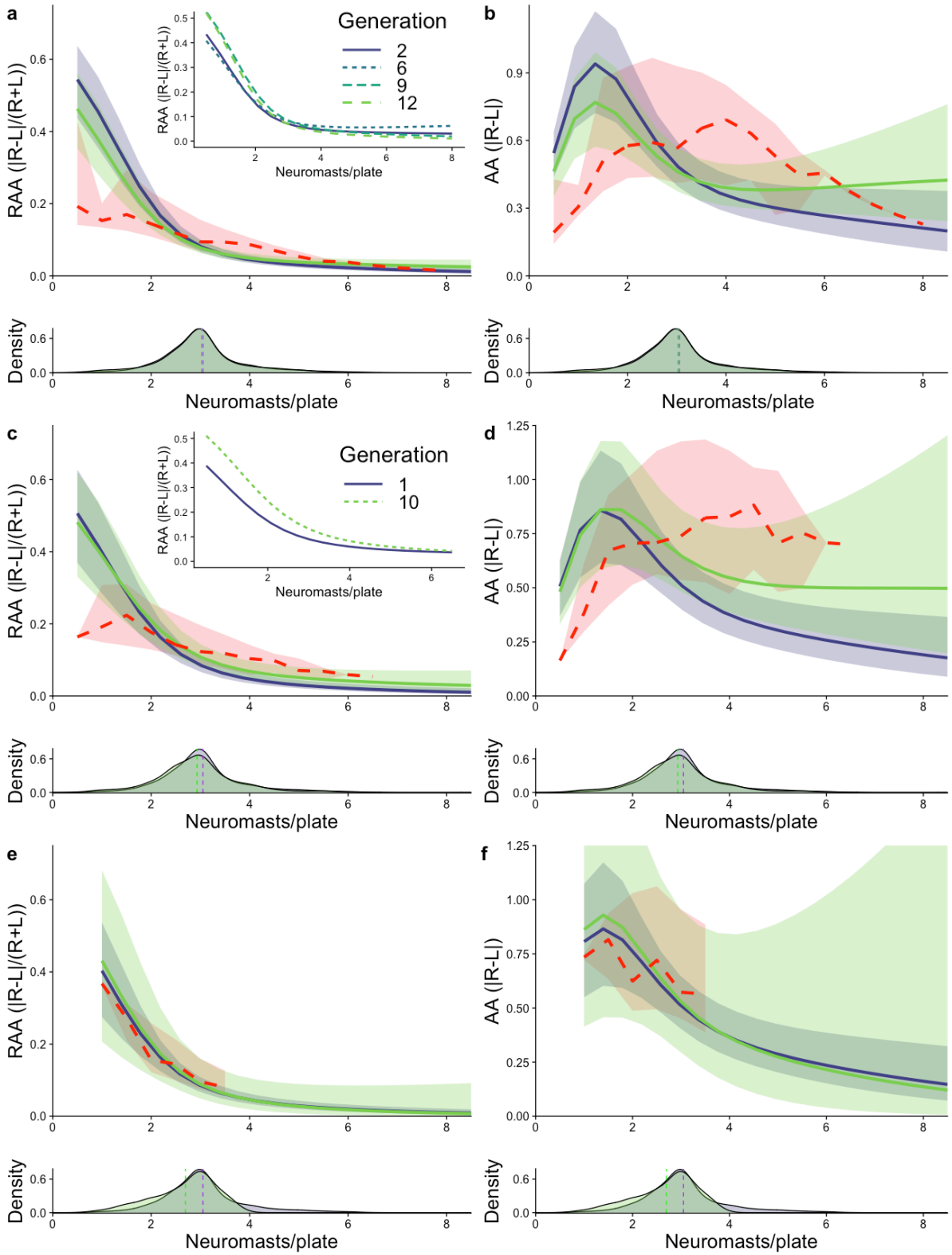
a
b
c
d
e
f
RAA (|R-L|/(R+L))
AA (|R-L|)
Density
Neuromasts/plate
Generation
2
6
9
12
1
10

Figure 24. Changes in (*a,c,e*) relative absolute asymmetry (RAA) and (*b,d,f*) absolute asymmetry (AA) following transplant from Mayer Lake (purple) to (*a,b*) Roadside Pond (green), (*c,d*) Bevan's Pond (green) and (*e,f*) Mayer Pond Two (green). Trend lines are estimated marginal means (EMMs), and shaded regions are their 95% CI. Dotted red lines are the expected RAA/AA for a pond population as predicted by the reduced equation 4, given its environmental and morphological characteristics. Stochasticity in expected RAA is due to differences in average standard length for a given neuromast count within pond samples, and the red shaded region spans the 2.5^{th} and 97.5^{th} quantiles of the model estimates. Inset figures indicate intergeneration change within pond populations, and density plots show the distribution of neuromasts per plate within the source and transplant populations, with vertical dashed lines indicating the population means. All EMMs are averaged over all predictors not being visualized.

3.5 Discussion

The buttressing plate neuromasts of coastal British Columbia threespine stickleback exhibit a wide degree of individual and population-level signed (SA) and absolute (AA) asymmetry. Frequencies of asymmetrical fish averaged 93% among the 64 populations, and while there is a marginal excess of right-biased populations, there was no evidence for any significant departures from a mean of zero in any population. AA increases with the number of neuromasts per lateral plate (NPP), at least for buttressing plates. Relative absolute asymmetry (RAA) is greater in stained water localities, except for those with few NPP. Furthermore, sexual dimorphism in RAA is elevated in these stained water localities, associated with an increase in body length. Despite the lateral line's role in rheotaxis and other behaviours expected to differ among major ecological regimes, I found no statistical differences in RAA between allopatric

lakes and streams, between parapatric lake-stream pairs, or between oceanic and freshwater fish. However, I did observe both increases and decreases in RAA in populations transplanted from stained lakes to unstained ponds over less than twelve generations, suggesting that changes in lateral line asymmetry observed across coastal British Columbia could have developed quickly following initial post-glacial colonization of the lakes.

I found that the lateral line of threespine stickleback is on average symmetrical, suggesting that stickleback have not specialized in the use of one side of the lateral line, even in habitats with limited light availability. In contrast, Mexican tetras that have adapted to survive in the absence of light (blind Mexican cavefish), exhibit a left bias in superficial neuromast counts and mechanosensory behaviour not seen in their surface-dwelling counterparts (Burt de Perera and Braithwaite 2005; Gross et al. 2016; Fernandes et al. 2018). The differences between the species may be due to the difference in response stimuli. The lateral line of Mexican cavefish is specialized for prey localization and navigation (Holzman et al. 2014; Yoshizawa et al. 2015), whereas threespine stickleback use their lateral line for rheotaxis (Jiang et al. 2017), and schooling (Greenwood et al. 2016). I have also examined trunk neuromasts which are associated with escape response (Faucher et al. 2006), rather than facial neuromasts that are used for feeding (Bleckmann et al. 1989) and which exhibit directional asymmetry in Mexican cavefish (Gross et al. 2016). Given that prey emit oscillations from a single point, whereas abiotic flow and schools provide a diffuse stimulus, lateralization may be less advantageous for stickleback. Furthermore, predatory fish can control which side they approach prey more readily than fish responding to abiotic flow or a school of conspecifics. Lastly, cavefish live in an aphotic environment, whereas stained water stickleback live in a low-light environment. While sub-

modalities of the lateral line may exhibit SA under the right circumstances, I do not see evidence of this in the anterior trunk neuromasts of threespine stickleback.

RAA is highly variable in threespine stickleback, reflecting a diversity of ecologies and life histories and a functional trade-off between visual and mechanosensation modalities. As far as I am aware, Trokovic et al. (2012) have conducted the only other study of habitat-dependent changes in lateral line asymmetry, finding that ninespine stickleback in ponds have much greater asymmetry than oceanic fish, which they interpreted as relaxed selection. My data suggest an alternative mechanism; that the changes in RAA observed by Trokovic et al. (2012) may be due to changes in neuromast count rather than developmental instability. I found similar RAA in oceanic and clear freshwater populations, and a loss of buttressing plate neuromasts in low-plated compared to fully-plated threespine stickleback (Chapter 2). Trokovic et al. (2011) found that the neuromast stitches that differed the most between oceanic and pond populations, ATr-c, CP and CP-c (roughly corresponding to the anterior main trunk line (Ma) and caudal peduncle (CP) lines of threespine stickleback), lost neuromasts in pond populations. These differences in neuromast count between oceanic and freshwater populations and the similarity in RAA between freshwater and oceanic fish with similar numbers of NPP suggests that differences in neuromast counts between oceanic and pond populations strongly influences RAA.

I found that water clarity is more important in determining RAA than predation by puncturing predators, with stained water populations having reduced RAA, except for fish with very few NPP. As tannin concentration causes low pH in tandem with reducing light transmission, the analysis cannot differentiate their effect on RAA. Given the inhibition of lateral line development for larval fish reared in low pH and that pH is likely a major factor in limiting the number of buttressing plate neuromasts, I would expect stained localities to have greater

RAA if pH was inducing developmental instability (Lin et al. 2019; Chapter 2). However, light limitation in these same environments would decrease RAA due to a shift from visual to mechanosensation mediated behaviour (Liao 2006; Schwalbe et al. 2012; York and Bartol 2014), which may restrict the development of asymmetry in the lateral line. As stickleback in stained water habitats with many neuromasts had very little RAA, spectral regime likely has a stronger influence on RAA than pH for fish with more than ~2 NPP, whereas pH has a greater influence on RAA for populations with extremely few NPP.

As with changes in the number of NPP, Mayer Lake and Swan lake provide two counterfactual examples of the influence of spectral landscape on RAA. Both populations have more than three NPP; however, Mayer Lake has some of the lowest RAA observed, whereas Swan Lake has the greatest RAA. The difference between these two populations suggests that a reliance on mechanosensation due to limited light availability and a shorter reaction distance does not necessarily reduce RAA without the presence of other selective pressures. If the development of neuromasts is physiologically 'cheaper' in Swan Lake than Mayer Lake, the conservations of symmetry in the lateral line may not provide as much of a fitness advantage for stickleback in Swan Lake versus those in Mayer Lake. The ponds studied by Trokovic et al. (2011; 2012) are also likely eutrophic like Swan Lake and had elevated RAA, suggesting similar ecological factors may be causing RAA to increase in these localities.

Like allopatric lakes and streams across Haida Gwaii, RAA is conserved in parapatric lake-stream pairs, suggesting that flow regime does not affect lateral line asymmetry. The paired lake and stream populations are genetically distinct, reproductively isolated and have undergone changes in phenotype, including lateral plate and defense traits (Deagle et al. 2012) and there appear to be no consistent changes in neuromast count between lakes and streams (Wark and

Peichel 2010; Jiang et al. 2017; Kelley et al. 2017; Chapter 2). The similarity in neuromast count between lakes and streams is particularly interesting, given the lateral line's role in mediating rheotaxis behaviour in threespine stickleback and other species of fish (Montgomery et al. 1997; Suli et al. 2012; Jiang et al. 2017). Lakes and streams may differ in the morphology of neuromasts themselves or how the central nervous system processes mechanosensory information, but given similar NPP and RAA between lake-stream pairs, I infer that rheotaxis is not associated with differences in neuromast count or neuromast count asymmetry.

In the transplant experiments from the stained Drizzle Lake and Mayer Lake to the stained Mayer Pond Two and unstained Drizzle Pond, Roadside Pond and Bevan's Pond, the observed changes in RAA in the transplants were relatively consistent with the expected effect of changes in clarity. All three transplants to unstained habitats underwent an increase in RAA for fish with more than three NPP as expected; however, only Roadside Pond fish showed a reduction in RAA for fish with fewer than three neuromasts. A possible explanation for this difference of outcome may be an increase in nocturnal foraging behaviour and benthic prey consumption by Roadside Pond fish (Leaver 2010), but Drizzle Pond and Bevan's pond stickleback have not been tested for behavioural changes. Mayer Pond Two stickleback also had similar RAA to Mayer Lake stickleback as expected due to their similar photo regimes. The Drizzle Pond transplant suggests phenotypic plasticity in RAA is possible, given the abrupt increase in RAA seen in the first generation and the similarity among subsequent generations. However, the degree of change in RAA is much smaller than changes in NPP (Chapter 2) and as expected by changes in clarity regime and standard length, suggesting that the population has not yet reached an equilibrium within twelve generations. If the underlying mechanism of phenotypic plasticity is epigenetic, this would suggest that epigenetic modification can also

influences the degree of asymmetry a trait expresses. If we assume that Drizzle Pond has undergone epigenetic change, the increased expression of genes which promote neuromast development has also increased the amount of asymmetry in the expression of these genes between the two sides of the body. In contrast, the Roadside Pond and Bevan's Pond transplants suggest a genetic mechanism undergoing small directional changes in subsequent generations. Drizzle Lake is relatively deep with a small littoral zone mostly lacking vegetation (Reimchen 1990), whereas Mayer Lake is shallow with a large and vegetated littoral zone (Moodie 1972); thus, the spatial heterogeneity of Mayer Lake is more similar to the transplant ponds and may be a cause for the slower change observed in its transplant populations. In all transplants, stickleback with fewer NPP tended to be more variable in RAA, which may be why Drizzle Lake fish exhibited greater changes in RAA than Mayer Lake fish following transplantation to a pond. Lastly, the patterns of change in RAA among ponds reflect their changes in the number of NPP, suggesting the same underlying mechanism controlling both aspects of morphology.

Independence of neuromast asymmetry and lateral plate count and asymmetry is surprising given their developmental link and overlapping ecological functions. Feeding behaviour and predator avoidance are associated with lateral line morphology (Mesa and Warren 1997; Coombs and Patton 2009; Junges et al. 2010; Schwalbe et al. 2012) and lateral plate asymmetry in threespine stickleback (Moodie and Reimchen 1976; Reimchen and Nosil 2001b), suggesting that these traits would be associated. Furthermore, the common genetic loci and closely linked developmental ontogeny of lateral plates and neuromasts (Wada et al. 2010; Wark et al. 2012; Mills et al. 2014) also suggests that asymmetry in these traits would be related. However, given the contention around the genetic basis of asymmetry in many species (Markow and Clarke 1997; Møller and Thornhill 1997; Houle 1997; Pomiankowski 1997), it is not wholly

unexpected that neuromast count asymmetry is independent of lateral plate asymmetry. While asymmetry in neuromast count and lateral plate count are common and despite their developmental and functional association, they seemingly interact with life history independently.

Given the importance of the lateral line for mechanosensation, it would be reasonable to predict that population average RAA would decrease over ontogeny as lower fitness asymmetric individuals are lost at a higher rate (Beasley et al. 2013). However, there was no decline in RAA over ontogeny within populations and older stickleback have increased lateral plate asymmetry in some populations (Reimchen and Bergstrom 2009), suggesting that asymmetry in some traits may not reduce fitness (Lens et al. 2002; Lajus et al. 2019).

Sexual dimorphism in threespine stickleback is dependent on a variety of ecological and life history traits (Reimchen et al. 2016). Sexual dimorphism in RAA is greater in stickleback populations that exhibit increased adult body length, suggesting that RAA changes with certain aspects of life history. Increased sexual dimorphism in RAA with larger body size may be due to a bigger difference in reproductive strategy, exposure to predation or trophic niche between the sexes in long stickleback populations (Moodie 1972; Oravec and Reimchen 2013; Reimchen et al. 2016). Males from giant stickleback populations also feed on more benthic prey, whereas females are predominantly limnetic (Reimchen and Nosil 2004). As the lateral line is used for detecting zooplankton (Montgomery 1989), this niche partitioning may be conserving symmetry in females and driving increased asymmetry in males. The relationship between length and RAA suggests that asymmetry in the lateral line plays a more complex role in life history than indicating reduced fitness.

Given the high fidelity required of the lateral line to detect subtle mechanosensory stimuli in the environment, one would expect that a symmetrical lateral line would be common in most fishes. However, I found that for threespine stickleback, asymmetry in the lateral line is widespread and highly variable. The prevalence of asymmetry in the lateral line suggests that differences in stimuli sensitivity between the two sides may impart additional sensory information in different ecological contexts. Asymmetry in neuromast counts may allow fish with very few neuromasts to gain more complete coverage of their body surface and glean more sensory information with fewer receptors. Sensory structure asymmetry may also be advantageous if it plays a role in the development of behavioural laterality, allowing individuals to respond more rapidly to certain environmental stimuli such as the vibrations produced by prey (Fernandes et al. 2018) or attacks by predators (Cantalupo et al. 1995). While I found no evidence that there is a directional bias at the population level, individuals may still exhibit lateralized behavioural syndromes associated with greater asymmetry in neuromast count. I also found that lateral line asymmetry is highly responsive to ecological change, in addition to changes in neuromast count. These findings show that asymmetry in the lateral line system can change rapidly in response to colonization of an ecologically divergent habitat, warranting future investigation into the functional ecology of lateral line asymmetry.

Chapter 4: Testing the role of neuromast count asymmetry in mechanosensory laterality

4.1 Abstract

Behavioural asymmetry, typically referred to as laterality, is widespread among bilaterians and is often associated with asymmetry in the structure of the brain. However, the influence of asymmetry in sensory receptors on laterality has undergone little investigation. This chapter aims to investigate the influence of neuromast count asymmetry on laterality in three mechanosensation dependent behaviours of threespine stickleback. The behaviour of 40 stickleback to simulated predator mechanosensation, simulated prey mechanosensation and abiotic flow were recorded and compared to asymmetry in their lateral line system. Furthermore, I tested each stickleback four times to determine the repeatability of individual lateralization and consistency in laterality among behavioural contexts. Stickleback 'protected' their right side against the arena wall 56.7% of the time ($p < 0.001$), responded 1.3 times as often to predatory stimuli from the right compared to predatory stimuli from the left ($p = 0.068$), 'hugged' the right wall 56% of the time in the dark ($p = 0.085$) and sat in a faster flow regime when making right turns ($p = 0.015$). A right bias in positioning was associated with more neuromasts in the light ($p = 0.007$), and fewer neuromasts in the dark ($p = 0.025$) and the only behaviour associated with directional asymmetry in the lateral line was the tendency of stickleback to escape towards their side with more neuromasts ($p = 0.020$). Lastly, laterality was not consistent within individuals or among behaviours.

4.2 Introduction

Fishes display behavioural laterality in a wide variety of settings. Lateralized responses have been observed in social interactions (Bisazza et al. 2000a; Reddon and Balshine 2010;

Roux et al. 2016), predator observation (De Santi et al. 2001), predator evasion (Cantalupo et al. 1995; Lippolis et al. 2009), feeding (Takeuchi and Hori 2008) and habitat navigation (Westin 1998). The dominant side often differs greatly between settings, being modulated by the context in which the behaviour occurs. Laterality of predator observation changes with the presence of conspecific social interaction (Bisazza et al. 1999) and previous exposure to predators (De Santi et al. 2000). Laterality of social interaction is influenced by sex and sexual motivation (Bisazza et al. 1998a; Kaarthigeyan and Dharmaretnam 2005). Laterality without social or predatory context is variable with temperature (Domenici et al. 2014; Lai et al. 2015), familiarity with objects (Burt de Perera and Braithwaite 2005) and with characteristics of the 'habitat,' *e.g.* the shape of a T-maze (Bisazza et al. 1997a). Laterality also shows signatures of changes on the evolutionary time scale, differing among species across behavioural contexts (Bisazza et al. 1998a, 2000a; Sovrano et al. 1999, 2001) and being heritable (Bisazza et al. 2000b, 2005; Dadda et al. 2007). This complex suite of lateralized behaviours suggests an interaction between potentially deeply rooted side biases for specific behaviours (Vallortigara et al. 1999) and context-specific lateralization (Demaree et al. 2005; Rogers 2010; Gainotti 2019).

Many studies have investigated visual laterality (Bisazza et al. 1999; Güntürkün et al. 2000; Agrillo et al. 2009; Farmer et al. 2010; Roux et al. 2016; Dadda and Bisazza 2016; Goursot et al. 2019); however, other sensory modalities such as olfaction (Westin 1998) and mechanosensation (Burt de Perera and Braithwaite 2005) have received little attention. As these other sensory modalities play an important role in the life history of fishes, it is essential that their degree of lateralization is understood, to better understand the full mosaic of the origins of behavioural laterality.

Laterality is associated with morphological asymmetry, in the case of mouth sidedness biasing the laterality of attack behaviour (Takeuchi and Hori 2008) and neuromast count influencing prey localization (Fernandes et al. 2018). However, the traits examined in these studies exhibit strong anti-symmetry or population-level directional asymmetry. Thus, more subtle differences between the left and right sides in sensory structures, which are much more common across taxa, have not yet been investigated with respect to behavioural laterality.

This chapter aims to determine if asymmetry in the lateral line influences laterality in the behaviour of threespine stickleback. Given that laterality is highly variable among contexts, I assessed the interaction between morphological and behavioural asymmetry in three different ecologically relevant behaviours; predator evasion, rheotaxis and prey localization. These behaviours are particularly relevant as they are all influenced by lateral line morphology or neuromast count (Yoshizawa et al. 2010; Olszewski et al. 2012; Jiang et al. 2017). Furthermore, given the recent evidence of individual laterality not being repeatable in subsequent trials (Leliveld 2019; Roche et al. 2020), I tested the repeatability of individual laterality in each of these behaviours and the potential association of laterality among behaviours.

4.3 Methods

4.3.1 Stickleback collection

Seventy-seven stickleback were captured at Eagles Lake (48.5088, -123.4633; Fig. 25) using minnow traps baited with aged cheddar cheese and transported to the University of Victoria Aquatics Facility in aerated 19 L buckets. The stickleback were housed in a 189 L tank at 15 °C, with artificial habitat enrichment, a 12:12 hour light-dark cycle and fed on a diet of bloodworms once daily.

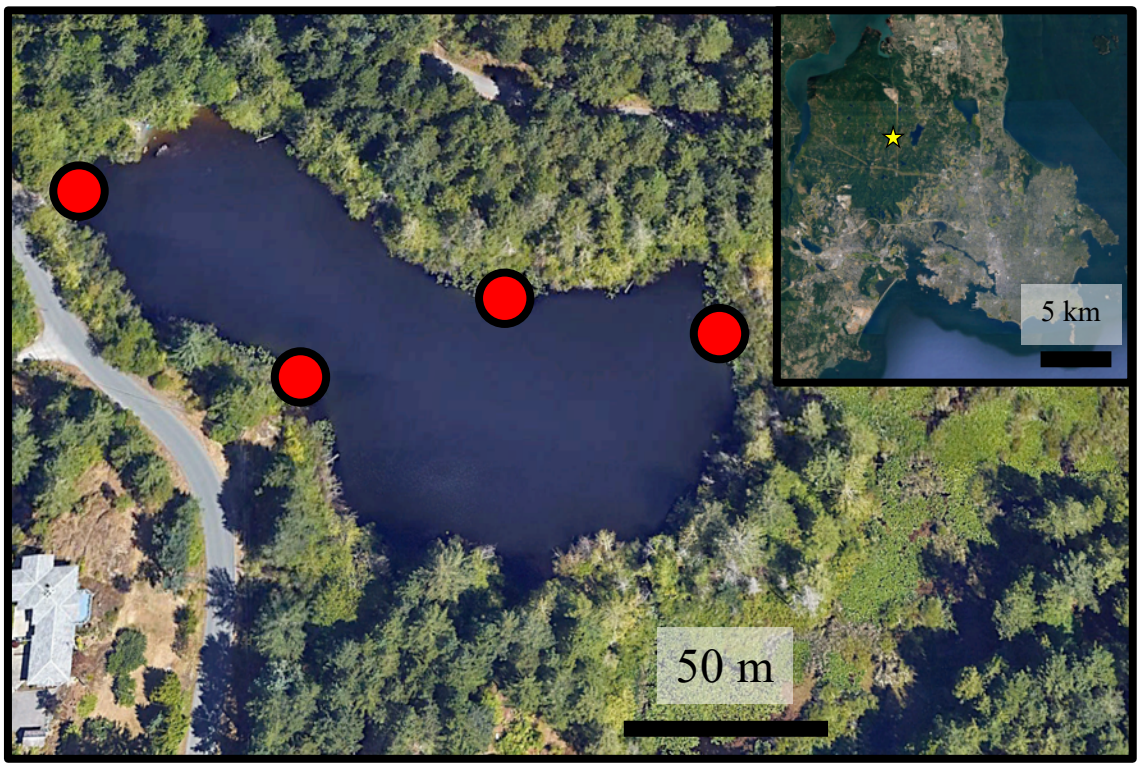

Figure 25. Eagle's Lake sampling site. Red dots indicate locations where I placed traps and successfully captured threespine stickleback. The inset figure is of the lower Saanich peninsula, with Eagle's Lake starred.

4.3.2 Vibration attraction behaviour experiment

I tested ten stickleback to determine the best frequencies for assessing vibration attraction behaviour (VAB; see Yoshizawa et al. 2010). The VAB tank consisted of a five-gallon bucket's midsection affixed to a piece of plexiglass with silicone. The tank was placed on the top of cinderblocks, separated by vibration-absorbing foam, illuminated with an ITT IR Illuminator (850 nm) and viewed by an ITT mini Monocular NIGHT-VISION SCOPE mounted onto the lens of a GoPro Hero4, taking a time-lapse at 0.667 images per second (Fig. 26). Oscillations were generated by a Speaker Craft MTR1C, connected via a Yamaha RS-V395 receiver and a Scarlet 2i2 audio interface to a MacBook Pro, generating tones with the oscillator plugin within

Ableton Live 9. Sound pressure was converted to mechanical displacement by affixing a glass rod to the speaker diaphragm dust cap, which I centered above the tank. I filled the tank with 6 cm of water from the aquatics facility throughflow system, enough that the glass rod extended 1 cm into the water. I placed a plastic lid on the tank, and turned off the room's lights for five minutes prior to testing to allow the stickleback to acclimate to the setup. The infrared light was strong enough that it shone through the plastic lid. Each stickleback was exposed to 10 Hz intervals from 20-100 Hz for three minutes in random order and three minutes of silence in between stimuli. Following the fifth trial, the water was refreshed, and stickleback were given another five minutes to re-acclimate.

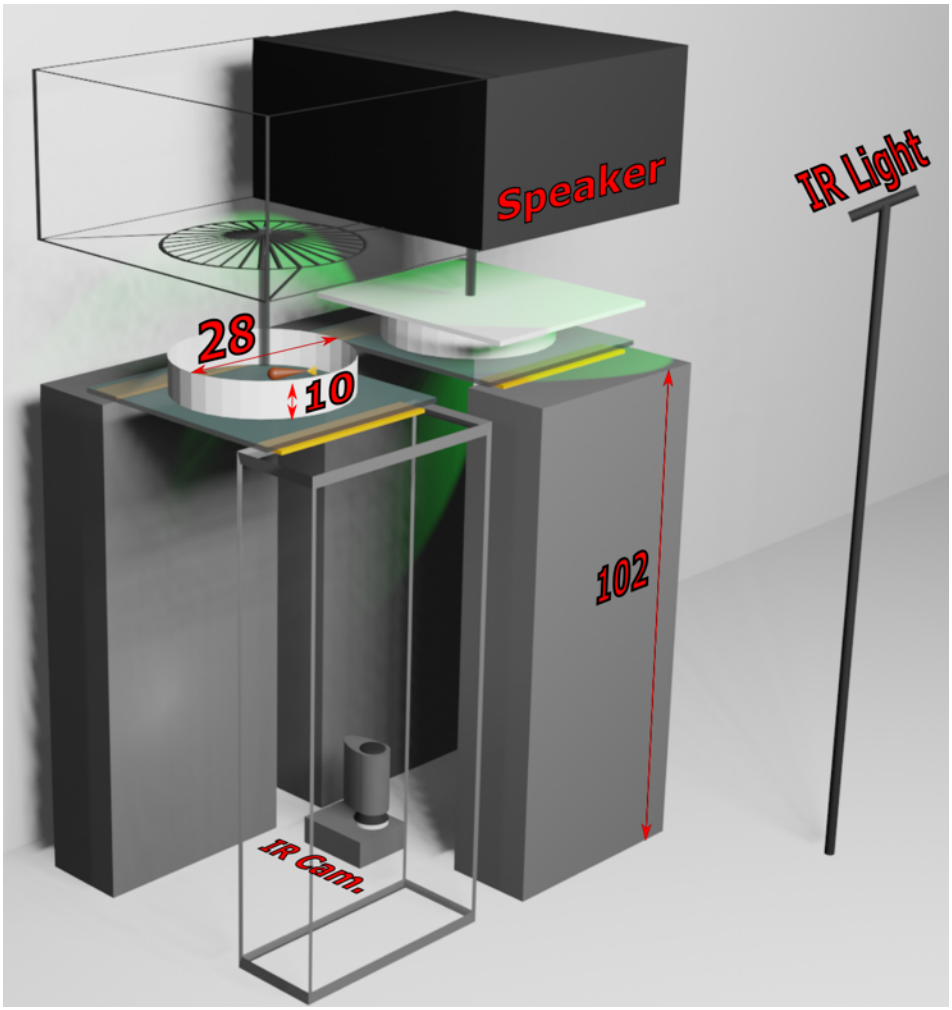

Figure 26. Schematic of vibration attraction behaviour (VAB) testing apparatus. The front support, front infrared (IR) light, half the speaker and the first tank's lid have been removed for visibility. Vibration absorbing foam is shown in yellow. All distances given are in cm.

I calibrated the amplitude and frequency of oscillations with fast Fourier transform analysis (R library *GeneCycle*; Ahdesmaki et al. 2019) of 240 fps video footage of the glass rod, verifying the rod was oscillating at the same frequency as the speaker and adjusting speaker volume so that displacement was 3 mm for all frequencies. 20 Hz and 60 Hz elicited similar numbers of approaches and more than other frequencies, so they were both used in subsequent testing.

I tested laterality of VAB using the same setup as preliminary testing; however, the apparatus was doubled up after the first four groups were tested (Fig. 26). Stickleback were acclimated to the dark for six minutes, with behaviour being recorded after the first three minutes as a control, followed by three minutes of exposure to either a 20 or 60 Hz oscillation. The same procedure was then repeated with the other frequency. I initiated video capture at the beginning of acclimation, and the room was kept dark throughout the VAB trial.

4.3.3 Rheotaxis experiment

I assessed rheotaxis behaviour in two circular tracks, with water flowing either clockwise or counterclockwise (Fig. 27). I placed two Sicce Mi-Mouse circulation pumps in a reservoir shared by both tanks, feeding into each track by a rubber hose and I cut an outlet hole out of each track 90° upstream of the flow source and covered it with a fine mesh. I mounted a GoPro Hero3+ above each track, and recorded a time-lapse at 0.667 images per second. I filled the tracks to 6 cm depth and calibrated flow to average 0.8 m/s in each track (~0.2 m/s at the outer

edge and ~0-0.04 m/s at the inner edge). Stickleback were placed in each track and acclimated to still water for five minutes, flow for five minutes, then five minutes of behavioural footage was recorded. I initiated video capture at the beginning of acclimation and I started the pumps with a switch hidden from view, as not to disturb the fishes' behaviour.

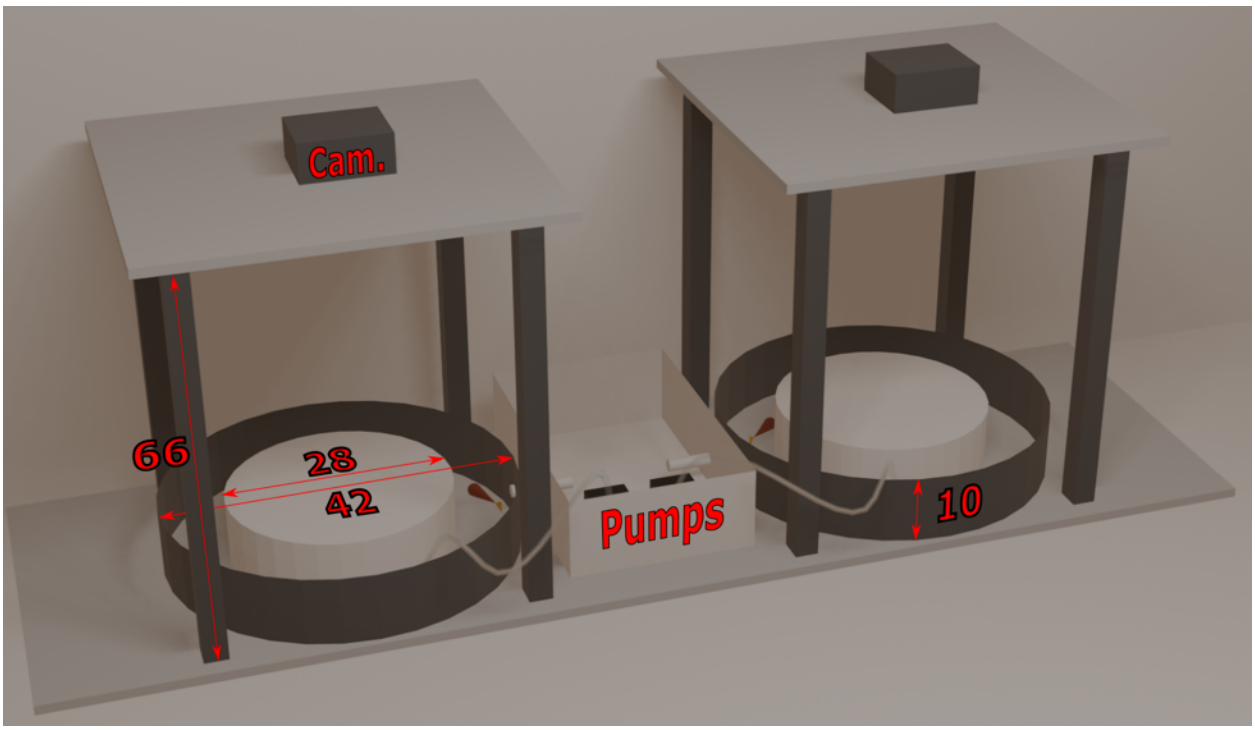

Figure 27. Schematic of rheotaxis testing apparatus. All distances given are in cm.

4.3.4 Evasion of a simulated predator attack experiment

I tested the evasion of a simulated predator attack, hereafter referred to as predator evasion, by dropping water adjacent to stickleback in a circular arena. Arenas consisted of five-gallon buckets with the base cut off, mounted to plexiglass sheets with silicon. I inserted a mesh 2 cm from the edge of the bucket to allow stimuli to be given from both sides, even if the stickleback was against the side of the tank (Fig. 28). A GoPro Hero4 and SJcam4000 were placed below the left and right tanks, respectively (from the observer's perspective), recording

1280x720 footage at 60 fps. I mounted a white sheet above the tanks to provide a consistent background, and after the first four groups, I mounted a mirror at 45° above each tank so that I could see the fish without looming over the tank. Fish were placed in the apparatus and acclimated for five minutes. Following acclimation, I dropped 10 ml of water from a stick-mounted-turkey-baster from a height of 18 cm. I bored a small hole into the baster and attached a rubber hose, so water was released consistently by removing my thumb from the top of the hose (Fig. 28). A 'drop' was repeated every 90 seconds for eleven 'drops,' with the sixth drop being a control with no water. I alternated positioning between sides, with the first side counterbalanced within pairs and distance haphazardly determined, usually placed about 2 cm from the fish's mid-section. The leftmost tank always received the drop first.

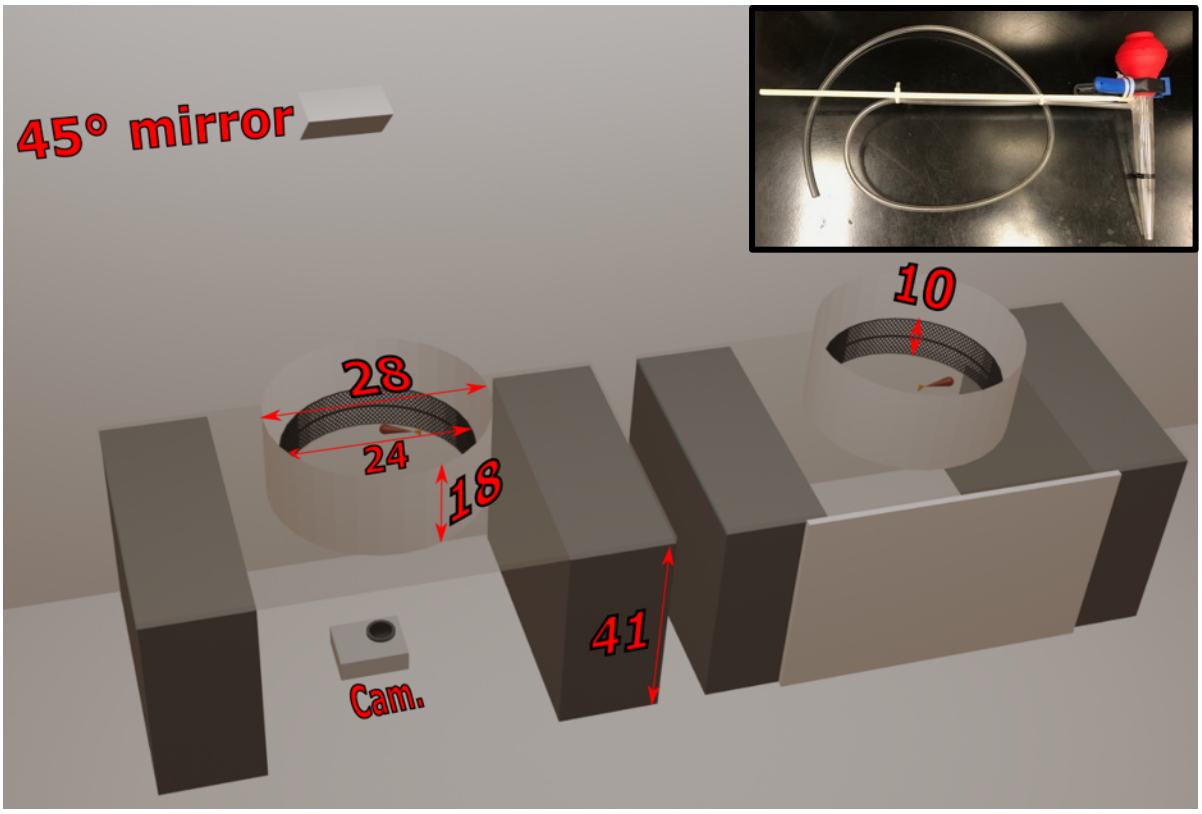

Figure 28. Schematic of predator evasion testing apparatus. All distances shown are in cm. The front cover from the left tank has been removed for visibility. The inset figure is an image of the predatory stimuli source.

4.3.5 Counter-balance design and repeat testing

I tested forty fish for each behaviour in four repeat trials in a counter-balanced design (Fig. 29; Table 4). I conducted two trials each day for two days, with at least a four-hour rest period in between. I tested fish in groups of four (two pairs). I always tested VAB first; if the first pair received 20 Hz then 60 Hz, the other pair would receive 60 Hz then 20 Hz. I would reverse the order of stimuli in the next trial and the day's sequence would be reversed on the second day. I tested one pair for rheotaxis first, with one receiving clockwise flow and the other counterclockwise flow. In the next trial, the order would be reversed and rheotaxis would be tested after predator evasion. The next day I would test flow regimes in the opposite order and the alternate sequence relative to predation evasion testing. I did the same alternation for placement in the two predator evasion arenas, and the first 'drop side.' The sequence of trials was such that each fish completed each behavioural test in each combination of orders. In between experiments, fish were housed in individual 19 L tanks with habitat enrichment, water throughflow and kept under cover. Feeding was withheld during the two-day testing period.

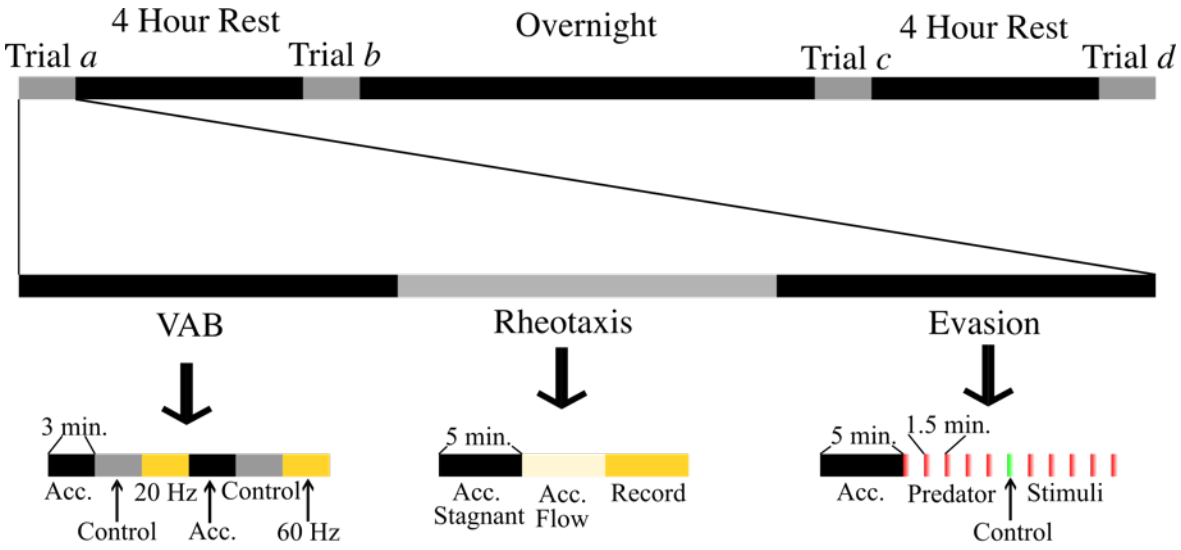

Figure 29. Example experimental sequence for one group of stickleback being tested for vibration attraction behaviour (VAB), rheotaxis and response to a simulated predatory stimulus (evasion). Acc. = acclimation.

Table 4. Counterbalancing of vibration attraction behaviour (VAB), rheotaxis and simulated predator evasion experiments. Numbers in the VAB table are fish's within-group IDs with the stimuli frequencies in brackets (first/second). Numbers in the rheotaxis table and predator evasion table are also fish's within-group IDs, with the letters in the predator evasion table indicating the side of the first drop for that trial.

VAB

Trial	Test seq	Tank 1 (1st fill)	Tank 1 (2nd fill)	Tank 2	Tank 3
a	1st	1 (20/60)	3 (60/20)	1 (20/60)	2 (20/60)
	2nd	2 (60/20)	4 (20/60)	3 (60/20)	4 (60/20)
b	1st	4 (60/20)	2 (20/60)	4 (20/60)	3 (20/60)
	2nd	3 (20/60)	1 (60/20)	2 (60/20)	1 (60/20)
c	1st	3 (60/20)	4 (20/60)	2 (20/60)	1 (20/60)
	2nd	1 (20/60)	2 (60/20)	4 (60/20)	3 (60/20)
d	1st	2 (20/60)	1 (60/20)	3 (20/60)	4 (20/60)
	2nd	4 (60/20)	3 (20/60)	1 (60/20)	2 (60/20)

Rheotaxis

Trial	Test seq	Track 1 (C)	Track 2 (CC)
a	1st	1	2
	2nd	3	4
b	1st	4	3
	2nd	2	1
c	1st	2	1
	2nd	4	3
d	1st	3	4
	2nd	1	2

Predator Evasion

Trial	Test seq	Arena 1	Arena 2
a	1st	3R	4L
	2nd	1L	2R
b	1st	2L	1R
	2nd	4R	3L
c	1st	4L	3R
	2nd	2R	1L
d	1st	1R	2L
	2nd	3L	4R

4.3.6 Microscopy

Either immediately after behavioural testing or the next day, the lateral line of live fish was viewed using fluorescent microscopy. I stained the lateral line using 2-(4-(dimethylamine)styryl)-N-ethylpyridinium iodide (DASPEI) using the procedure from Wark and Peichel (2010). I suspended DASPEI in dH2O to a concentration of 0.038%, then diluted this solution to 0.025% concentration with aquatics facility water. Fish could freely swim in the staining solution for 15 minutes, then rinsed with fresh water and anesthetized in 0.016% tricaine methylsulfonate (MS-222) solution until motionless and breathing shallowly (~2 minutes). Following anesthesia, fish were placed in a deep petri-dish containing 0.005% MS222 solution and viewed with an Olympus SZX-ILLD2-100 fluorescent microscope, illuminated by an

Olympus U-LH100HGAPO broad-spectrum UV light source and filtered by an Olympus SZX-MGF (excitation 460-490 nm; emission 510 nm longpass).

Neuromasts were counted on the left then the right sides. Counts were divided into the stitches described in Wark and Peichel (2010), but I divided the mandibular (MD) stitch into two sublines. I scored MD1 on the dentary and MD2 on the preopercular bone separately, as they were easily separable and the MD1 neuromasts were often abraded (Fig. 30). I also extended the Ma line to include the eighth lateral plate rather than stopping at the seventh, and recorded neuromasts counts on the fourth through eighth lateral plates individually, for inclusion in the analyses of Chapter 2 and Chapter 3. Following viewing, fish were euthanized with an overdose of 0.025% MS222, their isthmus was severed, and they were preserved in 70% ethanol. Following a few days of preservation, I scored fish for lateral plate count, standard length, sex and the presence of parasites.

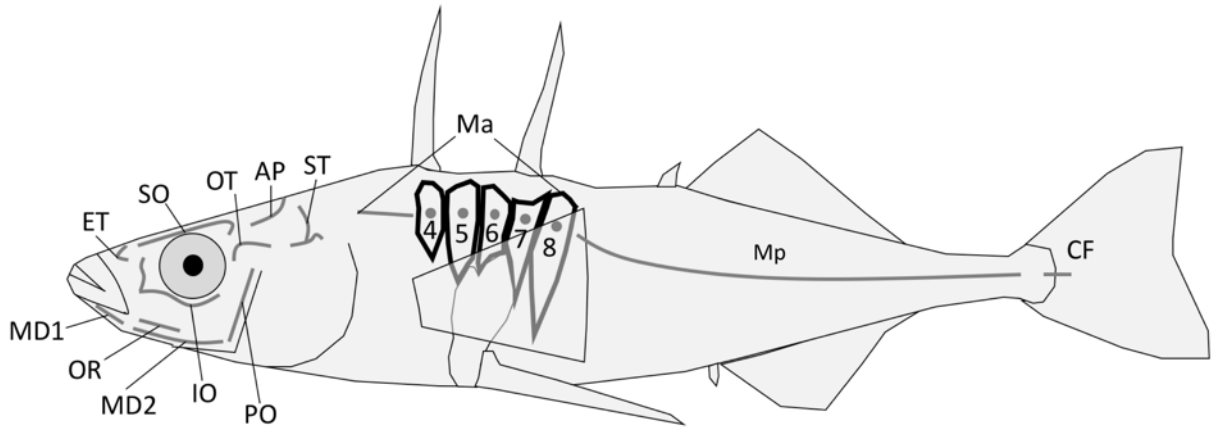

Figure 30. Diagram of lateral line stitches of threespine stickleback. Abbreviations are as follows: mandibular one / dentary (MD1), mandibular two / lower preopercular (MD2), oral (OR), infraorbital (IO), preopercular (PO), ethmoid (ET), supraorbital (SO), otic (OT), anterior

pit (AP), supratemporal (ST), main trunk line anterior (Ma), main trunk line posterior (Mp), and caudal fin (CF).

4.3.7 Video processing

I converted VAB and rheotaxis images to video using ImageJ macros, cropping out the clips of interest from the full footage and dividing VAB videos into control and stimuli clips. Videos were also cropped to the test tank to minimize future computation. I manually annotated predator evasion videos for the first frame each drop contacted the water surface (impact frame). I then extracted the impact frames and eleven seconds of footage (one second before and ten seconds after) for each drop using a python script. I converted impact frames into a video with ImageJ and manually annotated each drop's position using DLTdv8 (Hedrick 2008).

I annotated the position of the tip of the snout and the midsection between the pectoral fins in all videos using DeepLabCut (Mathis et al. 2018). I manually annotated the initial training frames, selecting up to 20 frames using k-fold selection from 100 predator evasion clips, 50 VAB clips and 10 rheotaxis videos. I iteratively assessed the quality of each model's tracking and retrained with additional 'outlier' training frames. I corrected errors in the tracking of the final neural networks in DLTdv8.

I corrected for distortion due to the camera lens and any angle between the camera and the center of the tank by using the edge of each tank as a reference. I annotated 30 points around the perimeter of each tank for each video and fit an ellipse to these points. Then I compressed the

fishes' positions along the major axis of the ellipse to the length of the minor axis (Fig. 31a).

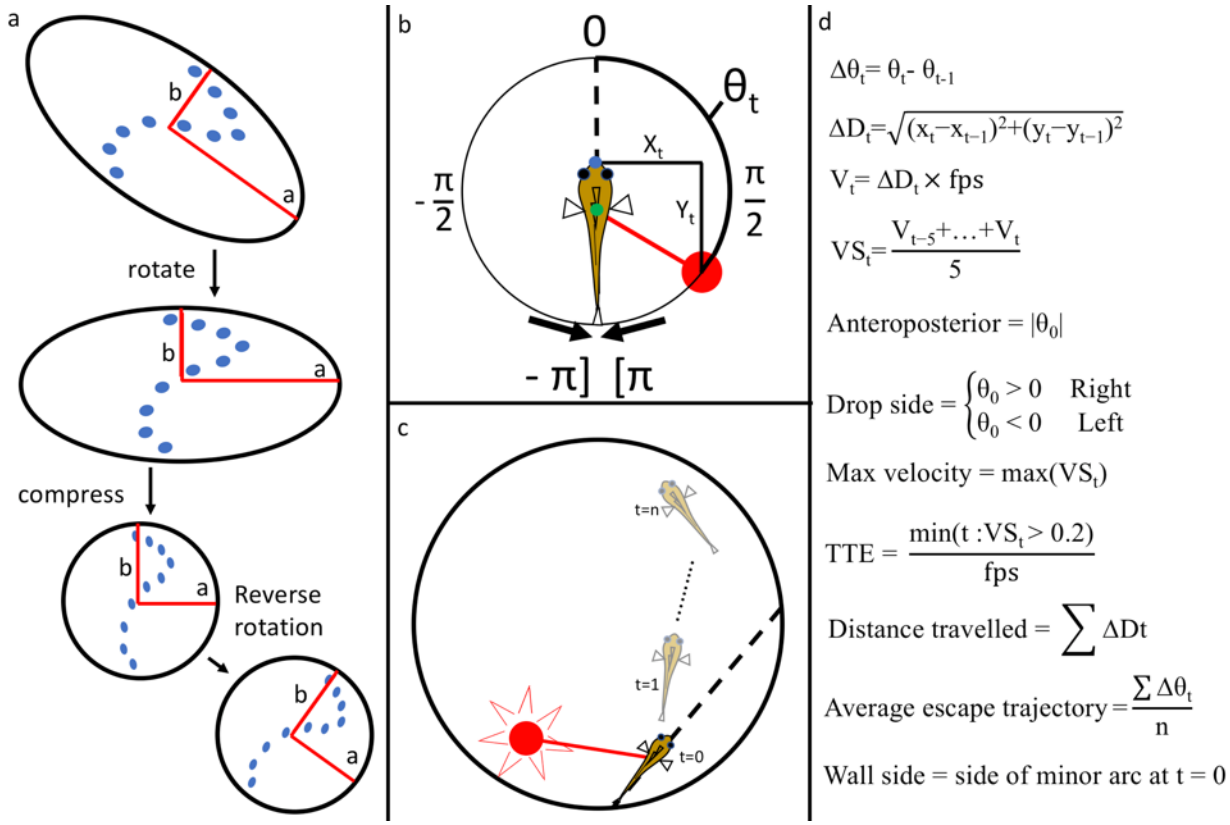

Figure 31. (*a*) The sequence of functions applied to raw tracking data to correct for camera angle. (*b*) Diagram of how angles and distances were calculated during the analysis of footage, t = frame number with the first frame that the drop hit the water's surface being 0. The red point is the drop, the blue point is the position of the snout, and the green dot is the position of the mid-section. Note that θ_t is bound between [-π, π] and rotations with a magnitude greater than π never occurred within a single frame (*c*) Diagram of a predator evasion event. The red dot is the drop. (*d*) Equations used to calculate kinematics for analysis. TTE = time to escape, fps = frames per second, (n : X) is the set of all n for which X is satisfied.

For predator evasion trials, the distance and angle of the drop relative to the fish's orientation was calculated, as well as the proportion of the arena on its left and right sides at the frame of impact (Fig. 31b-d). I divided drop angles into those on the left and right sides, and

calculated anteroposterior placement of the drop as the absolute value of the drop angle (0° being directly in front of the snout). I calculated velocity by taking the distance between snout positions on each frame and multiplying by frame rate; I used the snout since the position of the midpoint along the body was more variable during tracking. Distance travelled is a sum of all velocities over total elapsed time, and acceleration is the difference in velocity between subsequent frames. I calculated average escape trajectory as the sum of all changes in angle between frames divided by the number of frames. As velocity data are noisy, I used a rolling average with a window size of five frames for the calculation of maximum velocity. Each drop was classified as an escape if the fish reached at least 0.2 m/s, I chose this threshold as it matched the proportion of C-start escapes observed in my previous predator evasion experiments. I also tabulated time to reach 0.2 m/s (TTE) using the rolling average velocity.

I calculated distance travelled during VAB trials the same way as during predation evasion, and angles were calculated relative to the position of the glass rod (Fig. 32). An 'approach' occurred when the stickleback got within 5 cm of the glass rod (roughly one body length), with a three-frame buffer in between approaches to prevent double-counting from noise in position data. I considered the angle of the approach to be the fish's angle relative to the rod on the frame it passed the approach threshold (5 cm). I also calculated the total time spent in the center and the average angle while within the 5 cm radius zone. Approach side and wall side (the side facing the outer wall of the tank most often) were categorized as left or right, as both were highly bimodal.

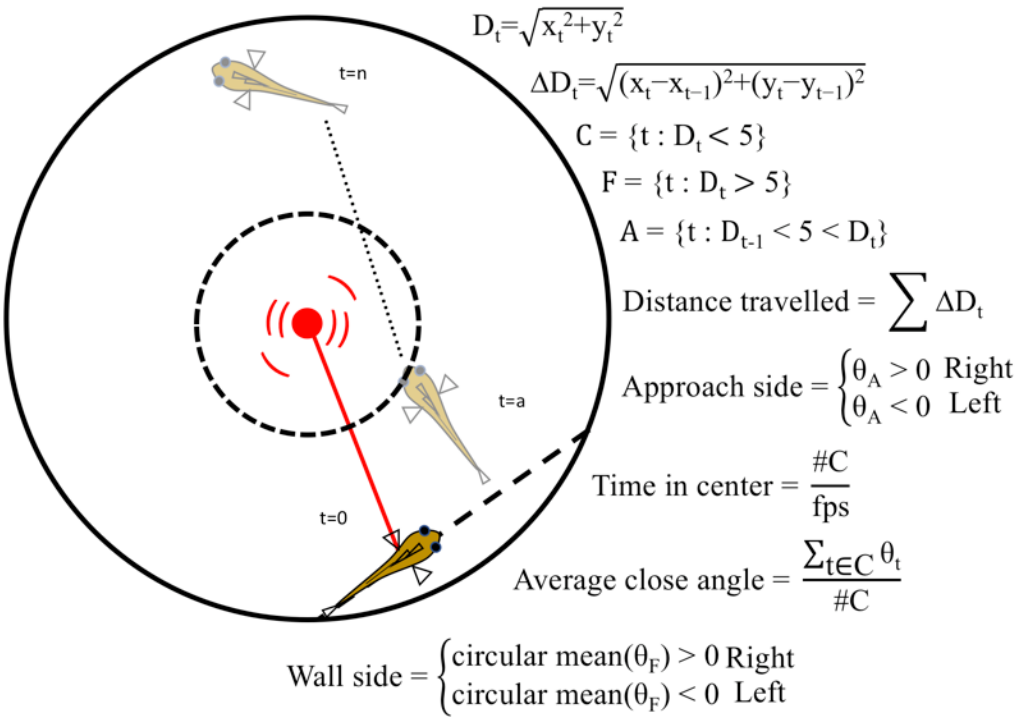

Figure 32. Diagram of how kinematics were calculated for vibration attraction behaviour experiment. The first frame that the tip of a stickleback's snout enters within 5 cm of the center rod is t=a. fps = frames per second. (n : X) is the set of all n for which equation X is satisfied. #C is the cardinality of set C, in this case the number of frames where the fish's snout was within 5 cm of the glass rod. Circular mean was calculated using the mean.circular function in the R package *circular* (Agostinelli and Lund 2017).

Following Jiang et al. (2017), I examined at four metrics of rheotaxis behaviour; net displacement (+upstream,-downstream), cumulative upstream movement, time oriented upstream and flow regime selection (distance from outer edge) (Fig. 33). I tabulated upstream and downstream movement as the change in angle relative to the vertical and center of the track between frames (ϕ in Fig. 33), with cumulative upstream movement being the summation of the distance travelled on all frames where the fish's position moved upstream. Time oriented

upstream was the number of frames with the stickleback orientated between 45° and 135° relative to the center (θ within 45° of the direction of flow) and distance from the outer edge was calculated using the calibration circle and averaged across all frames.

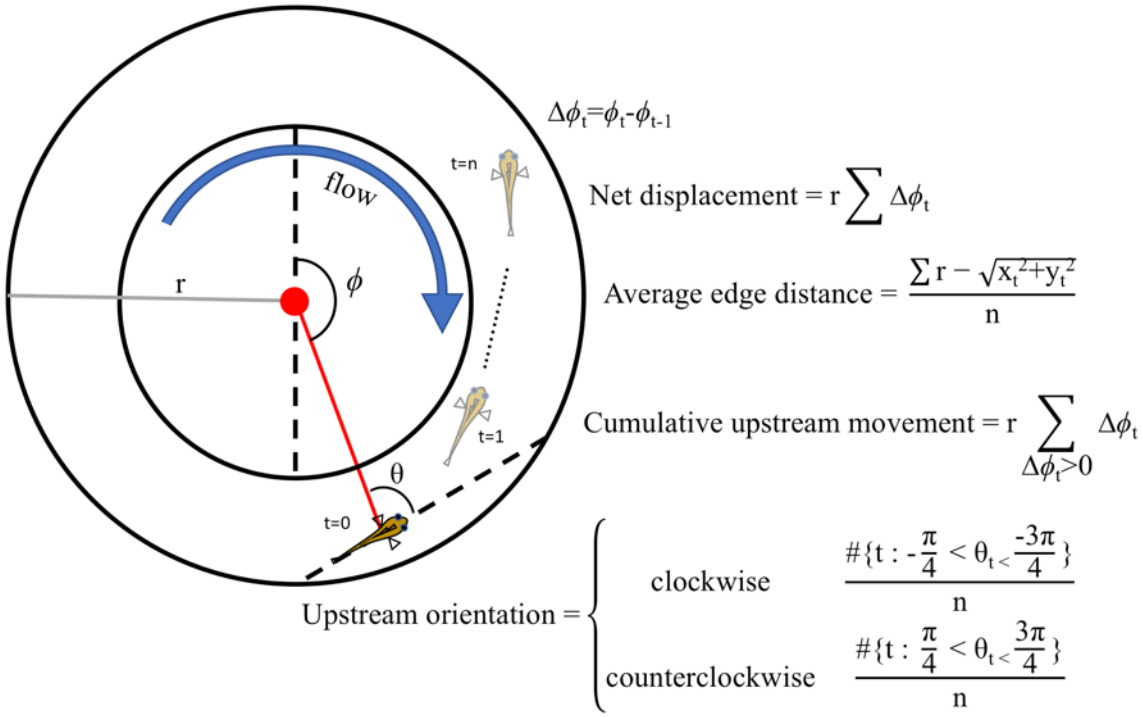

Figure 33. Diagram of how kinematics were calculated for rheotaxis experiment. (n : X) is the set of all n for which X is satisfied. #T is the cardinality of set T.

4.3.8 Statistical analyses

Predator evasion

I assessed five aspects of predator evasion behaviour for laterality; whether escape occurred, TTE, maximum velocity, the average trajectory of escape and positioning within the arena (see Table 5 for data transformations and error structures). Max velocity closely correlates with distance travelled (r = 0.64 [0.55,0.71], t_{237} = 12.7, p < 0.001) and acceleration (r = 0.44

[0.33,0.54], $t_{237} = 7.5$, $p < 0.001$), so the latter two were excluded from analyses. I first modeled all behaviours with the potential confounds due to experimental design: arena identity, test sequence (rheotaxis or predator evasion tested first), drop number within a trial, trial number, presence of drips, group, drop distance and anteroposterior position of drops (drop ang.), using equation 1 (Table 6). These models then underwent model selection at $\alpha = 0.05$ (Murtaugh 2009). I included predictors that were significant and not counterbalanced in the experimental design in the rest of the analysis. I tested the effect of sex, standard length, neuromast count (NC = $\sum(R_s+L_s)$), directional neuromast count asymmetry (DA = $\sum(R_s-L_s)$) and absolute neuromast count asymmetry (AA = $\sum(|R_s-L_s|)$) on behavioural laterality, with backwards model selection on equation 2 (Table 6). R_s and L_s are the number of neuromasts on the right and left sides of stitch S, respectively. Note that drop number was changed from a factor in equation 1 to a continuous predictor in equation 2 to save degrees of freedom since differences among drop numbers were approximately linear for all behaviours. Laterality of wall side selection was assessed using equation 3 (Table 6). If NC, DA or AA significantly influenced escape behavior, I substituted the sum over all stitches each stitch in the reduced model equation, *e.g.* if there was a significant effect of DA on TTE, TTE would be modeled by R – L neuromast counts for each stitch individually plus any other factors that had a significant effect on TTE. P-values from individual stitch analysis were Bonferroni corrected (n = 13) to account for multiple comparisons.

Table 5. Model types for behavioural metrics of predator evasion, vibration attraction behaviour (VAB) and rheotaxis. Transform is the transform applied the data prior to fitting model.

Experiment	Metric	Transform	Residual distribution	Link function
Predator evasion	Escape	none	binomial	logit
	Time to escape	cube root	Gaussian	none
	Max velocity	ln	Gaussian	none
	Escape angle	none	Gaussian	none
	Wall side	none	binomial	logit
VAB	Distance travelled	cube root	Gaussian	none
	# of approaches	none	general Poisson	log
	Time in center	ln	Gaussian	none
	Wall side	none	binomial	logit
	Approach side	none	binomial	logit
	Center angle	none	Gaussian	none
Rheotaxis	Net displacement	cube root	Gaussian	none
	Upstream movement	log	Gaussian	none
	% upstream orientation	none	binomial	logit
	Outer edge distance	none	beta	logit

Table 6. Model equations for model selection. Y is all the behaviours examined for a given experiment, except for wall side which has its own equation. SL = standard length, NC = neuromast count, DA = directional asymmetry in neuromast count (R - L), AA = absolute asymmetry in neuromast count (|R - L|).

Experiment	Eq.	Model Formula
Predation	1	$Y = drip + arena\ ID + test\ seq. + trial + cohort + drop\ seq. +$ drop distance + drop ang. + $(1\|individual\ ID)$
	2	$Y = drop\ side * (sex +$ SL + NC + DA + AA + $wall\ side +$ drop seq. + $trial) + (1\|individual\ ID)$
	3	wall side = $sex +$ SL + NC + DA + AA + drop seq. + $trial + (1\|individual\ ID)$
VAB	4	$Y = stimulus * (trial + cohort + tank\ seq. + tank\ ID) + (1\|individual\ ID)$
	5	$Y = stimulus * (sex +$ SL + NC + DA + AA + $trial) + (1\|individual\ ID)$
Rheotaxis	6	$Y = test\ seq. + trial + direction/track + cohort + (1\|individual\ ID)$
	7	$Y = direction/track * (trial + cohort + sex +$ SL + NC + DA + AA) + $(1\|individual\ ID)$

VAB

I tested three aspects of VAB behavior for the effect of 20 Hz and 60 Hz stimuli; distance travelled, number of approaches and time in the center (see Table 5 for data transformations and error structure). I first modeled all parameters with the potential confounds due to experimental

design: trial, tank ID, tank sequence and group, using equation 4 (Table 6). As with predator evasion, if predictors were significant and not counterbalanced in the experimental design, they were included in subsequent models. I compared non-lateralized and lateralized behaviours to morphological characteristics with equation 5 (Table 6). Analysis of lateralized and non-lateralized behaviours had to be separated for VAB analysis since laterality could not be encoded as an interaction effect *e.g.* drop side or flow direction. I tested individual stitches the same way as with predator evasion.

Rheotaxis

I examined four metrics of rheotaxis behaviour for laterality (see Table 5 for data transformations and error structure). I modelled the effects of experimental procedure: test sequence, trial, flow direction/track ID and group with equation 6 (Table 6). I tested the effect of morphology on lateralized and non-lateralized behaviour using equation 7 (Table 6). All models underwent the same backwards model selection procedure and I tested individual stitches in the same way as predator evasions and VAB trials.

Repeatability of behaviour

I tested the consistency of non-lateralized and lateralized behaviors using the *rptR* package (Stoffel et al. 2017), using the reduced model structure for experimental design effects, *i.e.* equations 1,4 and 6 (Table 6). Individual repeatability was tested on just the first drop and the first VAB control, to account for pseudo replication, *e.g.* a stickleback that starts on the right is more likely to stay on the right. I tested correlation in laterality among behaviours exhibiting the greatest laterality with the *psych* package (Revelle 2020) after summing / averaging the behaviour of each individual.

4.4 Results

4.4.1 Predator evasion

Experimental design

Fish never initiated escape response during control trials, however 6% of escape responses were initiated before drop impact. The probability of initiating escape response was (mean [95% CI]) 9.5% [6.6%,13.3%]. Escape was initiated less frequently in subsequent drops within trials ($\chi^2_9 = 102$, $p < 0.001$), with the minimum rate of response being reached by drop six (Fig. 34a) and in later trials ($\chi^2_3 = 49.2$, $p < 0.001$; Fig. 34b). Escape response was more likely to be initiated the further the drop distance was from the fish ($\chi^2_1 = 10.0$, $p = 0.002$; Fig. 34c). Group, test sequence, arena ID, drips and anteroposterior placement did not affect escape response (group: $\chi^2_9 = 8.5$, $p = 0.485$; all other $\chi^2_1 \leq 1.8$, $p \geq 0.185$).

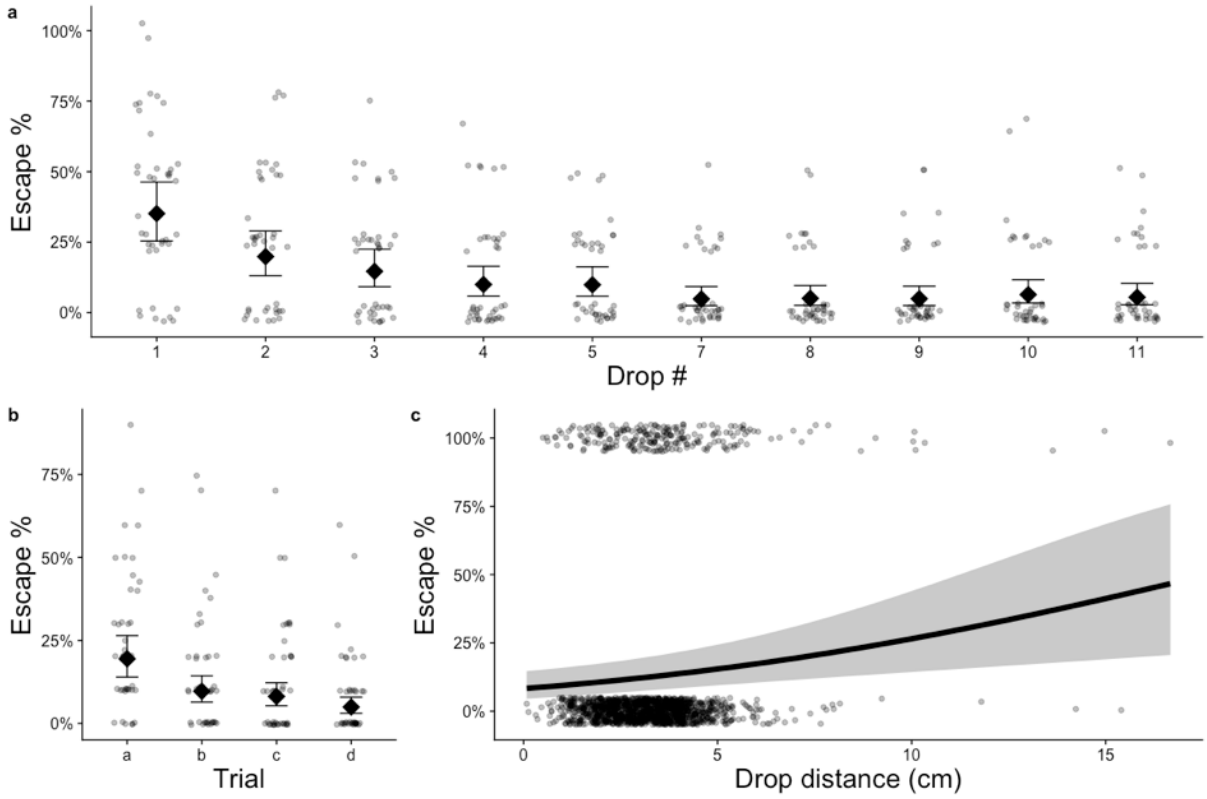

Figure 34. Percent of drops resulting in escape response being initiated among (*a*) drops, (*b*) trials and with (*c*) drop distance. (*a,b*) Diamonds are estimated marginal means (EMMs) with 95% CI error bars, and circular points are the average response of individuals jittered for visibility. (*c*) The line is the EMM with the shaded region indicating a 95% CI and points are each drop jittered for visibility. All EMMs are averaged over all predictors other than the one being visualized.

Average TTE was 1.2 [0.98,1.49] s and ranged from 0.02 s to 9.92 s for escape responses initiated after impact. TTE was faster in the first arena than the second arena (first arena = 0.98 [0.78,1.22]; second arena = 1.44 [1.18,1.75]; $\chi^2_1 = 8.11$, $p = 0.004$), increased in later trials ($\chi^2_3 = 55.9$, $p < 0.001$; Fig. 35a), decreased with drop distance ($\chi^2_1 = 6.77$, $p = 0.009$; Fig. 35b) and varied among groups ($\chi^2_9 = 23.8$, $p = 0.005$). TTE was not affected by test sequence, drop number, drips or anteroposterior placement (drop number: $\chi^2_9 = 13.3$, $p = 0.150$;

all other $\chi^2_1 \leq 1.3$, $p \geq 0.246$).

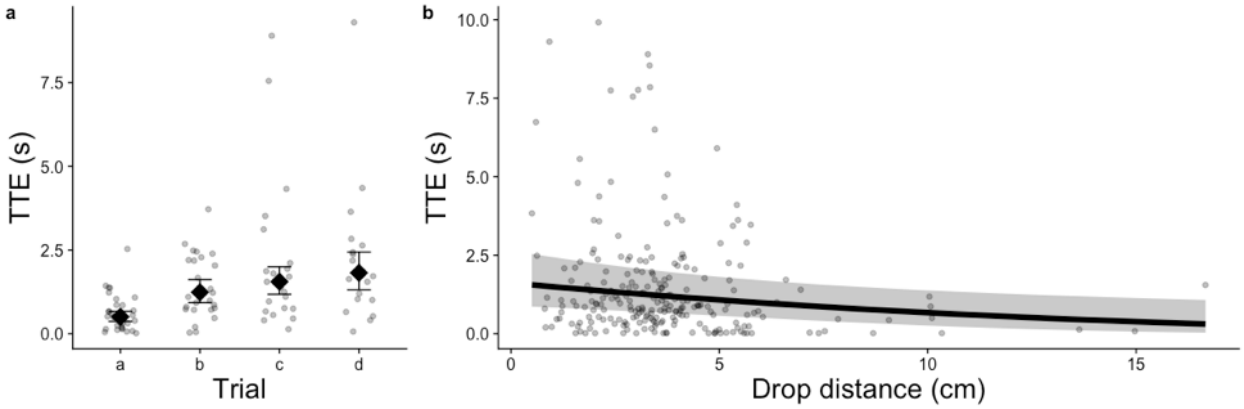

Figure 35. Time to escape (TTE), *i.e.* time to reach 0.2 m/s (*a*) among trials and (*b*) with drop distance. (*a*) Diamonds are estimated marginal means (EMMs) with 95% CI error bars, and

circular points are the average response of individuals jittered for visibility. (*b*) The line is the EMM with the shaded region indicating a 95% CI and points are each individual drop. All EMMs are averaged over all predictors other than the one being visualized.

Max velocity averaged 0.39 [0.34,0.44] m/s, ranging from 0.2 m/s to 2.2 m/s. Max velocity decreased in later trials ($\chi^2_3 = 89.6$, $p < 0.001$; Fig 36), but did not change with group, drop number, arena ID, test sequence, drips, drop distance or anteroposterior placement (all $\chi^2_9 \leq 13.2$, $p = 0.154$; all $\chi^2_1 \leq 0.48$, $p \geq 0488$).

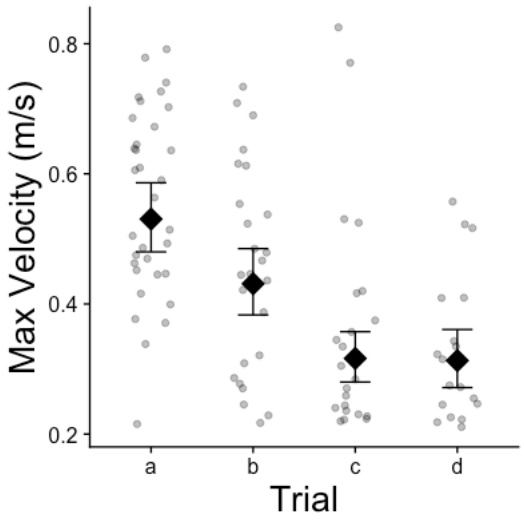

Figure 36. The difference in max velocity among predator evasion trials. Diamonds are estimated marginal means (EMMs) with 95% CI error bars, and circular points are the average response of individuals jittered for visibility.

Absolute escape angle was 8.6 [8.3,8.9] rad/m on average, ranging from 0.1 rad/m to 33.5 rad/m and varying among groups ($F_9 = 2.7$, $p = 0.006$). Absolute escape angle did not change with trial, drop number, arena ID, test sequence, drips, drop distance or anteroposterior placement (all $F_{1-9} \leq 1.1$, $p \geq 0.287$).

Laterality and morphology

The orientation of fish within the arena was highly bimodal, with fish 'hugging' the arena wall with their right side in 56.7% of drops and hugging the left in 43.3% of drops. Fish with fewer neuromasts were more likely to hug the right wall (neuromasts: $\chi^2_1 = 7.44$, $p = 0.006$; Fig 37a), and the preference for hugging the right wall was greatest during trial *a* (trial: $\chi^2_3 = 18.1$, $p < 0.001$; Fig 37b). Twelve of thirteen stitches negatively correlated with a bias towards right wall hugs, and the Mp stitch had the strongest and only significant correlation (Table 7).

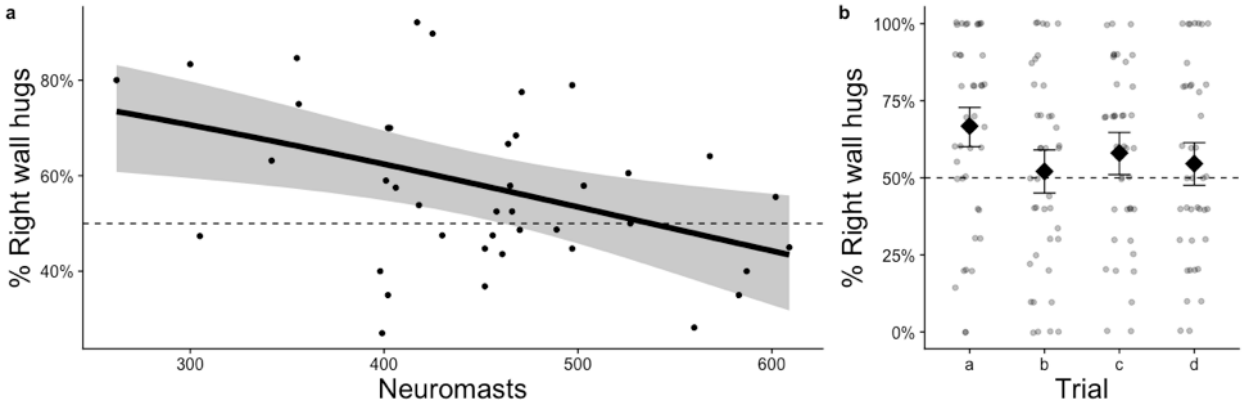

Figure 37. Change in probability of hugging the right wall with changes in (*a*) total neuromast count and (*b*) among trials. (*a*) The line is the estimated marginal mean (EMM) with the shaded region indicating a 95% CI and points are the average response of individuals. (*b*) Diamonds are EMMs with 95% CI error bars and, points are the average response of individuals jittered for visibility. All EMMs are averaged over all predictors other than the one being visualized.

Table 7. Effects of neuromast count of individual stitches on the percent of right wall hugs. Adjusted p-values have been Bonferroni adjusted for multiple comparisons (n = 13). Estimate is the change in the log-odds of right wall hugging per neuromast, whereas scaled estimate is the

change in the log-odds of right wall hugging per standard deviation of neuromast counts for that stitch. Stitches with significant effect are underlined and stitches with significant effect after correcting for multiple comparisons are also bolded.

Stitch	χ^2	p (adjusted)	estim. ± se	scaled estim. ± se
AP	2.57	0.109 (1)	-0.037 ± 0.023	-0.209 ± 0.13
SO	1.56	0.212 (1)	-0.022 ± 0.018	-0.159 ± 0.128
ET	0.21	0.646 (1)	-0.02 ± 0.043	-0.061 ± 0.132
IO	2.55	0.11 (1)	-0.023 ± 0.014	-0.192 ± 0.12
OR	1.35	0.246 (1)	-0.029 ± 0.025	-0.139 ± 0.12
MD1	0.46	0.497 (1)	-0.012 ± 0.018	-0.083 ± 0.122
MD2	2.08	0.149 (1)	0.024 ± 0.017	0.184 ± 0.127
PO	2.19	0.139 (1)	-0.039 ± 0.026	-0.174 ± 0.118
OT	1.3	0.254 (1)	-0.036 ± 0.032	-0.138 ± 0.121
ST	2.37	0.124 (1)	-0.023 ± 0.015	-0.19 ± 0.123
Ma	2.38	0.123 (1)	-0.009 ± 0.006	-0.197 ± 0.127
Mp	**10.83**	**0.001 (0.013)**	**-0.008 ± 0.003**	**-0.369 ± 0.112**
CF	0.07	0.785 (1)	-0.026 ± 0.096	-0.041 ± 0.149

Fish initiated escape behavior 10.7% [7.6%,14.7%] of the time when I placed the drop on the right and 8.2% [5.7%,11.6%] of the time on the left ($\chi^2_1 = 3.3$, $p = 0.068$). Fish with more neuromasts initiated escape response less frequently, with a stronger relationship for drops on the left side (neuromasts $\chi^2_1 = 7.2$, $p = 0.007$; neuromasts × drop side: $\chi^2_1 = 5.5$, $p = 0.02$; Fig. 38a). Escape response occurred more frequently with the arena wall on the left and the drop on the right, relative to other wall and drop positions (wall side × drop side: $\chi^2_1 = 4.9$, $p = 0.027$; Fig. 38b). There was a right bias in escape response in all trials but trial *d* (trial × drop side: $\chi^2_3 = 9.0$, $p = 0.029$; Fig. 38c). Escape response did not differ between sexes, with SL, DA or AA (all $\chi^2_1 \leq 1.2$, $p \geq 0.268$), including interactions with drop side (drop side × all: $\chi^2_1 \leq 1.8$, $p \geq 0.178$). Neuromasts counts in twelve of thirteen stitches had a negative association with escape behaviour, and eleven of thirteen had a stronger negative association

when drops came from the left side (Table 8). While the SO, IO and OR stitches had a significant association with the probability of initiating escape behaviour and the IO, MD2, OT, ST and Ma stitches had a significantly stronger association with drops from the left side, no individual stitches were significant after correction for multiple comparisons (Table 8).

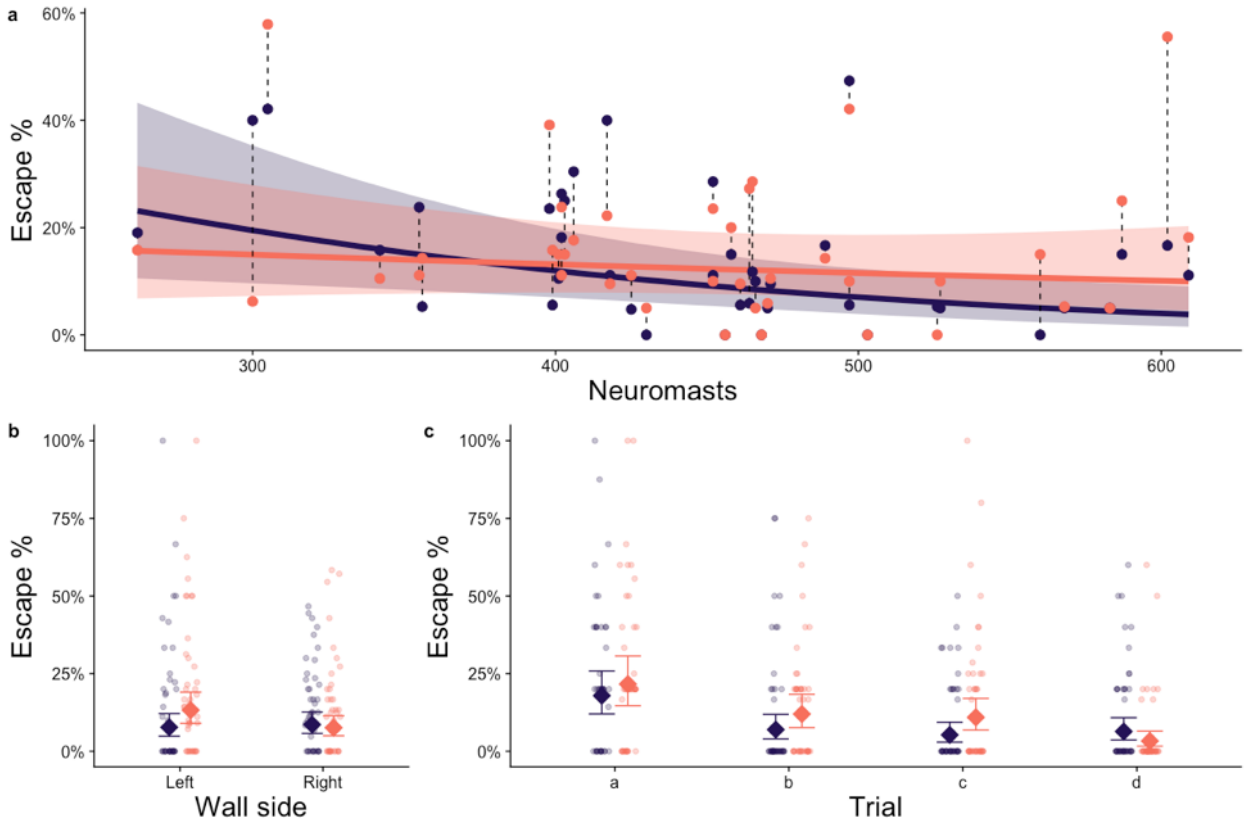

Figure 38. Change in probability of initiating escape behaviour from drops on the right (pink) and left (purple) with changes in (*a*) total neuromast count (*b*) wall side and (*c*) trial. (*a*) Lines are estimated marginal means (EMMs) with the shaded region indicating a 95% CI and points connected by dotted lines are the average response per side for each individual. (*b,c*) Diamonds are EMMs with 95% CI error bars, and circular points are the average response of individuals jittered for visibility. All EMMs are averaged over all predictors other than the one being visualized.

Table 8. Effects of neuromast count of individual stitches on the probability of initiating escape behaviour and on differences between the probability of escape from drops on the left versus the right (left - right). Adjusted p-values have been Bonferroni adjusted for multiple comparisons (n = 13). Estimate is the change in the log-odds of initiating escape per neuromast, whereas scaled estimate is the change in the log-odds of initiating escape per standard deviation of neuromast counts for that stitch. Stitches with significant effect are underlined, and stitches with significant effect after correcting for multiple comparisons are also bolded.

Predictor	Stitch	χ^2	p (adjusted)	estim. ± se	scaled estim. ± se
Neuromasts	AP	4.82	0.028 (0.365)	-0.066 ± 0.03	-0.396 ± 0.18
	SO	4.01	0.045 (0.589)	-0.046 ± 0.023	-0.349 ± 0.175
	ET	2.72	0.099 (1)	-0.091 ± 0.055	-0.341 ± 0.206
	IO	4.77	0.029 (0.376)	-0.041 ± 0.019	-0.337 ± 0.154
	OR	3.86	0.05 (0.644)	-0.066 ± 0.033	-0.328 ± 0.167
	MD1	3.6	0.058 (0.752)	-0.045 ± 0.024	-0.304 ± 0.16
	MD2	0.06	0.809 (1)	-0.006 ± 0.023	-0.045 ± 0.186
	PO	3.36	0.067 (0.866)	-0.065 ± 0.036	-0.283 ± 0.154
	OT	0.87	0.352 (1)	-0.041 ± 0.044	-0.147 ± 0.159
	ST	1.64	0.2 (1)	-0.027 ± 0.021	-0.203 ± 0.158
	Ma	0.82	0.366 (1)	-0.008 ± 0.008	-0.161 ± 0.178
	Mp	0.7	0.404 (1)	-0.003 ± 0.004	-0.147 ± 0.176
	CF	1.37	0.241 (1)	0.146 ± 0.125	0.24 ± 0.205
Neuromasts	AP	2.88	0.09 (1)	-0.048 ± 0.028	-0.139 ± 0.082
X Drop side	SO	3.65	0.056 (0.728)	-0.043 ± 0.022	-0.102 ± 0.053
	ET	0	0.947 (1)	-0.003 ± 0.049	-0.007 ± 0.099
	IO	4.83	0.028 (0.364)	-0.043 ± 0.019	-0.16 ± 0.073
	OR	0.58	0.446 (1)	-0.025 ± 0.033	-0.061 ± 0.08
	MD1	0.51	0.475 (1)	-0.017 ± 0.024	-0.047 ± 0.065
	MD2	0.05	0.824 (1)	0.005 ± 0.021	0.027 ± 0.123
	PO	0.63	0.427 (1)	0.028 ± 0.035	0.072 ± 0.091
	OT	4.22	0.04 (0.519)	-0.089 ± 0.043	-0.207 ± 0.101
	ST	5.02	0.025 (0.325)	-0.047 ± 0.021	-0.192 ± 0.086
	Ma	5.01	0.025 (0.328)	-0.018 ± 0.008	-0.072 ± 0.032
	Mp	3.58	0.059 (0.762)	-0.007 ± 0.004	-0.07 ± 0.037
	CF	3.8	0.051 (0.665)	-0.222 ± 0.114	-0.112 ± 0.058

TTE decreased with AA for drops from the right but increased with AA for drops from the left (drop side × AA: $\chi^2_1 = 10.1$, $p = 0.001$; Fig 39). TTE did not differ with wall side, sex, SL, neuromast count, or DA (all $\chi^2_1 \leq 0.2$, $p \geq 0657$), and none had a significant interaction with drop side (drop side × all: $\chi^2_{1\text{-}3} \leq 0.6$, $p \geq 0.667$). AA in nine of thirteen stitches was negatively associated with TTE; however, no individual stitches were significant (Table 9).

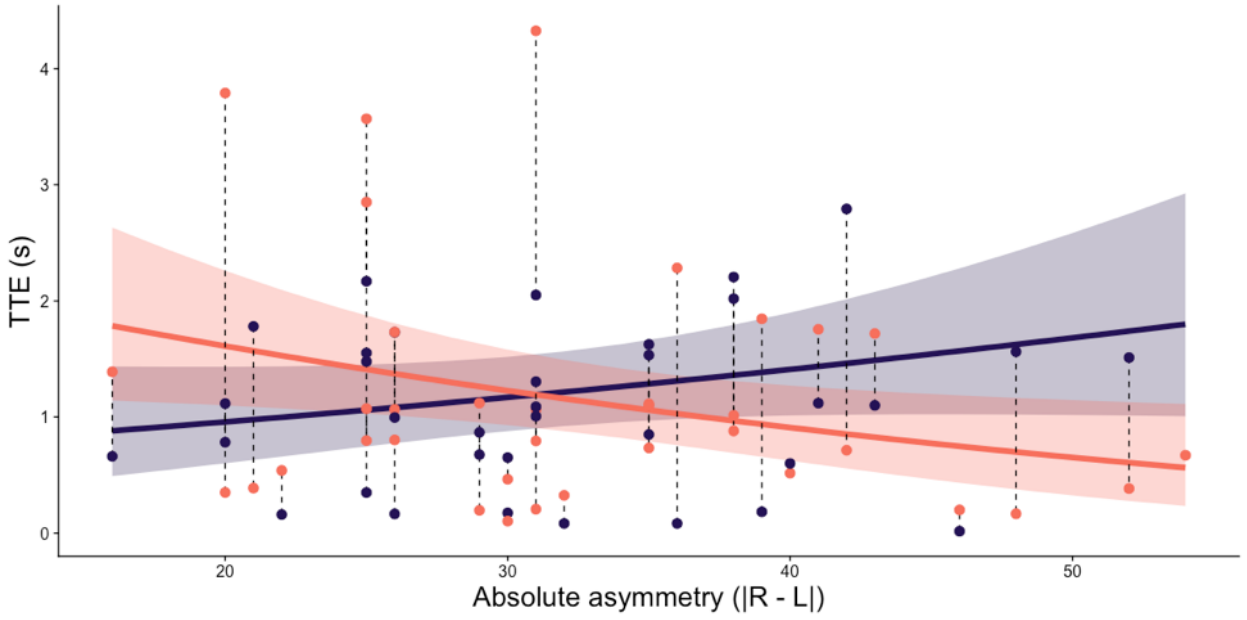

Figure 39. Change in time to escape (TTE) from drops on the left (purple) and right (pink) with changes in absolute asymmetry (AA). AA is calculated as the sum of |R - L| for all neuromast stitches. Lines are estimated marginal means (EMMs) with the shaded region indicating a 95% CI and points connected by dotted lines are the average response per side for each individual. EMMs are averaged over all predictors other than the one being visualized.

Table 9. Effects of individuals neuromast stitch absolute asymmetry (AA; |R - L|) on differences between time to escape (TTE) from drops on the left versus the right (left - right). Adjusted p-values have been Bonferroni adjusted for multiple comparisons (n = 13). Estimate is the change

in cube root transformed TTE per neuromast, whereas scaled estimate is the change in cube root transformed TTE per standard deviation of neuromast counts for that stitch. Stitches with significant effect are underlined, and stitches with significant effect after correcting for multiple comparisons are also bolded.

Stitch	χ^2	p (adjusted)	estim. ± se	scaled estim. ± se
AP	0.29	0.589 (1)	-0.012 ± 0.023	-0.073 ± 0.136
SO	0.85	0.355 (1)	-0.031 ± 0.034	-0.236 ± 0.255
ET	1	0.316 (1)	0.04 ± 0.04	0.149 ± 0.149
IO	0.01	0.933 (1)	0.002 ± 0.019	0.013 ± 0.155
OR	0.65	0.42 (1)	-0.019 ± 0.024	-0.096 ± 0.119
MD1	5.88	0.015 (0.199)	-0.049 ± 0.02	-0.33 ± 0.136
MD2	2.11	0.147 (1)	-0.018 ± 0.012	-0.146 ± 0.1
PO	0.32	0.57 (1)	-0.014 ± 0.024	-0.059 ± 0.104
OT	0.27	0.601 (1)	0.015 ± 0.028	0.052 ± 0.099
ST	0.02	0.876 (1)	0.003 ± 0.019	0.022 ± 0.142
Ma	0	0.964 (1)	-0.001 ± 0.016	-0.015 ± 0.336
Mp	2.6	0.107 (1)	-0.011 ± 0.007	-0.471 ± 0.292
CF	0.98	0.322 (1)	-0.094 ± 0.095	-0.155 ± 0.156

Fish with more neuromasts reached a lower max velocity on average ($\chi^2_1 = 5.3$, $p = 0.022$; Fig. 40a), and fish with more neuromasts on the right reached a higher max velocity on average ($\chi^2_1 = 4.1$, $p = 0.044$; Fig. 40b). Max velocity did not differ with drop side, wall side, sex, SL or AA (all $\chi^2_1 \leq 1.8$, $p \geq 0.183$) and no interactions with drop side were significant (drop side × all: $\chi^2_{1\text{-}3} \leq 1.9$, $p \geq 0.167$). Increased neuromast count in twelve of thirteen stitches had a negative association with max velocity, with the ST and Ma stitches having a significant association and the IO and MD1 stitches having a significant association without correction for multiple comparisons (Table 10). The effect of DA across stitches was inconsistent, with a right bias in eight of thirteen lines increasing max velocity, including the significantly associated IO stitch and the OR and MD2 stitches, which are significantly associated prior to correcting for

multiple comparisons (Table 10).

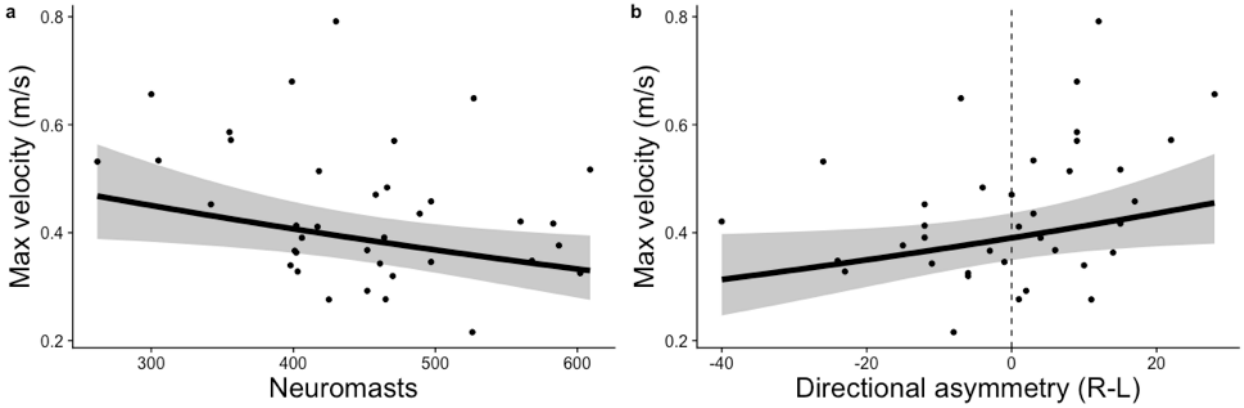

Figure 40. Change in max velocity with changes in (*a*) neuromast count and (*b*) directional asymmetry (DA). DA is calculated as a sum of R – L neuromast counts for each neuromast stitch. Lines are estimated marginal means and shaded regions 95% CIs, averaged over all predictors other than the one being visualized. Points are the average response of individuals.

Table 10. Effects of neuromast count of individuals neuromast stitches and directional asymmetry (DA; R - L) of individual stitch neuromast count on max velocity. Adjusted p-values have been Bonferroni adjusted for multiple comparisons (n = 13). Estimate is the change in log(max velocity) per neuromast, whereas scaled estimate is the change in log(max velocity) per standard deviation of neuromast counts for that stitch. Stitches with significant effect are underlined, and stitches with significant effect after correcting for multiple comparisons are also bolded.

Predictor	Stitch	χ^2	p (adjusted)	estim. ± se	scaled estim. ± se
Neuromasts	AP	0.44	0.506 (1)	-0.005 ± 0.008	-0.031 ± 0.046
	SO	5.52	0.019 (0.244)	-0.013 ± 0.005	-0.095 ± 0.04
	ET	3.73	0.054 (0.696)	-0.025 ± 0.013	-0.092 ± 0.048
	IO	3.83	0.05 (0.654)	-0.009 ± 0.005	-0.074 ± 0.038
	OR	0.81	0.367 (1)	-0.008 ± 0.009	-0.039 ± 0.043
	MD1	4.14	0.042 (0.546)	-0.012 ± 0.006	-0.081 ± 0.04
	MD2	0.07	0.786 (1)	0.002 ± 0.006	0.013 ± 0.046
	PO	1.11	0.292 (1)	-0.01 ± 0.009	-0.041 ± 0.039
	OT	0	0.952 (1)	-0.001 ± 0.011	-0.002 ± 0.041
	ST	**8.53**	**0.004 (0.046)**	**-0.014 ± 0.005**	**-0.104 ± 0.036**
	Ma	**11.91**	**0.001 (0.007)**	**-0.006 ± 0.002**	**-0.13 ± 0.038**
	Mp	1.92	0.166 (1)	-0.001 ± 0.001	-0.058 ± 0.042
	CF	1.1	0.294 (1)	-0.031 ± 0.029	-0.051 ± 0.048
DA	AP	1.59	0.208 (1)	-0.019 ± 0.015	-0.056 ± 0.045
	SO	0.27	0.604 (1)	0.009 ± 0.018	0.022 ± 0.042
	ET	0.84	0.361 (1)	-0.02 ± 0.022	-0.04 ± 0.044
	IO	**9.93**	**0.002 (0.021)**	**0.03 ± 0.01**	**0.114 ± 0.036**
	OR	5.17	0.023 (0.298)	0.034 ± 0.015	0.082 ± 0.036
	MD1	1.71	0.191 (1)	0.022 ± 0.017	0.061 ± 0.046
	MD2	7.77	0.005 (0.069)	0.018 ± 0.006	0.107 ± 0.039
	PO	0.33	0.568 (1)	-0.01 ± 0.018	-0.027 ± 0.047
	OT	0.31	0.581 (1)	-0.011 ± 0.02	-0.026 ± 0.046
	ST	0.13	0.714 (1)	0.004 ± 0.011	0.016 ± 0.044
	Ma	0.48	0.488 (1)	-0.007 ± 0.01	-0.027 ± 0.039
	Mp	0.12	0.729 (1)	0.001 ± 0.004	0.014 ± 0.041
	CF	0.44	0.509 (1)	0.044 ± 0.067	0.023 ± 0.034

Average trajectory of escape was away from the nearest wall ($\chi^2_1 = 4.9$, $p = 0.028$; Fig. 41a). Fish with more neuromasts on their right side escaped away from the drop, whereas fish with more neuromasts on the left escaped towards it more often (DA × drop side: $\chi^2_1 = 5.4$, $p = 0.020$; Fig. 41b). Sex, SL, neuromast count and AA did not affect escape trajectory (all $\chi^2_1 \leq 0.4$, $p \geq 0.545$) and wall side, sex, SL, neuromast count and AA did not interact with drop side (all $\chi^2_{1\text{-}3} \leq 1.2$, $p \geq 0.393$). A right bias in twelve of thirteen stitches was associated with increased rightward trajectory when starting with the arena wall on the left, with the ET and

MD1 having a significant interaction between DA and drop side, although no individual stitches were significant after correction for multiple comparisons (Table 11).

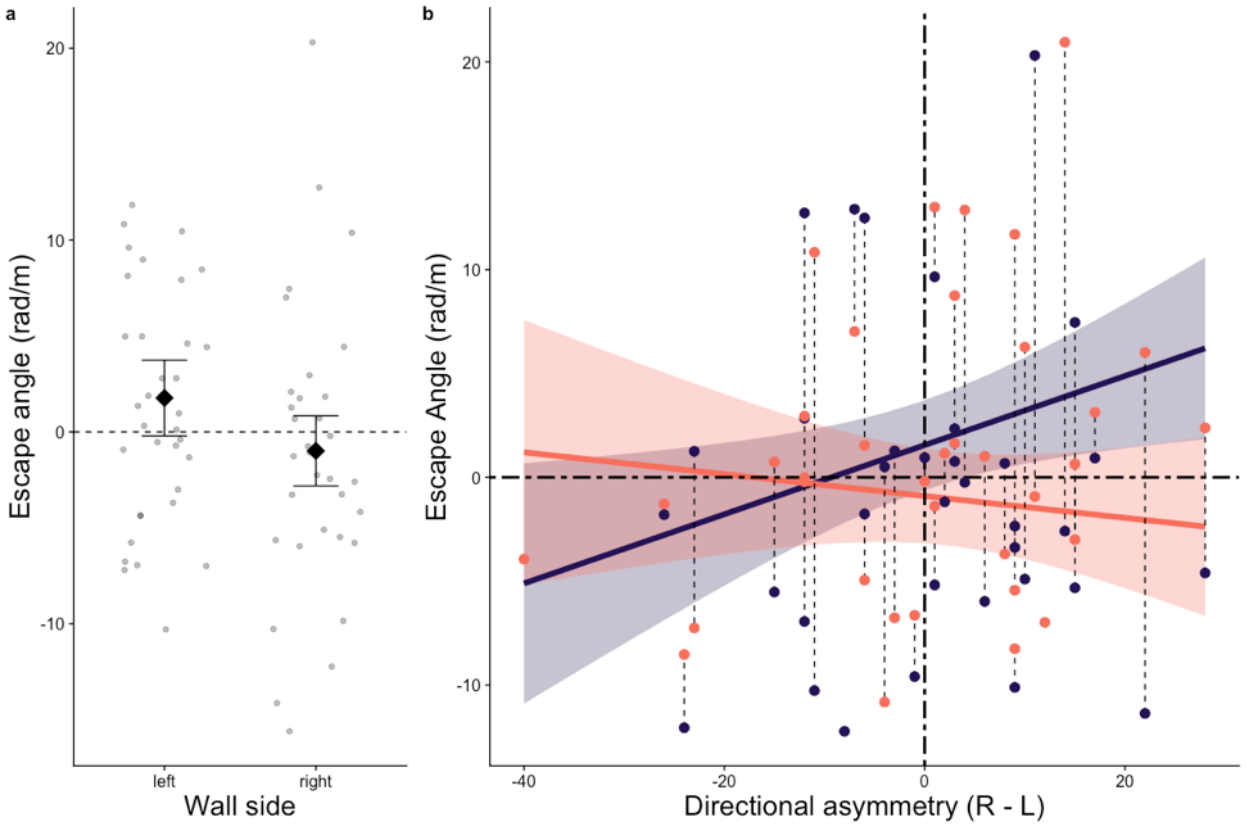

Figure 41. (a) Average angle of escape when stickleback had the arena wall on their left or right. (*b*) Changes in escape angle with directional asymmetry (DA), when responding to drops from either the left (purple) or right (pink). DA calculated as a sum of R – L neuromast counts for each neuromast stitch. (*a*) Diamonds are estimated marginal means (EMMs) with 95% CI error bars, and circular points are the average response of individuals jittered for visibility. (*a*) Lines are EMMs with the shaded region indicating a 95% CI and points connected by dotted lines are the average response per side for each individual. All EMMs are averaged over all predictors other than the one being visualized.

Table 11. Effects of individual neuromast stitch right directional asymmetry (DA; right - left) in neuromast count on the difference in escape angle between drops from the left and right (left - right). Adjusted p-values have been Bonferroni adjusted for multiple comparisons (n = 13). Estimate is the change in escape angle per neuromast, whereas scaled estimate is the change in escape angle per standard deviation of neuromast counts for that stitch. Stitches with significant effect are underlined, and stitches with significant effect after correcting for multiple comparisons are also bolded.

Stitch	χ^2	p (adjusted)	estim. ± se	scaled estim. ± se
AP	0	0.981 (1)	-0.255 ± 0.332	-0.74 ± 0.962
SO	0.14	0.711 (1)	-0.326 ± 0.379	-0.779 ± 0.906
ET	7.71	0.006 (0.072)	-1.072 ± 0.422	-2.183 ± 0.86
IO	0.12	0.724 (1)	-0.237 ± 0.245	-0.89 ± 0.919
OR	0.51	0.475 (1)	-0.375 ± 0.378	-0.904 ± 0.911
MD1	5.66	0.017 (0.225)	-0.746 ± 0.275	-2.044 ± 0.753
MD2	0.22	0.638 (1)	-0.189 ± 0.203	-1.128 ± 1.213
PO	0.02	0.89 (1)	-0.275 ± 0.366	-0.717 ± 0.954
OT	0.11	0.741 (1)	0.344 ± 0.41	0.796 ± 0.949
ST	0.23	0.633 (1)	-0.093 ± 0.239	-0.376 ± 0.971
Ma	0.78	0.378 (1)	0.283 ± 0.237	1.126 ± 0.944
Mp	0.02	0.889 (1)	-0.071 ± 0.092	-0.7 ± 0.914
CF	0.13	0.718 (1)	-0.273 ± 2.011	-0.138 ± 1.018

4.4.2 Vibration attraction behaviour

Experimental design

Fish travelled 2.24 [1.77, 2.80] m per three-minute vibration attraction behaviour (VAB) video on average. However, the distance travelled was much higher during trial *a* relative to other trials, was less when fish were in the VAB tank second, and differed among tanks (trial:

$\chi^2_3 = 262$, $p < 0.001$; tank sequence: $\chi^2_1 = 26.3$, $p < 0.001$; tank ID: $\chi^2_2 = 7.7$, $p = 0.021$; Fig. 42a-c). Group did not have a significant effect on distance travelled ($\chi^2_9 = 9.1$, $p = 0.432$).

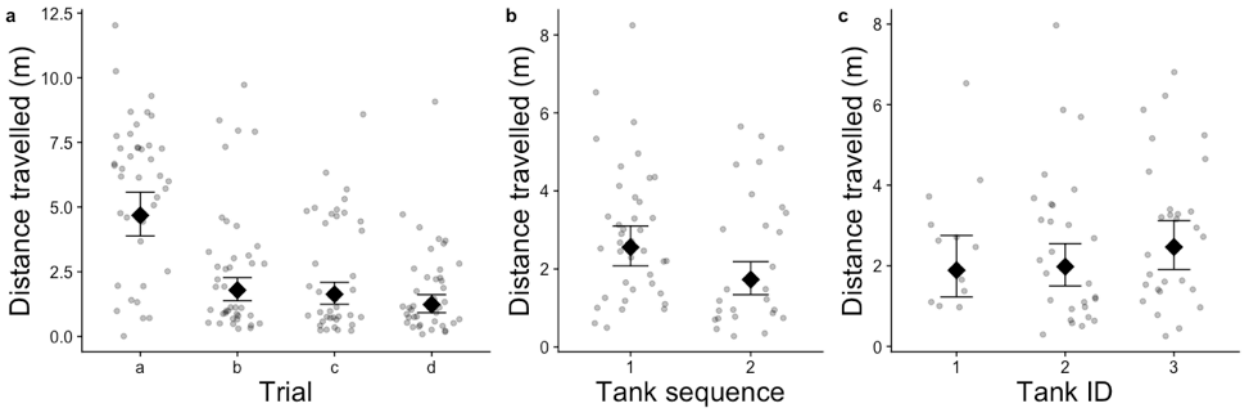

Figure 42. Distance travelled among (*a*) trials, with (*b*) tank sequence and with (*c*) tank ID. Diamonds are estimated marginal means (EMMs) with 95% CI error bars, and circular points are the average response of individuals jittered for visibility. All EMMs are averaged over all predictors other than the one being visualized.

In each VAB video 2.2 [1.9, 2.6] approaches were made on average. There were fewer approaches after trial *a* and variation in approaches among tanks (trial: $\chi^2_3 = 71.9$, $p < 0.001$; tank sequence: $\chi^2_3 = 7.2$, $p = 0.007$; tank ID: $\chi^2_2 = 11.9$, $p = 0.003$; Fig. 43a-c). Group had a near significant effect on the number of approaches ($\chi^2_9 = 16.2$, $p = 0.062$) and test sequence had no effect ($\chi^2_1 = 2.4$, $p = 0.12$).

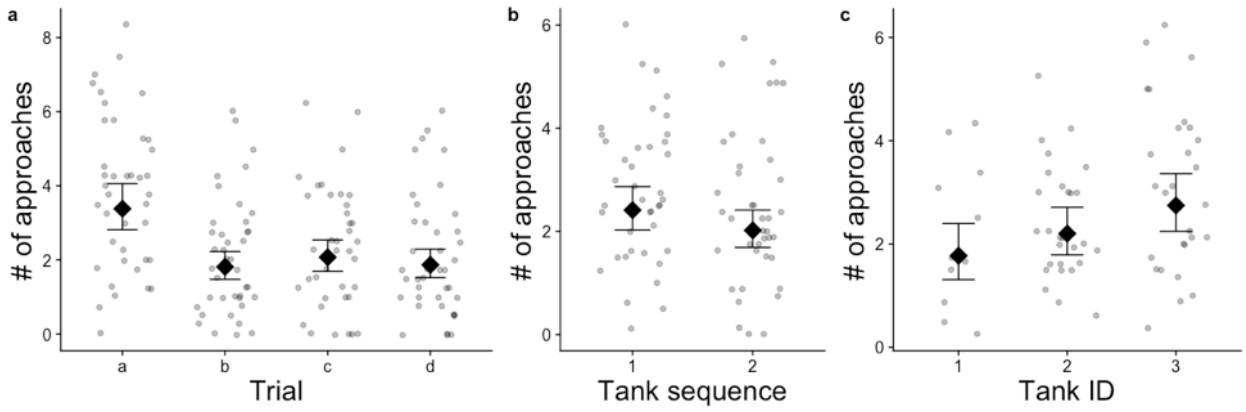

Figure 43. The number of approaches among (*a*) trials, with (*b*) tank sequence and with (*c*) tank ID. Diamonds are estimated marginal means (EMMs) with 95% CI error bars, and circular points are the average response of individuals jittered for visibility. All EMMs are averaged over all predictors other than the one being visualized.

The average time spent in the center was 28.6 [22.8,36.0] s, which increased in subsequent trials and when the fish was in the VAB tank second (trial: $\chi^2_3 = 31.0$, $p < 0.00$; tank sequence: $\chi^2_1 = 4.0$, $p = 0.045$; Fig. 44a-b). Tank ID ($\chi^2_2 = 4.5$, $p = 0.105$) and group ($\chi^2_1 = 7.2$, $p = 0.615$) had no significant effect on time spent in the center.

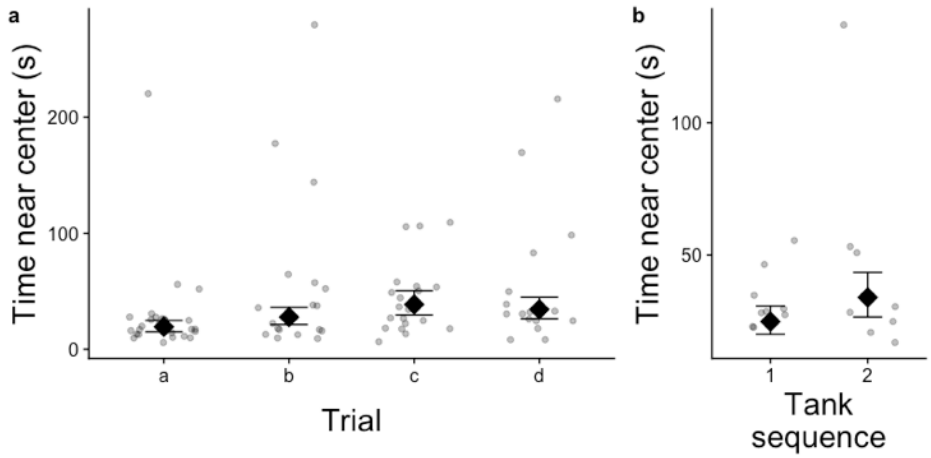

Figure 44. Changes in time near center rod among (*a*) trials and with (*b*) tank sequence. Diamonds are estimated marginal means (EMMs) with 95% CI error bars, and circular points are the average response of individuals jittered for visibility. All EMMs are averaged over all predictors other than the one being visualized.

VAB and morphology

Neither the 60 Hz stimulus or 20 Hz stimulus induced greater travel distance or number of approaches when compared to controls (all $t_{437\text{-}622} \leq 1.67$, $p \geq 0.218$). However, more time was spent in the center during the 20 Hz than control stimuli for trial *d*, ($t_{431} = 3.5$, $p = 0.002$; trial × stimulus: $\chi^2_6 = 16.8$, $p = 0.010$; Fig. 45a). The effect of oscillatory stimuli was not modulated by any morphological characteristics (all × stimulus: $\chi^2_2 \leq 1.1$, $p \geq 0.578$). Fish with greater AA did not travel as far during VAB trials ($\chi^2_1 = 4.1$, $p = 0.040$; Fig 45b) and no other morphological characteristics affected any behaviours directly (all $\chi^2_1 \leq 2.1$, $p \geq 0.150$). AA in seven of thirteen stitches had a negative association with distance travelled, and the IO, MA, and Mp stitches had a significant association, although the IO stitch had the only significant association after correction for multiple comparisons (Table 12).

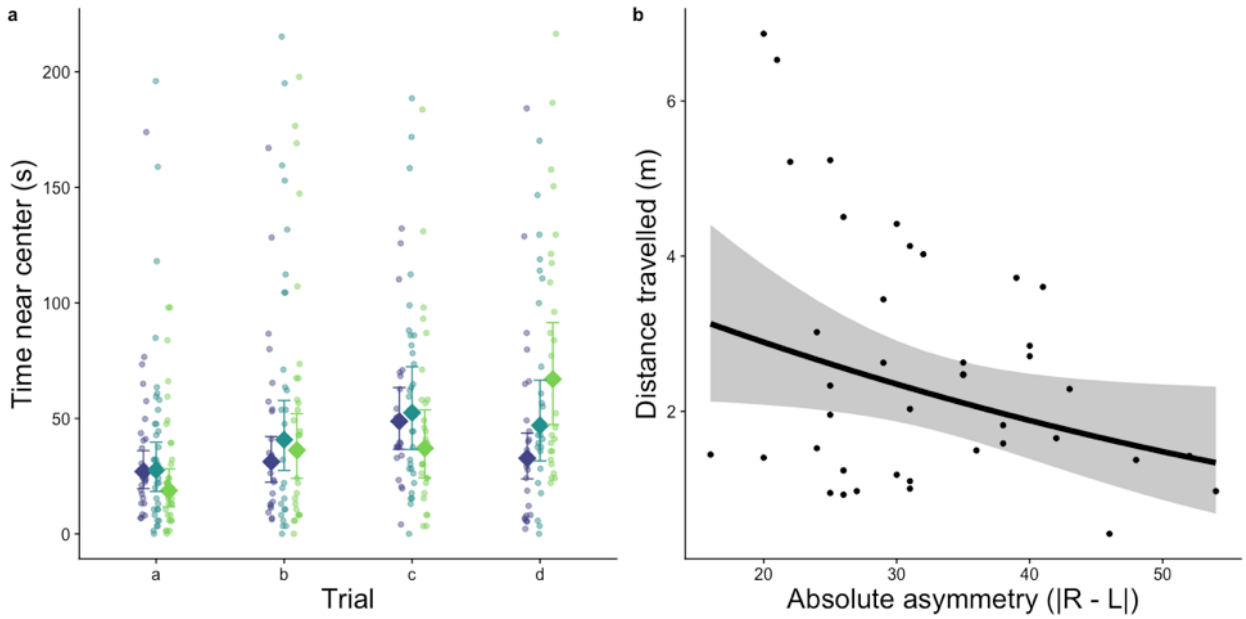

Figure 45. (*a*) Changes in time near center rod with stimulus (purple = control; blue = 60 Hz; green = 20 Hz) among trials. (*b*) Change in distance travelled with absolute asymmetry of neuromasts (AA = |R-L|). (*a*) Diamonds are estimated marginal means (EMMs) with 95% CI error bars, and circular points are the average response of individuals jittered for visibility. (*b*) The line is the EMM with the shaded region indicating a 95% CI, and points are the average response of an individual. All EMMs are averaged over all predictors other than the one being visualized.

Table 12. Effects of absolute asymmetry (AA = |R-L|) of individual stitch neuromast count on distance travelled during vibration attraction behaviour (VAB) trials. Adjusted p-values have been Bonferroni adjusted for multiple comparisons (n = 13). Estimate is the change in cube root transformed distance travelled per neuromast, whereas scaled estimate is the change in cube root transformed distance travelled per standard deviation of neuromast counts for that stitch. Stitches with significant effect are underlined, and stitches with significant effect after correcting for multiple comparisons are also bolded.

Stitch	χ^2	p (adjusted)	estim. ± se	scaled estim. ± se
AP	0.04	0.842 (1)	-0.006 ± 0.03	-0.027 ± 0.133
SO	0.04	0.838 (1)	-0.007 ± 0.036	-0.028 ± 0.136
ET	3.4	0.065 (0.849)	0.03 ± 0.016	0.248 ± 0.134
IO	**9.78**	**0.002 (0.023)**	**0.02 ± 0.006**	**0.412 ± 0.132**
OR	2.14	0.143 (1)	0.005 ± 0.003	0.199 ± 0.136
MD1	0.06	0.814 (1)	-0.026 ± 0.109	-0.04 ± 0.168
MD2	2.75	0.097 (1)	-0.016 ± 0.009	-0.132 ± 0.08
PO	0.03	0.865 (1)	0.003 ± 0.016	0.013 ± 0.076
OT	0.36	0.551 (1)	0.006 ± 0.011	0.044 ± 0.074
ST	0.01	0.938 (1)	0.001 ± 0.011	0.006 ± 0.083
Ma	7.25	0.007 (0.092)	-0.042 ± 0.015	-0.186 ± 0.069
Mp	4.02	0.045 (0.585)	-0.039 ± 0.019	-0.148 ± 0.074
CF	4.64	0.031 (0.407)	-0.021 ± 0.01	-0.171 ± 0.08

Laterality and morphology

Fish tended to orient themselves with the wall on the right more often than the left (proportion wall on right ± se = 0.56 ± 0.02; $\chi^2_1 = 3.0$, p = 0.085). Fish with few neuromasts were more likely to orient with the wall on their left, whereas fish with many neuromasts were more likely to orient with the tank wall on their right ($\chi^2_1 = 5.0$, p = 0.025; Fig. 46a). The same trend occurred with increasing standard length, except during the 60 Hz stimulus where the relationship was reversed ($\chi^2_2 = 6.2$, p = 0.044; Fig 46b). Effect of stimuli on positioning along the VAB tank edge was not affected by sex, neuromast count, DA or AA (all × stimulus: $\chi^2_2 \leq 1.8$, $p \geq 0.407$) and sex, DA and AA did not affect positioning directly (all $\chi^2_1 \leq 0.5$, $p \geq 0.496$). Nine of the thirteen stitches were associated with an increase in the number of right wall hugs, including the ET and Ma stitches, whose correlation was significant after correction for multiple comparisons (Table 13).

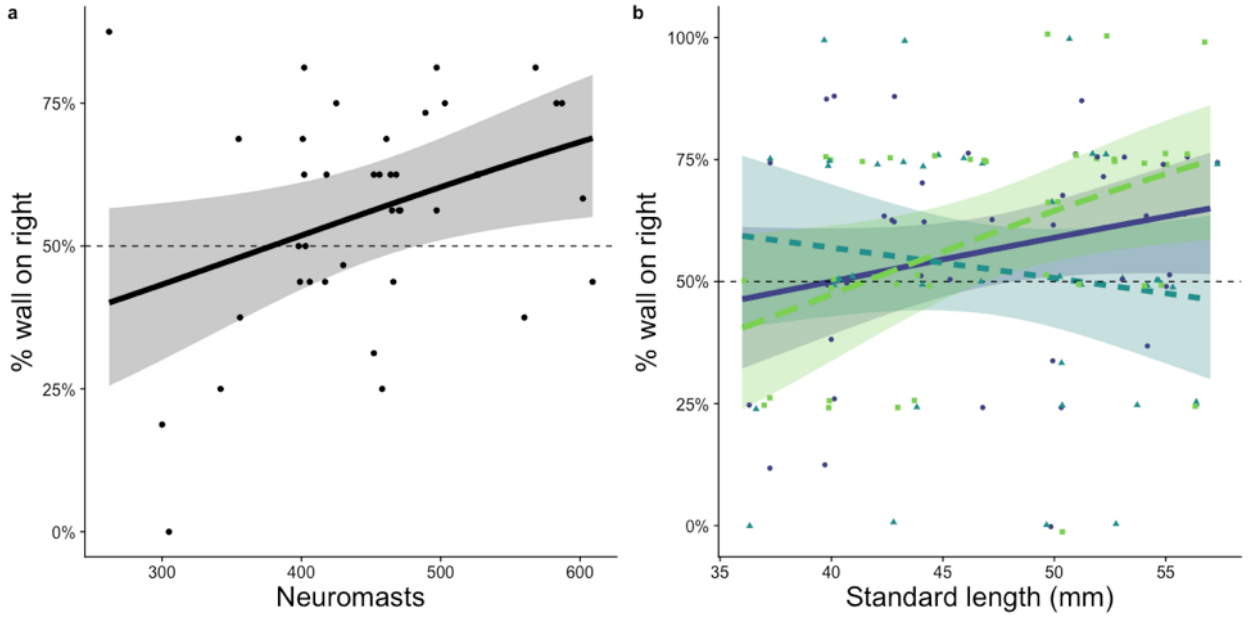

Figure 46. Changes in proportion of time with the outer wall on the right with (*a*) neuromast count and (b) standard length (SL) across stimuli (purple circles / solid line = control; blue triangles / dotted line = 60 Hz; green squares / dashed line = 20 Hz). Lines are estimated marginal means (EMMs) with the shaded region indicating a 95% CI and points are the average response of an individual jittered for visibility. All EMMs are averaged over all predictors other than the one being visualized.

Table 13. Effects of individual stitch neuromast count on time spent with the outer wall on the right side during VAB trials. Adjusted p-values have been Bonferroni adjusted for multiple comparisons (n = 13). Estimate is the change in log-odds of having the outer wall on the right per neuromast, whereas scaled estimate is the change in log-odds of having the outer wall on the right per standard deviation of neuromast counts for that stitch. Stitches with significant effect are underlined, and stitches with significant effect after correcting for multiple comparisons are also bolded.

Stitch	χ^2	p (adjusted)	estim. ± se	scaled estim. ± se
AP	0.03	0.871 (1)	0.004 ± 0.026	0.024 ± 0.146
SO	2.14	0.143 (1)	0.029 ± 0.02	0.205 ± 0.14
ET	**9.37**	**0.002 (0.029)**	**0.143 ± 0.047**	**0.445 ± 0.145**
IO	2.65	0.104 (1)	0.025 ± 0.015	0.213 ± 0.131
OR	1.53	0.217 (1)	0.034 ± 0.028	0.162 ± 0.131
MD1	0.26	0.609 (1)	0.01 ± 0.02	0.068 ± 0.134
MD2	0.12	0.732 (1)	-0.006 ± 0.019	-0.048 ± 0.141
PO	0.04	0.842 (1)	-0.006 ± 0.03	-0.027 ± 0.133
OT	0.04	0.838 (1)	-0.007 ± 0.036	-0.028 ± 0.136
ST	3.4	0.065 (0.849)	0.03 ± 0.016	0.248 ± 0.134
Ma	**9.78**	**0.002 (0.023)**	**0.02 ± 0.006**	**0.412 ± 0.132**
Mp	2.14	0.143 (1)	0.005 ± 0.003	0.199 ± 0.136
CF	0.06	0.814 (1)	-0.026 ± 0.109	-0.04 ± 0.168

The proportion of left and right approaches to the center were the same (proportion right approaches ± se = 0.522±0.19; $\chi^2_1 = 1.42$, p = 0.234) and the average angle while in the center was facing directly in (angle ± se = 0.078 ± 0.050; $\chi^2_1 = 2.42$, p = 0.120). During trial *a* fish approached from the right more often during the 60 Hz stimulus and from the left more often during the 20 Hz stimulus (trial × stimulus; $\chi^2_6 = 13.8$, p = 0.032; Fig. 47a). The same trend occurred with angle while in the center (trial × stimulus; $\chi^2_6 = 14.5$, p = 0.241; Fig. 47b). Fish with more neuromasts tended to approach the center from the left more frequently (log-odds ± se = -0.277±0.151; $\chi^2_1 = 3.3$, p = 0.069) and sex, SL, DA and AA had no effect ($\chi^2_1 \leq 0.43$, p ≥ 0.512). No morphological characteristics interacted with stimuli to influence the proportion of right approaches (all × stimulus: $\chi^2_2 \leq 3.1$, p ≥ 0.209). No morphological characteristics influenced the average angle of the fish while in the center, including interactions with stimuli (All $\chi^2_{1\text{-}2} \leq 2.1$, p ≥ 0.348). Nine of thirteen stitches were associated with a greater number of right approaches, and the SO, ET, OT, and ST stitches had a significant association but not after correction for multiple comparisons (Table 14).

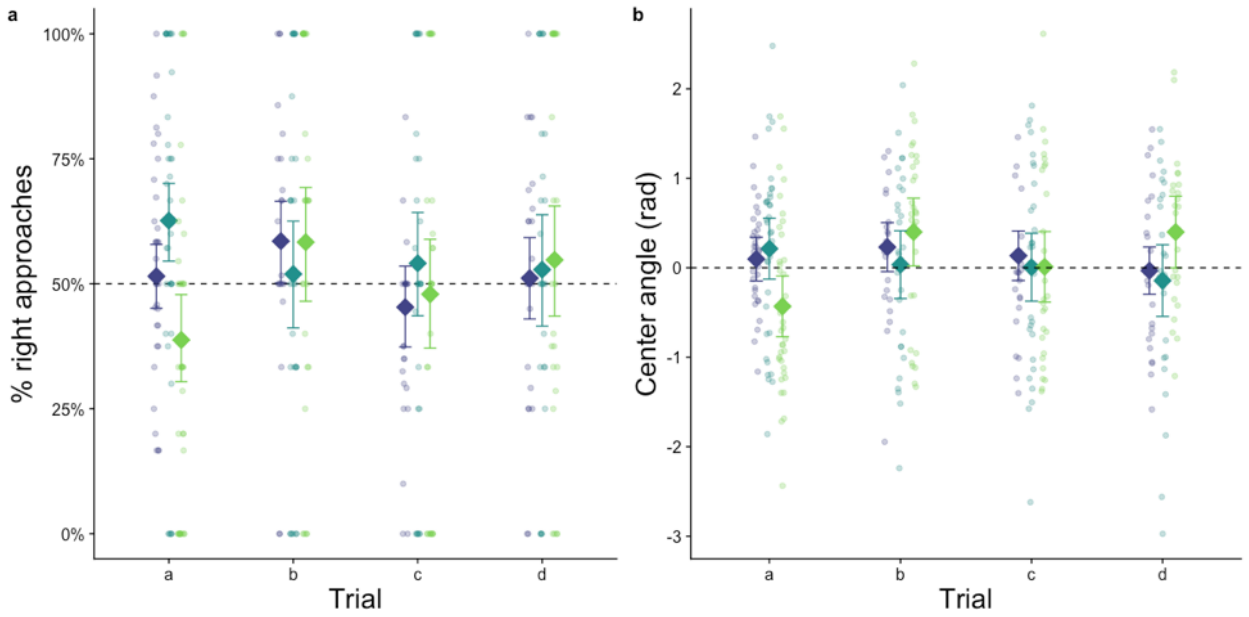

Figure 47. (*a*) Changes in proportion of right approaches with stimulus (purple = control; blue = 60 Hz; green = 20 Hz) and trial. (*b*) Changes in the average angle while in the center with stimulus and trial. Diamonds are estimated marginal means (EMMs) with 95% CI error bars, and circular points are the average response of individuals jittered for visibility. All EMMs are averaged over all predictors other than the one being visualized.

Table 14. Effects of neuromast count of individual neuromast stitches on time spent with the center rod on the right during vibration attraction behaviour (VAB) trials. Adjusted p-values have been Bonferroni adjusted for multiple comparisons (n = 13). Estimate is the change in log-odds of having the center rod on the right per neuromast, whereas scaled estimate is the change in log-odds of having the center rod on the right per standard deviation of neuromast counts for that stitch. Stitches with significant effect are underlined, and stitches with significant effect after correcting for multiple comparisons are also bolded.

Stitch	χ^2	p (adjusted)	estim. ± se	scaled estim. ± se
AP	0.52	0.471 (1)	-0.011 ± 0.015	-0.061 ± 0.084
SO	6.12	0.013 (0.174)	-0.027 ± 0.011	-0.193 ± 0.078
ET	5.8	0.016 (0.208)	-0.064 ± 0.027	-0.198 ± 0.082
IO	2.75	0.097 (1)	-0.016 ± 0.009	-0.132 ± 0.08
OR	0.03	0.865 (1)	0.003 ± 0.016	0.013 ± 0.076
MD1	0.36	0.551 (1)	0.006 ± 0.011	0.044 ± 0.074
MD2	0.01	0.938 (1)	0.001 ± 0.011	0.006 ± 0.083
PO	7.25	0.007 (0.092)	-0.042 ± 0.015	-0.186 ± 0.069
OT	4.02	0.045 (0.585)	-0.039 ± 0.019	-0.148 ± 0.074
ST	4.64	0.031 (0.407)	-0.021 ± 0.01	-0.171 ± 0.08
Ma	2.79	0.095 (1)	-0.007 ± 0.004	-0.137 ± 0.082
Mp	1.11	0.291 (1)	-0.002 ± 0.002	-0.083 ± 0.078
CF	3.61	0.058 (0.748)	0.104 ± 0.055	0.161 ± 0.085

4.4.3 Rheotaxis

Lab characteristics

Fish were displaced 0.7 [0.23, 1.65] m downstream on average. Fish that were tested for rheotaxis prior to predator avoidance were displaced further downstream (rheotaxis first: mean [95% CI] = 1.36 [0.45, 3.03] m; rheotaxis second: mean [95% CI] = 0.03 [0, 0.27]; $\chi^2_1 = 14.4$, $p < 0.001$), downstream displacement varied among groups ($\chi^2_9 = 23.1$, $p = 0.006$), and there was much less net downstream displacement in trial *b* compared to all other trials ($\chi^2_1 = 9.8$, $p = 0.020$; Fig. 48a).

The average distance from the outer edge was 4.70 [4.32, 5.08] cm. Edge distance varied among groups ($\chi^2_9 = 31.4$, $p < 0.001$), and fish tended to position closer to the outer edge in trial *a* than other trials ($\chi^2_3 = 6.7$, $p = 0.082$; Fig. 48b), but test sequence had no effect ($\chi^2_1 = 2.6$, $p < 0.110$).

Fish faced upstream 78.5% [75.0%, 81.6%] of the time, which did not vary with any control parameters (All $\chi^2_{1\text{-}9} \leq 12.0$, $p \geq 0.213$). Cumulative upstream movement was 3.54 [2.72, 4.59] m on average. Upstream movement was greatest in trial *a* ($\chi^2_3 = 9.4$, $p = 0.025$; Fig. 48c) and when rheotaxis behavior was tested prior to predator evasion (rheotaxis first: mean [95% CI] = 4.25 [3.24,5.48] m; rheotaxis second: mean [95% CI] = 2.86 [2.21,3.70] m; $\chi^2_1 = 5.90$, $p = 0.015$), but did not differ among groups ($\chi^2_2 = 11.74$, $p = 0.228$).

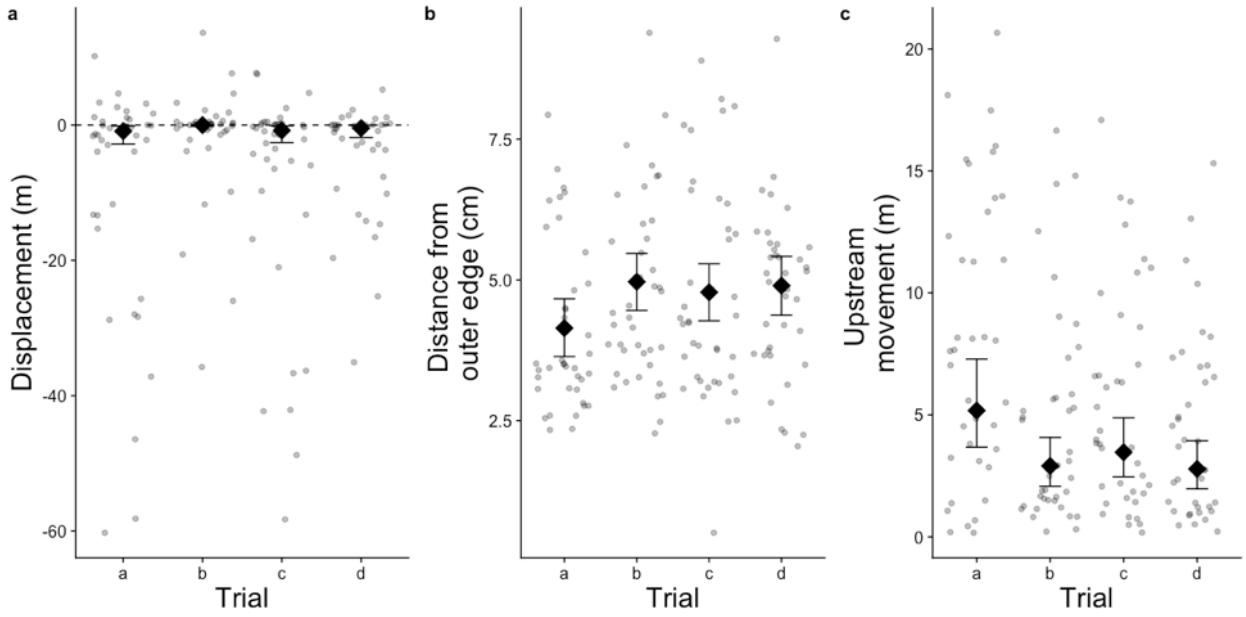

Figure 48. Changes (*a*) net displacement, (*b*) distance from the outer edge and (c) upstream movement among rheotaxis trials. Diamonds are estimated marginal means (EMMs) with 95% CI error bars, and circular points are the average response of individuals jittered for visibility. All EMMs are averaged over all predictors other than the one being visualized.

Laterality and morphology

Females were closer to the outer edge of the tank than males on average (females: mean distance from outer edge [95% CI] = 4.42 [4.06, 4.79] cm; males: mean [95% CI] = 5.17 [4.68 ,

5.65] cm; $\chi^2_1 = 5.09$, $p = 0.023$) and average distance from the outer edge of the tank was greater when water flow was clockwise (clockwise: mean [95% CI] = 5.11 [4.73, 5.48] cm; counterclockwise: mean [95% CI] = 4.48 [4.11, 4.86]; $\chi^2_1 = 5.96$, $p = 0.015$). SL, neuromast count, DA and AA did not affect distance from the outer edge (all $\chi^2_1 \leq 0.5$, $p \geq 0.466$) and no morphological characteristics interacted with flow direction (all $\chi^2_1 \leq 0.6$, $p \geq 0.426$). Net downstream displacement, cumulative upstream movement and time facing upstream were not influenced by any morphological characteristics (all $\chi^2_1 \leq 1.65$, $p \geq 0.199$), including interactions with flow direction (all $\chi^2_1 \leq 1.23$, $p \geq 0.268$).

4.4.4 Consistency of behaviour

Max velocity was the only repeatable behaviour during predator evasion trials (R [95% CI] = 0.45 [0.24,0.71], $p < 0.001$). TTE (R [95% CI] = 0 [0,0.33], $p = 1$), probability of escape (R [95% CI] = 0.02 [0,0.13], $p = 0.40$), laterality of escape probability (R [95% CI] = 0.02 [0,0.12], $p = 0.426$), wall side selection (R [95% CI] = 0.0 [0,0.06], $p = 1$) and escape angle (R [95% CI] = 0 [0,0.36], $p = 1$) were not repeatable. During VAB trials, distance travelled (R [95% CI] = 0.23 [0.07,0.44], $p = 0.019$) and number of approaches (R [95% CI] = 0.41 [0.06,0.51], $p < 0.001$) were repeatable; however, wall side selection (R [95% CI] = 0.0 [0,0.07], $p = 0.5$) and approach laterality (R [95% CI] = 0 [0,0.006], $p = 0.5$) were not repeatable. No rheotaxis behaviours were repeatable, *i.e.* net displacement (R [95% CI] = 0.10 [0,0.30], $p = 0.34$), cumulative upstream movement (R [95% CI] = 0.09 [0,0.29], $p = 0.41$), time oriented upstream (R [95% CI] = 0 [0,0.18], $p = 1$) and laterality of flow regime selection (R [95% CI] = 0.13 [0,0.35], $p = 0.22$).

Laterality of predator avoidance, rheotaxis and VAB were not correlated. However, the laterality of wall side selection was correlated with escape laterality and VAB wall selection was highly correlated with approach angle (Table 15).

Table 15. Correlation in laterality of behaviours. Significantly correlated behaviours have been bolded. Numbers in the upper table are correlation coefficients, and bracketed numbers are 95% CI.

Correlation	(Rheo.) edge dist.	(Pred.) wall side	(Pred.) esc. side	(VAB) wall side	(VAB) appr. side
(Rheo.) edge dist.	-				
(Pred.) wall side	-0.17 [-0.46,0.16]	-			
(Pred.) esc. side	0.05 [-0.29,0.38]	**0.36 [0.03,0.62]**	-		
(VAB) wall side	-0.2 [-0.49,0.12]	0.15 [-0.,18,0.45]	0.03 [-0.31,0.36]	-	
(VAB) appr. side	-0.14 [-0.44,0.18]	-0.11 [-0.42,0.21]	0.03 [-0.3,0.36]	**-0.47 [-0.68,-0.17]**	-
p-values	(Rheo.) edge dist.	(Pred.) wall side	(Pred.) esc. side	(VAB) wall side	(VAB) appr. side
(Rheo.) edge dist.	-				
(Pred.) wall side	0.31	-			
(Pred.) esc. side	0.77	**0.03**	-		
(VAB) wall side	0.22	0.37	0.87	-	
(VAB) appr. side	0.39	0.5	0.85	**< 0.001**	-

4.5 Discussion

I have found evidence of laterality in mechanosensation behaviour and an association between neuromast count asymmetry and laterality; however, the extent is limited. When evading a model predator stimulus, stickleback were more likely to expose their left side, and they were more likely to initiate escape behaviour when the stimulus came from the right. Furthermore, stickleback with few neuromasts were more likely to escape when the stimuli came from the left side. Neuromasts also influenced escape behaviour kinematics inconsistently. Stickleback with more neuromasts escaped more slowly, stickleback with more neuromasts on the right had higher average escape velocity and time to escape (TTE) declined with increased absolute asymmetry of neuromast counts (AA) when responding to drops from the right but

increased with AA when responding to drops form the left. Stickleback with more neuromasts on the right also escaped towards the left more often, whereas stickleback with more neuromasts on the left escaped towards the right more often. Stickleback did not display vibration attraction behaviour (VAB) towards 20 Hz or 60 Hz stimuli. Despite the lack of VAB, stickleback tended to face the arena's outer wall with their right side, with a stronger right bias in stickleback with more neuromasts. Neuromasts did not influence rheotaxis behaviour; however, stickleback occupied a slower flow regime when consistently making left turns (clockwise flow). The only case of sexual dimorphism in behaviour was flow regime selection during rheotaxis, and standard length showed some weak association with VAB laterality. No individual stitches stood out as a consistent predictor of either predator evasion, VAB or rheotaxis behaviour, rather most stitches tended have a similar effect on behaviour, suggesting the integration of information across the lateral line rather than functional specialization of individual stitches. No lateralized behaviours were repeatable; however, few non-lateralized behaviours were repeatable either, *i.e.* max escape velocity, distance travelled during VAB and number of VAB approaches. Usually, behaviour during the first trial was markedly different from the following three, including changes in laterality.

Laterality in predator evasion is common but inconsistent, in both my experimentation and across studies. Stickleback were most likely to respond to drops that came from the right; however, they were also more likely to place their right side against the arena's wall. The preference to expose the left side and respond to stimuli from the right may suggest that the stickleback were more effective at determining that the simulated predatory stimulus was not a true threat when the stimuli came from their left. The notion that initiating escape behaviour was due to a misidentification of the mechanosensory stimuli is further supported by fish with fewer

neuromasts responding more often and more vigorously to drops. Dominance in the function of neuromasts on the left side would explain why neuromasts influence escape probability more when drops came from the left, and the reduced intensity of response when individuals have more neuromasts on the left. Interestingly, a left bias in neuromasts is also associated with feeding behaviour in blind Mexican cavefish (Fernandes et al. 2018). However, the trend I observed differs from the most directly comparable study of the Australian lungfish, *Neoceratodus forsteri* (Krefft, 1870), which found that lungfish were more likely to escape to the left in response to a vertically plunging model predator (Lippolis et al. 2009). Predator evasion is also variable among other species, as Heuts (1999) found two species that preferred to escape to the right and four with no directional bias in escape behaviour when startled by a mechanosensory stimulus. Laterality of escape response also differs between juvenile and adult goldbelly topminnows, *Girardinus falcatus* (Eigenmann, 1903), with mature individuals exhibiting stronger laterality than juveniles (Cantalupo et al. 1995). Furthermore, there is contrasting evidence for the advantage of lateralized escape response. Lateralized shiner perch, *Cymatogaster aggregata* (Gibbons, 1854), exhibited shorter latency, greater distance travelled and higher turning rates than non-lateralized individuals when responding to a plunging model predator (Dadda et al. 2010). Whereas lateralized female *G. falcatus* had no such advantage when responding to visual predatory stimuli (Agrillo et al. 2009). Overall, there does not seem to be a consistent population-level side bias in escape behaviour among fishes, a trend which occurs in other potentially lateralized behaviours (Bisazza et al. 1997b, 2000a; Sovrano et al. 2001) and other taxa such as amphibians (Lippolis et al. 2002).

Drawing broad conclusions from studies of laterality in predator evasion is made difficult by two primary factors. First, due to inconsistent predatory stimuli and laterality metrics

across studies, it is impossible to differentiate between a difference due to species or context versus lab procedure. Second, many metrics of lateralized behaviour are ambiguous with regard to which side is dominant and why. For example, a stronger response to predators attacking from the left may be due to stronger musculature on the right (Heuts 1999) or a preference for viewing predators with the left eye (Bisazza et al. 1997b, a). Given that the model predator is not an actual threat, a more vigorous escape when attacked from the left may be indicative of greater acuity or propensity for generating false positives by the sensory structures on the left, with the fishes perceived level of threat influenced the most likely interpretation (Helfman 1989). Since escape behaviour does not always improve survival (Nair et al. 2017) and is energetically costly (Domenici and Blake 1997), further nuance and a cost-benefit framing are required for understanding the functional ecology of laterality.

While I found an association between escape behaviour and lateral line morphology, I cannot exclude the influence of visual sensory information. Despite the use of water to minimize the amount of 'predator-like' visual stimuli during testing, visual and mechanosensory information were present during escape response trials and visually mediated response occurred in at least 6% of trials. This confounding factor is not only important as it reduces the power of my experiments in determining the role of the lateral line in escape behaviour, but it also affects interpretations of side dominance. Innervation of Mauthner cells by mechanosensory afferents is predominantly ipsilateral (Mirjany and Faber 2011), whereas innervation of the optic tectum (Schwassmann and Kruger 1965) and nucleus isthmi (Northmore 1991) by the optic nerve is predominantly contralateral. These opposing innervation patterns mean that an individual who is right-lateralized would have a dominant left eye and/or the right side of the lateral line, putting the two sensory modalities at odds. Furthermore, visual and mechanosensory stimuli may be

required to initiate escape response (McIntyre and Preuss 2019), and both modalities show evidence of integration of both ipsilateral and contralateral stimuli (Mirjany and Faber 2011; Gebhardt et al. 2019), suggesting that they do not operate entirely independently. Despite this, laterality in different modalities is often independent (McGreevy and Rogers 2005; Oltedal and Hugdahl 2017).

Lateralized behaviour may be causing neuromast asymmetry due to abrasion. During fluorescent microscopy, it was clear that the MD1 and Mp stitches often had damaged or missing neuromasts, suggesting that fish that tended to escape towards the arena's outer wall would have lost neuromasts on that side. The average escape trajectory was opposite of neuromast asymmetry, supporting abrasion; however, lateralized behaviour does not explain why there is only interaction between neuromast asymmetry and escape trajectory when stickleback were responding to drops from the left. Abrasion would also explain why less active fish tended to have more neuromasts, but not why laterality would differ with neuromast count. If abrasion of the MD1 and Mp lines drove all associations between laterality and neuromast count, I would expect them to be outliers in the individual stitch analyses. As the MD1 and Mp stitches did not consistently drive associations between neuromast count and behaviour, natural variation in neuromast counts likely does play a role in determining behaviour.

Stickleback do not exhibit VAB. A lack of mechanosensory mediated prey localization in stickleback is to be expected given that only cave varieties of *A. mexicanus* exhibit this behaviour (Yoshizawa et al. 2010). While we might expect that stickleback in low light environments, *e.g.* stained lakes, would have a similar adaptation for finding prey in the absence of visual information, these populations typically have undergone a reduction in their number of neuromasts (Chapter 2) rather than the proliferation seen in cavefish (Yoshizawa et al. 2010).

When navigating in the dark, stickleback tended to hug the wall with their right sides, exposing their left. This side bias is the same as in the predator avoidance test and matches the laterality of cavefish exploring novel objects in the dark (Burt de Perera and Braithwaite 2005). The relationship between neuromast count and right biased 'wall hugs' is also opposite in predator evasion and VAB trials. While cavefish use mechanosensation for navigation in the dark (Holzman et al. 2014) and may have a greater ability to develop lateralized mechanosensory navigation behaviour with more neuromasts, if we use VAB as a benchmark, stickleback are not likely to exhibit this adaptation.

Perhaps the most surprising finding of these experiments is the lack of association between neuromast count and rheotaxis behaviour, opposed to the results of Jiang et al. (2017). While Jiang et al. demonstrate that ablation of the entire lateral line affects rheotaxis behaviour, they utilized canonical correlation analysis (CAA) to examine the interaction between natural variation in neuromast counts and rheotaxis behaviour. In short, this generated the ordinal axis with the strongest relationship between three dimensions of rheotaxis behaviour and twelve dimensions of neuromast counts (one for each stitch), regardless of directionality. Thus, a strong positive association between the two primary canonical variables may be due to a mix of positive, and negative associations between rheotaxis behaviour and neuromast counts and this is likely what occurred in Jiang et al. (2017). Wild-caught, and lab-reared fish also showed inconsistency in the directionality and extent of the association between rheotaxis behaviour and natural variation in neuromast counts, further suggesting that there is no clear linear relationship between neuromast number and rheotaxis behaviour. While the lateral line is important for rheotaxis in stickleback, natural variation in neuromast counts within populations likely does not have a linear relationship with displacement downstream.

Laterality and sexual dimorphism in rheotaxis are subtle. As the rheotaxis tack's outer edge had faster flow, this population of stickleback prefered to occupy a faster flow regime when the stonger mechanosensory stimuli came from the left side. Whether this behaviour indicates dominance of one side is unclear; however, this behaviour is not associated with the lateral line. This asymmetry may be due to biases in musculature (Heuts 1999), but this is speculative. It is also unclear why females would prefer to remain in a faster flow regime. While females typically have fewer neuromasts than males (Ahnelt et al. 2021; Chapter 2), neuromast ablation did not affect flow regime selection by stickleback (Jiang et al. 2017). Laterality and sexual dimorphism in rheotaxis are not likely associated with the lateral line.

Despite sexual dimorphism being widespread in stickleback behavioural ecology, I observed little to no sexual dimorphism in behaviour. The most likely explanation for this is that the ecology of Eagle's lake does not promote morphological sexual dimorphism. Sexual dimorphism typically arises due to a differentiation of the sexes along a benthic-limnetic axis, which corresponds to differences in multiple aspects of ecology (Reimchen and Nosil 2001c, 2004; Reimchen et al. 2008, 2016). Given that Eagle's lake is small and relatively shallow, there has probably not been the ecological opportunity for sexual dimorphism to arise. While there is evidence of sexual dimorphism in brain volume of stickleback (Kotrschal et al. 2012), either Eagle's lake does not have such dimorphism, or it had not elicited any functional consequences in the aspects of behaviour studied here.

I found that the laterality of individuals changed over time through both consistent and inconsistent mechanisms. Changes in the laterality of behaviours with subsequent testing are common. Juvenile fish may swap their side bias during predator evasion when tested multiple times for laterality and exhibit opposite laterality once mature (Cantalupo et al. 1995). Laterality

of detour behaviour can also change with time in captivity (Bisazza et al. 1997b), the novelty of stimuli (Burt de Perera and Braithwaite 2005), over months (Bisazza et al. 1998a), and over minutes (Sovrano et al. 2001). My data suggest that laterality also changes with the novelty of stimuli in a few hours. The right bias in wall hugging behaviour during the predator evasion trial was lost after trial *a*, right bias in escape probability was lost by trial *d,* and sidedness of approaches to the center of the VAB tank also changed after trial *a*. While these changes in behaviour cannot be viewed independently from the overall reduction in activity level in subsequent trials, changes in laterality suggest that novelty of the stimuli is important for the lateralization of behaviour. I suggest that testing behaviour after a very long period of acclimation to both the environment and test stimuli would give a more accurate representation of behavioural laterality in natural environments.

Recent concern has grown over the use of T-mazes in assessing the laterality of fishes, as the laterality of individuals is not consistent with repeat testing (McLean and Morrell 2020; Roche et al. 2020). Laterality in stickleback also does not appear to be repeatable across the behaviours I tested. However, many non-lateralized behaviours which are likely ecologically relevant, such as the probability of initiating escape behaviour, were also not repeatable. The lack of repeatability across behaviours suggests that all metrics of behaviour should be examined for repeatability before their use in studies of animal behaviour. The commonly used categorization of fish as bold or shy has been tested for repeatability multiple times and appears to be repeatable, although as with laterality, the degree of repeatability differs with context and among study systems (Wilson and Stevens 2005; Wilson and Godin 2009; Mazué et al. 2015; Jolles et al. 2019). There is also a degree of artificiality in repeat testing as it requires breaking the continuity of a fish's behaviour that does not occur in the wild. Initially, while examining

repeatability, I found that most behaviours were repeatability to some degree, including laterality. However, this was due to mistakenly including multiple data from a single behavioural trial and individuals who started on one side tended to stay on that side. While this is a clear confounding factor in a lab experiment, it more accurately reflects the experience of fish in a natural habitat: at no point in the life history of most fish are they suddenly moved to a new environment in a net. I suggest that there are metrics of laterality that are repeatable in a natural context; however, more work is needed in order to determine the best behaviours to measure. Furthermore, repeatability testing should be done with minimal disturbance between repeat trials, to more accurately reflect the natural ecology of fishes.

There was no association between the directionality of predator evasion, navigation in the absence of light and during rheotaxis, but biases in how individuals orient themselves within the tank influence the laterality of their subsequent behaviour. As stickleback were more likely to initiate escape behaviour when stimuli came from the same side as the one they had against the arena wall and more likely to pass objects with the side facing away from the wall, habitat structure, and the interaction of the individual with it likely determines much of the lateralization of inter/intraspecific interactions. Thus, assessing the laterality of an individual's orientation prior to stimuli such as predators, prey or conspecifics, is important context that is often ignored in studies of laterality. The importance of prior orientation is further evidence that the assessment of laterality as a continuity of behaviour is important in understanding its temporal dynamics.

Individual stickleback are lateralized in habitat orientation, which is associated with the neuromast count of their lateral line. While there is not a clear one-sided dominance in the function of the lateral line of stickleback, it likely plays a role in many aspects of life history, especially the evasion of predators. The short timescales that laterality changes over suggest that

this behavioural trait is rapidly adaptive, rather than being the result of deeply rooted evolutionary history (Wiper 2017) and the presence of feedback loops such as lateralized behaviour creating asymmetric abrasions which further bias sensory information emphasizes the importance of events within the life history of individuals. Thus, the laterality of populations is likely highly variable over time, and small scales changes in ecology such as the trade-off between density-dependent selection and population coordination dynamics are its key drivers (Vallortigara and Rogers 2005). This discussion has been focused on laterality in fishes for the sake of clarity, but the same dynamical processes must play a role across all Bilateria, including humans.

Chapter 5: Synthesis

In my thesis research, I have examined the extent to which lateral line neuromast count and neuromast count asymmetry differ among populations of threespine stickleback inhabiting different ecological regimes and the behavioural consequences of variation in neuromast count and neuromast count asymmetry within a population.

Ecology shapes lateral line morphology. Lateral line morphology is influenced by abiotic flow regime (Kelley et al. 2017; Rudolfsen et al. 2018), predator-prey interaction (Pohlmann et al. 2004; Bassett et al. 2007; Junges et al. 2010) and schooling (Partridge and Pitcher 1980; Mekdara et al. 2018). Given the right selective landscape, functional specializations in the lateral line, such as obstacle detection (Holzman et al. 2014) or surface wave detection (Bleckmann et al. 1989) can also evolve. While the contemporary evolution underlying this deeply seeded functional diversity is cryptic, observing threespine stickleback in adapting to a wide diversity of ecological landscapes helps elucidate this process. Across coastal British Columbia, stickleback range from completely lacking neuromasts on their lateral plates to a proliferation of neuromasts beyond the oceanic ancestral phenotype. This range of morphologies is due to the diversity of habitats in coastal British Columbia and interaction with other traits, recreating a model of interspecific divergence in microcosm. Water chemistry imposes a stronger selective effect than spectral regime on the development of neuromasts in low-light acidic environments, and the presence of predatory fishes promotes the proliferation of buttressing plate neuromasts. The differences in neuromast count among freshwater localities of divergent ecology elucidate some of the proximal mechanisms for the differences between oceanic and freshwater stickleback (Wark and Peichel 2010; Ahnelt et al. 2021). The rate of adaptation to this diversity of environments is fast and likely in-part due to phenotypic plasticity, as seen by the large increase

in neuromasts over just a couple generations in Drizzle Pond and the more gradual intergenerational change observed in Roadside Pond. Thus, lateral line morphology joins the growing list of rapidly adapting traits in stickleback (Spoljaric and Reimchen 2007; Leaver and Reimchen 2012; Marques et al. 2018), with the potential for epigenetic modification to infleunce lateral line phenotype. Adaptation in the lateral line facilitates the colonization of new habitats in addition to facilitating dispersal (Jiang et al. 2017).

Morphological asymmetry is widespread and highly variable. While slight deviations from symmetry are ubiquitous among Bilateria, they have typically been used as an indicator of developmental instability (Beasley et al. 2013) rather than a potentially functional trait. However, the evolution of stark directional asymmetry by gradual incrementation, such as that of flatfishes (Friedman 2008), suggests that deviations from symmetry can incur a selective advantage, given the exposure of a bilaterally symmetrical ancestor to the right ecological landscape. While asymmetry in many aspects of stickleback morphology exhibit a possible intermediate between full directional asymmetry and purely fluctuating asymmetry (Reimchen 1980; Bell et al. 1985; Bergstrom and Reimchen 2003), the lateral line does not display a consistent side bias. However, ecology still shapes non-directional asymmetry in the lateral line of threespine stickleback. The attenuation of asymmetry in the lateral line of populations with limited light availability suggests a functional trade-off between mechanosensation and vision, such as seen in bats (Wu et al. 2018) but on a finer scale. It is difficult to determine the functional implications of these subtle, non-directional changes in sensory structure symmetry, given the redundant innervation of neuromasts (Liao and Haehnel 2012). However, I suggest that this functional redundancy has arisen, in part, as an adaptation to these deviations from symmetry. Whether due to ontogeny or abrasion, the symmetry of the lateral line is highly

variable throughout life history and redundant innervation will buffer against these changes in addition to improving signal-to-noise ratio.

The findings of this work support the notion that behavioural laterality is widespread. Invertebrates (Frasnelli 2013) and a diversity of vertebrates (Bisazza et al. 1998b; Leliveld 2019) regularly exhibit laterality. Furthermore, this laterality is highly variable among behaviours and ecological contexts (Bisazza et al. 1997b; O'Shea-Wheller 2019; Jozet-Alves et al. 2019) and can be influenced by sensory structure asymmetry (Hart et al. 2000, p. 200; Lychakov et al. 2006, 2008; Krings et al. 2019), suggesting that behavioural laterality would differ among stickleback from diverse ecological regimes and with asymmetry in their mechanosensory structure. I found evidence of laterality across multiple aspects of stickleback life history, including interaction with lateral line morphology. However, individual lateralization was inconsistent, and there was a stronger association between total neuromast count and laterality than neuromast count asymmetry. My results suggest that population-level laterality can arise without significant individual-level lateralization and that population-level laterality correlates with individual morphology despite a lack of repeatability within individuals, leaving me puzzled. Right biases in low neuromast individuals during predator avoidance and left biases in low neuromast individuals while navigating in the dark may suggest that sensory trade-offs influence laterality and would support the efficient use of neural tissue (Levy 1977) and improved parallel processing (Rogers et al. 2004) as drivers of laterality. Stickleback from stained habitats may also be further lateralized than the clear water population which I examined, as cave varieties of the Mexican tetra exhibit stronger laterality than surface fish (Fernandes et al. 2018)

Laterality and morphological asymmetry are ultimately the same process evolving through two different evolutionary media, and both fields would benefit from being viewed through the opposing lens. Given that laterality must be a behavioural manifestation of structural differences between the two hemispheres of the brain, it too is a form of morphological asymmetry. However, brain structure greatly changes with ontogeny and experiences (Bottjer et al. 1985; Draganski et al. 2006). External morphological asymmetries have typically been viewed as a stochastic process due to random deviations during development, whereas laterality has been viewed as deterministic, shaped by asymmetries in interaction with the environment. However, both must exist somewhere in-between.

By viewing morphological asymmetry as a product of the external environment, we can see how ecology can shape asymmetry beyond the paradigms of relaxed selection (Trokovic et al. 2012) and stress-induced developmental instability (Rott and Press 2003). Behavioural context often shapes laterality (Bisazza et al. 1997b; O'Shea-Wheller 2019; Jozet-Alves et al. 2019), so I expect that it affects external morphological asymmetries as well. One example of behavioural context shaping asymmetry may be the stickleback of British Columbia (Reimchen 1997; Reimchen and Bergstrom 2009). Changes in external morphological asymmetry within the lifetime of individuals also must occur. If asymmetries arise due to developmental instability, there must be some previous point in ontogeny where a trait was symmetrical. The accumulation of scarring will also influence the morphological and behavioural asymmetries of individuals (Reist et al. 1987; Reimchen 1992).

By viewing laterality as a noisy process, which constantly approaches but does not settle on the optimal phenotype, we can elucidate similar temporal dynamics. As temporal patterns in morphological asymmetry unfold over contemporary evolutionary timescales and as a

demographic process within populations (Reimchen 1980; Bergstrom and Reimchen 2003; Rubio et al. 2020), behavioural laterality likely undergoes similar fluctuations within the lifetime of individual organisms. Studies often extend evidence of behavioral laterality as evidence of morphological asymmetry in the brain (Oltedal and Hugdahl 2017), and if taken to its logical extreme, this association between morphological and behavioural asymmetries could be fruitful for understanding the dynamics of asymmetry.

I believe that the evolution of asymmetry usually occurs over short time scales rather than having a common evolutionary history among taxa. It has been suggested that laterality among different species is related due to adaptations in a common ancestor and that evolutionary history can shape individual and population laterality (Bisazza et al. 1998b; Vallortigara et al. 1999; Rogers 2000, 2002; Wiper 2017; Prieur et al. 2019). This evolutionary hypothesis has spurred investigation into the laterality of evolutionary link species such as lungfish (Lippolis et al. 2009) and into the heritability of lateralization (Bisazza et al. 2000b, 2005; Dadda et al. 2007). However, given the high degree of differences among closely related species of fish (Bisazza et al. 1997b, 1998a, 2000a; Heuts 1999; Sovrano et al. 1999, 2001) and the loss of laterality with arbitrary changes to the environment such as the curvature of a T-maze (Bisazza et al. 1997a), I doubt a consistent evolutionary origin of laterality. While the dominance of the left eye for viewing novel stimuli is a common narrative within the field of laterality (Malashichev 2006), the evidence for this interpretation is not immediately clear. For example, mosquitofish tend to view conspecifics with the left eye; however, this is variable among contexts (Bisazza et al. 1997a, 1998a, 1999; Sovrano et al. 1999, 2001; De Santi et al. 2001), and there is variation in eye preference among closely related avian species (Franklin and Lima 2001). The dynamism of laterality among contexts suggests that there is not a deep evolutionary history in which novel

stimuli are preferentially viewed by the left-eye / right hemisphere. Furthermore, while the strength of laterality has a heritable component (Bisazza et al. 2000b, 2005; Dadda et al. 2007), the direction of laterality does not appear to be heritable. The influence of light *in ovo* on laterality differs among species, inducing left dominance, right dominance, increased laterality but with no directional bias and having no effect (Rogers 1990; Dadda and Bisazza 2012; Sovrano et al. 2016; George et al. 2021), suggesting that even the potential for the environment to induce lateralized behaviour does not have a consistent origin among species. Finally, individual laterality may not be repeatable with multiple testing (McLean and Morrell 2020; Roche et al. 2020). I interpret that these differences among studies indicate that laterality arises quickly due to the environment and widespread lateralization among species is indicative of independent evolutionary events rather than deeply rooted adaptation. This conclusion is further supported by my own investigation of threespine stickleback, as their morphological asymmetry changed substantially over a couple generations and their laterality changed within a single day.

Consistent asymmetry in the environment is likely required for the development of high degrees of asymmetry, as demonstrated by species that exhibit strong and consistent morphological or behaviour laterality. Many species that exhibit strong directional asymmetry are substrate-bound (Ludwig 1932; Palmer 2009), providing species with a starkly asymmetric environment to develop asymmetry in response to. These evolutionary dynamics unfold in the asymmetry of scallop shells, in which differences between the left and right shell evolve faster for sessile, substrate-bound species (Sherratt et al. 2017). However, it is important to consider that a benthic life history does not necessitate the breaking of bilateral symmetry but does require breaking of symmetry along at least one body axis. For example, monkfish (*Lophius spp.*) have a relatively similar life history to flatfishes but exhibit dorsoventral compression and

differenttation rather than dextral-sinistral rotation, and barnacles orient rostro-caudally against the substrate rather than bilaterally like scallops. If consistent, environmental asymmetry also affects laterality. During interactions where it is beneficial for two individuals to 'match' their laterality, it would be advantageous for population laterality to evolve. This is a possible explanation for the tendency for juvenile mammals to keep their mother on their right (Karenina et al. 2017) or laterality in species that demonstrate teaching behaviour (Frasnelli et al. 2012; Rogers et al. 2013), since both interacting individuals benefit from the other being able to use its dominant side.

Coordination dynamics can also shape morphological asymmetry, such as the coordination of copulation driving snails to evolve to either dextral or sinistral dominance (Schilthuizen and Davison 2005). Even if an individual is interacting with the abiotic environment, if they can decide the laterality of the interaction consistently, such as in solving rope puzzles, it can be advantageous to be lateralized (Magat and Brown 2009). Furthermore, behavioural anti-symmetry can arise if one or both individuals in an interaction can consistently choose the orientation of interaction. As male fiddler crabs generally start displays and bouts from their burrows (Wolfrath 1993), they can consistently present their dominant side. Yet, since the interaction is competitive, a population bias does not arise. Red crossbills (*Loxia curvirostra*) and lodgepole pine (*Pinus contorta*) also exhibit similar competitive dynamics of asymmetry in an interaction where the crossbill chooses the geometry of interactions (Benkman et al. 2003). Lastly, asymmetric reproductive behaviour and gonadal structure may also support the development of directional or anti-symmetry, depending on sexual selection for coordination or competition (Seligmann 1998; Calhim et al. 2019; Torres-Dowdall et al. 2020). An interesting counter-example is termite fishing in chimpanzees, which does not exhibit consistent laterality

despite chimpanzees being able to continually fish with the same hand (Palmer 2002; Marchant and McGrew 2007). Predator-prey interaction between two motile species seems to be a case where the laterality of two interacting individuals is always at odds, creating strong selective pressure for randomized sidedness and the ability of individuals to respond to stimuli from both sides, which may explain why I found only weak signals of laterality in stickleback predator-prey behaviour. The predator-prey arms race may also explain why handedness of chimp fishing is not as strongly lateralized as their other behaviours. Perhaps it is advantageous for chimps to change handedness in response to termite mound structure and vice versa.

The lateral line of threespine stickleback is a powerful model for investigating the interaction between sensory ecology and asymmetry. The diversity of buttressing plate neuromast counts observed across coastal British Columbia is indicative of the adaptability of the lateral line system and provides a rich adaptive landscape for the development of divergent asymmetries among populations. While the association between morphological asymmetry in the lateral line and mechanosensory laterality is not immediately clear, lateralization is likely to occur across ecological contexts, albeit with inconsistent directionality. I suggest two major avenues of future investigation. One, the role of brain structure asymmetry is pivotal in understanding asymmetry in sensory structures, behavioural laterality and their interaction. While broad-scale metrics like weight and regions of activation in of some regions of the brain have been investigated for laterality, it is likely more fine-scaled structures that are responsible for processes such as functional trade-offs between sensory modalities and context-dependent laterality. Second, further investigation into the repeatability of laterality within individuals is required, not just in the context of whether repeatability occurs but viewed as a dynamic and continuous process. If morphological asymmetry (Leung and Forbes 1996; Beasley et al. 2013)

and laterality (Leliveld 2019; Lesniak 2020) are to be used as indicators of fitness or ecology, a further understanding of their nuances is required. The evolutionary dynamics of morphological and behavioural asymmetry are powerful tools to study evolution under strong canalization (Waddington 1942) and what is required to break it.

References

Agostinelli C, Lund U (2017) R package "circular": Circular Statistics (version 0.4-93). CA: Department of Environmental Sciences, Informatics and Statistics, Ca' Foscari University, Venice, Italy. UL: Department of Statistics, California Polytechnic State University, San Luis Obispo, California, USA

Agrillo C, Dadda M, Bisazza A (2009) Escape behaviour elicited by a visual stimulus. A comparison between lateralised and non-lateralised female topminnows. Laterality 14:300–314

Ahdesmaki M, Fokianos K, Strimmer K (2019) GeneCycle: Identification of Periodically Expressed Genes

Ahnelt H, Ramler D, Madsen MØ, et al (2021) Diversity and sexual dimorphism in the head lateral line system in North Sea populations of threespine sticklebacks, *Gasterosteus aculeatus* (Teleostei: Gasterosteidae). Zoomorphology 140:103–117

Almeida D, Almodóvar A, Nicola GG, Elvira B (2008) Fluctuating asymmetry, abnormalities and parasitism as indicators of environmental stress in cultured stocks of goldfish and carp. Aquaculture 279:120–125

Anfora G, Rigosi E, Frasnelli E, et al (2011) Lateralization in the invertebrate brain: left-right asymmetry of olfaction in bumble bee, *Bombus terrestris*. PLoS ONE 6:e18903

Archambeault SL, Bärtschi LR, Merminod AD, Peichel CL (2020) Adaptation via pleiotropy and linkage: association mapping reveals a complex genetic architecture within the stickleback *Eda* locus. Evol Lett 4:282–301

Baker CF, Montgomery JC (1999) The sensory basis of rheotaxis in the blind Mexican cave fish, *Astyanax fasciatus*. J Comp Physiol A 184:519–527

Barrett RDH, Vines TH, Bystriansky JS, Schulte PM (2009) Should I stay or should I go? The *Ectodysplasin* locus is associated with behavioural differences in threespine stickleback. Biol Lett 5:788–791

Bassett DK, Carton AG, Montgomery JC (2007) Saltatory search in a lateral line predator. J Fish Biol 70:1148–1160

Bates D, Mächler M, Bolker B, Walker S (2015) Fitting linear mixed-effects models using lme4. J Stat Softw 67:1–48

Beasley DAE, Bonisoli-Alquati A, Mousseau TA (2013) The use of fluctuating asymmetry as a measure of environmentally induced developmental instability: A meta-analysis. EcolIndic 30:218–226

Bell MA, Foster SA (1994) Introduction to the evolutionary biology of the threespine stickleback. In: Bell MA, Forster SA (eds) The evolutionary biology of the threespine stickleback 1st edn. Oxford University Press, pp 1–27

Bell MA, Francis RC, Havens AC (1985) Pelvic reduction and its directional asymmetry in threespine sticklebacks from the Cook Inlet region, Alaska. Copeia 1985:437–444

Benkman CW, Parchman TL, Favis A, Siepielski AM (2003) Reciprocal selection causes a coevolutionary arms race between crossbills and lodgepole pine. Am Nat 162:182–194

Bergstrom CA, Reimchen TE (2000) Functional implications of fluctuating asymmetry among endemic populations of *Gasterosteus aculeatus*. Behaviour 137:1097–1112

Bergstrom CA, Reimchen TE (2003) Asymmetry in structural defenses: insights into selective predation in the wild. Evolution 57:2128–2138

Bergstrom CA, Reimchen TE (2005) Habitat dependent associations between parasitism and fluctuating asymmetry among endemic stickleback populations. J Evol Biol 18:939–948

Bisazza A, Cantalupo C, Capocchiano M, Vallortigara G (2000a) Population lateralisation and social behaviour: a study with 16 species of fish. Laterality 5:269–284

Bisazza A, Dadda M (2005) Enhanced schooling performance in lateralized fishes. Proc R Soc B-Biol Sci 272:1677–1681

Bisazza A, Dadda M, Cantalupo C (2005) Further evidence for mirror-reversed laterality in lines of fish selected for leftward or rightward turning when facing a predator model. Behav Brain Res 156:165–171

Bisazza A, De santi A, Vallortigara G (1999) Laterality and cooperation: mosquitofish move closer to a predator when the companion is on their left side. Anim Behav 57:1145–1149

Bisazza A, Facchin L, Pignatti R, Vallortigara G (1998a) Lateralization of detour behaviour in poeciliid fish: the effect of species, gender and sexual motivation. Behav Brain Res 91:157–164

Bisazza A, Facchin L, Vallortigara G (2000b) Heritability of lateralization in fish: concordance of right–left asymmetry between parents and offspring. Neuropsychologia 38:907–912

Bisazza A, J. Rogers L, Vallortigara G (1998b) The origins of cerebral asymmetry: a review of evidence of behavioural and brain lateralization in fishes, reptiles and amphibians. Neurosci Biobehav R 22:411–426

Bisazza A, Pignatti R, Vallortigara G (1997a) Detour tests reveal task- and stimulus-specific behavioural lateralization in mosquitofish (*Gambusia holbrooki*). Behav Brain Res 89:237–242

Bisazza A, Pignatti R, Vallortigara G (1997b) Laterality in detour behaviour: interspecific variation in poeciliid fish. Anim Behav 54:1273–1281

Bjorksten T, David P, Pomiankowski A, Fowler K (2000) Fluctuating asymmetry of sexual and nonsexual traits in stalk-eyed flies: a poor indicator of developmental stress and genetic quality. J Evol Biol 13:89–97

Blaxter JHS, Fuiman LA (1990) The role of the sensory systems of herring larvae in evading predatory fishes. J Mar Biol Assoc UK 70:413–427

Bleckmann H, Tittel G, Blübaum-Gronau E (1989) The lateral line system of surface-feeding fish: anatomy, physiology, and behavior. In: Coombs S, Görner P, Münz H (eds) The Mechanosensory Lateral Line. Springer, New York, NY, pp 501–526

Bottjer SW, Glaessner SL, Arnold AP (1985) Ontogeny of brain nuclei controlling song learning and behavior in zebra finches. J Neurosci 5:1556–1562

Brooks ME, Kristensen K, Benthem KJ van, et al (2017) glmmTMB balances speed and flexibility among packages for zero-inflated generalized linear mixed modeling. R J 9:378–400

Brown EEA, Simmons AM (2016) Variability of rheotaxis behaviors in larval bullfrogs highlights species diversity in lateral line function. PLoS ONE 11:e0166989

Burt de Perera T, Braithwaite VA (2005) Laterality in a non-visual sensory modality — the lateral line of fish. Curr Biol 15:R241–R242

Butler JM, Maruska KP (2016) Mechanosensory signaling as a potential mode of communication during social interactions in fishes. J Exp Biol 219:2781–2789

Calhim S, Pruett-Jones S, Webster MS, Rowe M (2019) Asymmetries in reproductive anatomy: insights from promiscuous songbirds. Biol J Linn Soc 128:569–582

Cantalupo C, Bisazza A, Vallortigara G (1995) Lateralization of predator-evasion response in a teleost fish (*Girardinus falcatus*). Neuropsychologia 33:1637–1646

Casey MB, Martino CM (2000) Asymmetrical hatching behaviors influence the development of postnatal laterality in domestic chicks (*Gallus gallus*). Dev Psychobiol 37:13–24

Colosimo PF, Hosemann KE, Balabhadra S, et al (2005) Widespread parallel evolution in sticklebacks by repeated fixation of *Ectodysplasin* alleles. Science 307:1928–1933

Coombs S, Bleckmann H, Fay RR, Popper AN (eds) (2014) The lateral line system. Springer-Verlag, New York

Coombs S, Patton P (2009) Lateral line stimulation patterns and prey orienting behavior in the Lake Michigan mottled sculpin (*Cottus bairdi*). J Comp Physiol A 195:279

Dadda M, Bisazza A (2016) Early visual experience influences behavioral lateralization in the guppy. Anim Cogn 19:949–958

Dadda M, Bisazza A (2012) Prenatal light exposure affects development of behavioural lateralization in a livebearing fish. Behav Process 91:115–118

Dadda M, Koolhaas WH, Domenici P (2010) Behavioural asymmetry affects escape performance in a teleost fish. Biol Lett 6:414–417

Dadda M, Zandonà E, Bisazza A (2007) Emotional responsiveness in fish from lines artificially selected for a high or low degree of laterality. Physiol Behav 92:764–772

Darvill CM, Menounos B, Goehring BM, et al (2018) Retreat of the western Cordilleran ice sheet margin during the last deglaciation. Geophys Res Lett 45:9710–9720

De Santi A, Bisazza A, Cappelletti M, Vallortigara G (2000) Prior exposure to a predator influences lateralization of cooperative predator inspection in the guppy, *Poecilia reticulata*. Ital J Zool 67:175–178

De Santi A, Sovrano VA, Bisazza A, Vallortigara G (2001) Mosquitofish display differential left- and right-eye use during mirror image scrutiny and predator inspection responses. Anim Behav 61:305–310

Deagle BE, Jones FC, Chan YF, et al (2012) Population genomics of parallel phenotypic evolution in stickleback across stream–lake ecological transitions. Proc R Soc B-Biol Sci 279:1277–1286

Demaree HA, Everhart DE, Youngstrom EA, Harrison DW (2005) Brain lateralization of emotional processing: historical roots and a future incorporating "dominance." Behav Cogn Neurosci Rev 4:3–20

Dingemanse NJ, Wright J, Kazem AJ, et al (2007) Behavioural syndromes differ predictably between 12 populations of three-spined stickleback. J Anim Ecol 76:1128-1138

Domenici P, Allan BJM, Watson S-A, et al (2014) Shifting from right to left: the combined effect of elevated CO2 and temperature on behavioural lateralization in a coral reef fish. PLoS ONE 9:e87969

Domenici P, Blake R (1997) The kinematics and performance of fish fast-start swimming. J Exp Biol 200:1165–1178

Dongen SV (2006) Fluctuating asymmetry and developmental instability in evolutionary biology: past, present and future. J Evol Biol 19:1727–1743

Draganski B, Gaser C, Kempermann G, et al (2006) Temporal and spatial dynamics of brain structure changes during extensive learning. J Neurosci 26:6314–6317

Edgley DE, Genner MJ (2019) Adaptive diversification of the lateral line system during cichlid fish radiation. iScience 16:1–11

Engqvist L (2005) The mistreatment of covariate interaction terms in linear model analyses of behavioural and evolutionary ecology studies. Anim Behav 70:967–971

Fain GL (2019) Sensory transduction. Oxford University Press

Farmer K, Krueger K, Byrne RW (2010) Visual laterality in the domestic horse (*Equus caballus*) interacting with humans. Anim Cogn 13:229–238

Faucher K, Fichet D, Miramand P, Lagardère JP (2006) Impact of acute cadmium exposure on the trunk lateral line neuromasts and consequences on the "C-start" response behaviour of the sea bass (*Dicentrarchus labrax* L.; Teleostei, Moronidae). Aquat Toxicol 76:278–294

Faucherre A, Pujol-Martí J, Kawakami K, López-Schier H (2009) Afferent neurons of the zebrafish lateral line are strict selectors of hair-cell orientation. PLoS ONE 4:e4477

Fernandes VFL, Macaspac C, Lu L, Yoshizawa M (2018) Evolution of the developmental plasticity and a coupling between left mechanosensory neuromasts and an adaptive foraging behavior. Dev Biol 441:262–271

Filipski GT, Wilson MVH (1984) Sudan Black B as a nerve stain for whole cleared fishes. Copeia 1984:204–208

Fischer EK, Soares D, Archer KR, et al (2013) Genetically and environmentally mediated divergence in lateral line morphology in the Trinidadian guppy (*Poecilia reticulata*). J Exp Biol 216:3132–3142

Franklin WE, Lima SL (2001) Laterality in avian vigilance: do sparrows have a favourite eye? Anim Behav 62:879–885

Frasnelli E (2013) Brain and behavioral lateralization in invertebrates. Front Psychol 4:

Frasnelli E, Iakovlev I, Reznikova Z (2012) Asymmetry in antennal contacts during trophallaxis in ants. Behav Brain Res 232:7–12

Friedman M (2008) The evolutionary origin of flatfish asymmetry. Nature 454:209–212

Gainotti G (2019) The role of the right hemisphere in emotional and behavioral disorders of patients with frontotemporal lobar degeneration: an updated review. Front Aging Neurosci 11:

Gamse JT, Thisse C, Thisse B, Halpern ME (2003) The parapineal mediates left-right asymmetry in the zebrafish diencephalon. Development 130:1059–1068

García-Berthou E, Moreno-Amich R (2000) Food of introduced pumpkinseed sunfish: ontogenetic diet shift and seasonal variation. J Fish Biol 57:29–40

Gebhardt C, Auer TO, Henriques PM, et al (2019) An interhemispheric neural circuit allowing binocular integration in the optic tectum. Nat Commun 10:5471

George I, Lerch N, Jozet-Alves C, Lumineau S (2021) Effect of embryonic light exposure on laterality and sociality in quail chicks (*Coturnix coturnix japonica*). Appl Anim Behav Sci 105270

Golovin PV, Bakhvalova AE, Ivanov MV, et al (2019) Sex-biased mortality of marine threespine stickleback (*Gasterosteus aculeatus* L.) during their spawning period in the White Sea. Evol Ecol Res 20:279–295

Goursot C, Duepjan S, Tuchscherer A, et al (2019) Visual laterality in pigs: monocular viewing influences emotional reactions in pigs. Anim Behav 154:183–192

Greenwood AK, Jones FC, Chan YF, et al (2011) The genetic basis of divergent pigment patterns in juvenile threespine sticklebacks. Heredity 107:155–166

Greenwood AK, Mills MG, Wark AR, et al (2016) Evolution of schooling behavior in threespine sticklebacks is shaped by the *Eda* gene. Genetics 203:677-681

Gross HP, Anderson JM (1984) Geographic variation in the gillrakers and diet of European threespine sticklebacks, *Gasterosteus aculeatus*. Copeia 1984:87–97

Gross JB, Gangidine A, Powers AK (2016) Asymmetric facial bone fragmentation mirrors asymmetric distribution of cranial neuromasts in blind Mexican cavefish. Symmetry 8:118

Gummer DL, Brigham RM (1995) Does fluctuating asymmetry reflect the importance of traits in little brown bats (*Myotis lucifugus*)? Can J Zool 73:990-992

Güntürkün O, Diekamp B, Manns M, et al (2000) Asymmetry pays: visual lateralization improves discrimination success in pigeons. Curr Biol 10:1079–1081

Haehnel M, Taguchi M, Liao JC (2012) Heterogeneity and dynamics of lateral line afferent innervation during development in zebrafish (*Danio rerio*). J Comp Neurol 520:1376–1386

Hagen DW (1967) Isolating Mechanisms in Threespine Sticklebacks (*Gasterosteus*). J Fish Res Bd Can 24:1637–1692

Halpern ME, Liang JO, Gamse JT (2003) Leaning to the left: laterality in the zebrafish forebrain. Trends Neurosci 26:308–313

Harrison XA, Donaldson L, Correa-Cano ME, et al (2018) A brief introduction to mixed effects modelling and multi-model inference in ecology. PeerJ 6:e4794

Hart NS, Partridge JC, Cuthill IC (2000) Retinal asymmetry in birds. Curr Biol 10:115–117

Hartig F (2019) DHARMa: residual diagnostics for hierarchical (multi-level / mixed) regression models

Hedrick TL (2008) Software techniques for two- and three-dimensional kinematic measurements of biological and biomimetic systems. Bioinspir Biomim 3:034001

Helfman GS (1989) Threat-sensitive predator avoidance in damselfish-trumpetfish interactions. Behav Ecol Sociobiol 24:47–58

Heuts BA (1999) Lateralization of trunk muscle volume, and lateralization of swimming turns of fish responding to external stimuli. Behav Process 47:113–124

Heuts MJ (1947) Experimental Studies on Adaptive Evolution in *Gasterosteus aculeatus* L. Evolution 1:89–102

Holzman R, Perkol-Finkel S, Zilman G (2014) Mexican blind cavefish use mouth suction to detect obstacles. J Exp Biol 217:1955–1962

Houle D (1997) A meta-analysis of the heritability of developmental stability - Comment. J Evol Biol 10:17–20

Jiang Y, Peichel CL, Torrance L, et al (2017) Sensory trait variation contributes to biased dispersal of threespine stickleback in flowing water. J Evol Biol 30:681–695

Jolles JW, Briggs HD, Araya-Ajoy YG, Boogert NJ (2019) Personality, plasticity and predictability in sticklebacks: bold fish are less plastic and more predictable than shy fish. Anim Behav 154:193–202

Jozet-Alves C, Percelay S, Bouet V (2019) Olfactory laterality is valence-dependent in mice. Symmetry 11:1129

Junges CM, Lajmanovich RC, Peltzer PM, et al (2010) Predator-prey interactions between *Synbranchus marmoratus* (Teleostei: Synbranchidae) and *Hypsiboas pulchellus* tadpoles (Amphibia: Hylidae): Importance of lateral line in nocturnal predation and effects of fenitrothion exposure. Chemosphere 81:1233–1238

Kaarthigeyan J, Dharmaretnam M (2005) Relative levels of motivation and asymmetries of viewing and detour task in guppies (*Poecilia reticulata*). Behav Brain Res 159:37–41

Karenina K, Giljov A, Ingram J, et al (2017) Lateralization of mother–infant interactions in a diverse range of mammal species. Nat Ecol Evol 1:1–4

Kelley JL, Grierson PF, Davies PM, Collin SP (2017) Water flows shape lateral line morphology in an arid zone freshwater fish. Evol Ecol Res 18:411–428

Kitano J, Mori S, Peichel CL (2007) Sexual dimorphism in the external morphology of the threespine stickleback (*Gasterosteus aculeatus*). Copeia 2007:336–349

Kitano J, Mori S, Peichel CL (2012) Reduction of sexual dimorphism in stream-resident forms of three-spined stickleback *Gasterosteus aculeatus*. J Fish Biol 80:131-146

Kotrschal A, Räsänen K, Kristjánsson BK, et al (2012) Extreme sexual brain size dimorphism in sticklebacks: a consequence of the cognitive challenges of sex and parenting? PLoS ONE 7:e30055

Krings M, Mueller-Limberger E, Wagner H (2019) EvoDevo in owl ear asymmetry-The little owl (*Athene noctua*). Zoology 132:1–5

Lai F, Jutfelt F, Nilsson GE (2015) Altered neurotransmitter function in CO2-exposed stickleback (*Gasterosteus aculeatus*): a temperate model species for ocean acidification research. Conserv Physiol 3:cov018

Lajus DL, Golovin PV, Yurtseva AO, et al (2019) Fluctuating asymmetry as an indicator of stress and fitness in stickleback: a review of the literature and examination of cranial structures. Evol Ecol Res 20:83–106

Larsson M (2009) Possible functions of the octavolateralis system in fish schooling. Fish Fish 10:344–353

Leaver S (2010) Morphological and behavioural responses of threespine stickleback (*Gasterosteus aculeatus*) to abrupt alterations in their selective landscape. MSc thesis, University of Victoria

Leaver SD, Reimchen TE (2012) Abrupt changes in defence and trophic morphology of the giant threespine stickleback (*Gasterosteus* sp.) following colonization of a vacant habitat. Biol J Linn Soc 107:494–509

Ledent V (2002) Postembryonic development of the posterior lateral line in zebrafish. Development 129:597–604

Leliveld LMC (2019) From science to practice: a review of laterality research on ungulate livestock. Symmetry 11:1157

Lens L, Dongen SV, Kark S, Matthysen E (2002) Fluctuating asymmetry as an indicator of fitness: can we bridge the gap between studies? Biol Rev 77:27–38

Lenth R (2019) emmeans: estimated marginal means, aka least-squares means

Lesniak K (2020) The incidence of, and relationship between, distal limb and facial asymmetry, and performance in the event horse. Comp Exerc Physiol 16:47–53

Leung B, Forbes MR (1996) Fluctuating asymmetry in relation to stress and fitness: effects of trait type as revealed by meta-analysis. Ecoscience 3:400–413

Leung B, Forbes MR, Houle D (2000) Fluctuating asymmetry as a bioindicator of stress: comparing efficacy of analyses involving multiple traits. Am Nat 155:101–115

Levy J (1977) The mammalian brain and the adaptive advantage of cerebral asymmetry. Ann NY Acad Sci 299:264–272

Liao JC (2006) The role of the lateral line and vision on body kinematics and hydrodynamic preference of rainbow trout in turbulent flow. J Exp Biol 209:4077–4090

Liao JC, Haehnel M (2012) Physiology of afferent neurons in larval zebrafish provides a functional framework for lateral line somatotopy. J Neurophysiol 107:2615–2623

Lin L-Y, Hung G-Y, Yeh Y-H, et al (2019) Acidified water impairs the lateral line system of zebrafish embryos. Aquat Toxicol 217:105351

Lippolis G, Bisazza A, Rogers LJ, Vallortigara G (2002) Lateralisation of predator avoidance responses in three species of toads. Laterality 7:163–183

Lippolis G, Joss JMP, Rogers LJ (2009) Australian Lungfish (*Neoceratodus forsteri*): A Missing Link in the Evolution of Complementary Side Biases for Predator Avoidance and Prey Capture. Brain Behav Evol 73:295–303

Lloyd E, Olive C, Stahl BA, et al (2018) Evolutionary shift towards lateral line dependent prey capture behavior in the blind Mexican cavefish. Dev Biol 441:328–337

López-Schier H, Starr CJ, Kappler JA, et al (2004) Directional cell migration establishes the axes of planar polarity in the posterior lateral-line organ of the zebrafish. Dev Cell 7:401–412

Ludwig W (1932) Rechts-Links-Blindheit und Dressierbarkeit auf rechts und links. In: Das Rechts-Links-Problem im Tierreich und beim Menschen. Springer, pp 361–365

Lychakov DV, Rebane YT, Lombarte A, et al (2006) Fish otolith asymmetry: morphometry and modeling. Hearing Res 219:1–11

Lychakov DV, Rebane YT, Lombarte A, et al (2008) Saccular otolith mass asymmetry in adult flatfishes. J Fish Biol 72:2579–2594

Magat M, Brown C (2009) Laterality enhances cognition in Australian parrots. Proc Biol Sci 276:4155–4162

Malashichev YB (2006) Behavioural and morphological asymmetries in vertebrates. CRC Press

Manns M (2006) The epigenetic control of asymmetry formation: lessons from the avian visual system. In: Maleashichev YB, Deckel AW (eds) Behavioral and morphological asymmetries in vertebrates. Landes Bioscience, Georgetown, pp 13–23

Marchant LF, McGrew WC (2007) Ant fishing by wild chimpanzees is not lateralised. Primates 48:22–26

Marchinko KB (2009) Predation's role in repeated phenotypic and genetic divergence of armor in threespine stickleback. Evolution 63:127–138

Markow TA, Clarke GM (1997) Meta-analysis of the heritability of developmental stability: a giant step backward. J Evol Biol 10:31–37

Marques DA, Jones FC, Di Palma F, et al (2018) Experimental evidence for rapid genomic adaptation to a new niche in an adaptive radiation. Nat Ecol Evol 2:1128-+

Marques DA, Taylor JS, Jones FC, et al (2017) Convergent evolution of *SWS2* opsin facilitates adaptive radiation of threespine stickleback into different light environments. PLoS Biol 15:e2001627

Marranzino AN, Webb JF (2018) Flow sensing in the deep sea: the lateral line system of stomiiform fishes. Zool J Linnean Soc 183:945–965

Marshall NJ (1996) Vision and Sensory Physiology. The lateral line systems of three deep-sea fish. J Fish Biol 49:239–258

Martín J, López P (2001) Hindlimb asymmetry reduces escape performance in the lizard *Psammodromus algirus*. Physiol Biochem Zool 74:619–624

Mathis A, Mamidanna P, Cury KM, et al (2018) DeepLabCut: markerless pose estimation of user-defined body parts with deep learning. Nat Neurosci 21:1281–1289

Mazué GPF, Dechaume-Moncharmont F-X, Godin J-GJ (2015) Boldness–exploration behavioral syndrome: interfamily variability and repeatability of personality traits in the young of the convict cichlid (*Amatitlania siquia*). Behav Ecol 26:900–908

McGreevy PD, Rogers LJ (2005) Motor and sensory laterality in thoroughbred horses. Appl Anim Behav Sci 92:337–352

McGrew W, Marchant L (1999) Laterality of hand use pays off in foraging success for wild chimpanzees. Primates 40:509–513

McHenry M, Feitl K, Strother J, Van Trump W (2009) Larval zebrafish rapidly sense the water flow of a predator's strike. Biol Lett 5:477–479

McIntyre C, Preuss T (2019) Influence of stimulus intensity on multimodal integration in the startle escape system of goldfish. Front Neural Circuits 13:7

McLean S, Morrell LJ (2020) Consistency in the strength of laterality in male, but not female, guppies across different behavioural contexts. Biol Lett 16:20190870

McPhail J (1969) Predation and the evolution of a stickleback (*Gasterosteus*). J Fish Res Bd Can 26:3183–3208

Mekdara PJ, Schwalbe MAB, Coughlin LL, Tytell ED (2018) The effects of lateral line ablation and regeneration in schooling giant danios. J Exp Biol 221:jeb175166

Mesa MG, Warren JJ (1997) Predator avoidance ability of juvenile chinook salmon (*Oncorhynchus tshawytscha*) subjected to sublethal exposures of gas-supersaturated water. Can J Fish Aquat Sci 54:757–764

Middlemiss KL, Cook DG, Jerrett AR, Davison W (2017) Morphology and hydro-sensory role of superficial neuromasts in schooling behaviour of yellow-eyed mullet (*Aldrichetta forsteri*). J Comp Physiol A 203:807–817

Mills MG, Greenwood AK, Peichel CL (2014) Pleiotropic effects of a single gene on skeletal development and sensory system patterning in sticklebacks. EvoDevo 5:5

Mirjany M, Faber DS (2011) Characteristics of the anterior lateral line nerve input to the Mauthner cell. J Exp Biol 214:3368–3377

Møller AP, Pomiankowski A (1993) Fluctuating asymmetry and sexual selection. Genetica 89:267

Møller AP, Thornhill R (1997) A meta-analysis of the heritability of developmental stability. J Evol Biol 10:1–16

Montgomery JC (1989) Lateral line detection of planktonic prey. In: Coombs S, Görner P, Münz H (eds) The mechanosensory lateral line. Springer, New York, NY, pp 561–574

Montgomery JC, Baker CF, Carton AG (1997) The lateral line can mediate rheotaxis in fish. Nature 389:960–963

Moodie GEE (1972) Predation, natural selection and adaptation in an unusual threespine stickleback. Heredity 28:155–167

Moodie GEE, Moodie PF (1996) Do asymmetric sticklebacks make better fathers? Proc R Soc B-Biol Sci 263:535–539

Moodie GEE, Reimchen TE (1976) Phenetic variation and habitat differences in *Gasterosteus* populations of the Queen Charlotte Islands. Syst Biol 25:49–61

Moorman S, Gobes SMH, van de Kamp FC, et al (2015) Learning-related brain hemispheric dominance in sleeping songbirds. Sci Rep 5:9041

Murtaugh PA (2009) Performance of several variable-selection methods applied to real ecological data. Ecol Lett 12:1061–1068

Nair A, Nguyen C, McHenry MJ (2017) A faster escape does not enhance survival in zebrafish larvae. Proc R Soc B-Biol Sci 284:20170359

Nishikawa KC (1987) Staining amphibian peripheral nerves with Sudan Black B: progressive vs regressive methods. Copeia 1987:489–491

Northmore DPM (1991) Visual responses of nucleus isthmi in a teleost fish (*Lepomis macrochirus*). Vis Res 31:525–535

Nosil P, Reimchen TE (2005) Ecological opportunity and levels of morphological variance within freshwater stickleback populations. Biol J Linn Soc 86:297–308

Olszewski J, Haehnel M, Taguchi M, Liao JC (2012) Zebrafish larvae exhibit rheotaxis and can escape a continuous suction source using their lateral line. PLoS ONE 7:e36661

Oltedal L, Hugdahl K (2017) Opposite brain laterality in analogous auditory and visual tests. Laterality 22:690–702

Oravec TJ, Reimchen TE (2013) Divergent reproductive life histories in Haida Gwaii stickleback (*Gasterosteus* spp.). Can J Zool 91:17–24

O'Shea-Wheller TA (2019) Honeybees show a context-dependent rightward bias. Biol Lett 15:20180877

Palmer AR (2009) Animal asymmetry. Curr Biol 19:R473–R477

Palmer AR (2002) Chimpanzee right-handedness reconsidered: evaluating the evidence with funnel plots. Am J Phys Anthropol 118:191–199

Palmer AR, Strobeck C (1986) Fluctuating asymmetry: measurement, analysis, patterns. Annu Rev Ecol Syst 17:391–421

Partridge BL, Pitcher TJ (1980) The sensory basis of fish schools: relative roles of lateral line and vision. J Comp Physiol 135:315–325

Planidin NP, Reimchen TE (2019) Spatial, sexual, and rapid temporal differentiation in neuromast expression on lateral plates of Haida Gwaii threespine stickleback (*Gasterosteus aculeatus*). Can J Zool 97:988–996

Pohlmann K, Atema J, Breithaupt T (2004) The importance of the lateral line in nocturnal predation of piscivorous catfish. J Exp Biol 207:2971–2978

Pomiankowski A (1997) Genetic variation in fluctuating asymmetry. J Evol Biol 10:51–55

Pressley PH (1981) Parental effort and the evolution of nest-guarding tactics in the threespine stickleback, *Gasterosteus aculeatus* L. Evolution 35:282–295

Prieur J, Lemasson A, Barbu S, Blois-Heulin C (2019) History, development and current advances concerning the evolutionary roots of human right-handedness and language: brain lateralisation and manual laterality in non-human primates. Ethology 125:1–28

Reddon AR, Balshine S (2010) Lateralization in response to social stimuli in a cooperatively breeding cichlid fish. Behav Process 85:68–71

Reimchen T (1995) Predator-induced cyclical changes in lateral plate frequencies of *Gasterosteus*. Behaviour 132:1079–1094

Reimchen T, Bergstrom C, Nosil P (2013) Natural selection and the adaptive radiation of Haida Gwaii stickleback. Evol Ecol Res 15:241–269

Reimchen T, Nosil P (2001a) Dietary differences between phenotypes with symmetrical and asymmetrical pelvis in the stickleback *Gasterosteus aculeatus*. Can J Zool 79:533–539

Reimchen TE (1989) Loss of nuptial color in threespine sticklebacks (*Gasterosteus aculeatus*). Evolution 43:450–460

Reimchen TE (1980) Spine deficiency and polymorphism in a population of *Gasterosteus aculeatus*: an adaptation to predators? Can J Zool 58:1232–1244

Reimchen TE (1997) Parasitism of asymmetrical pelvic phenotypes in stickleback. Can J Zool 75:2084–2094

Reimchen TE (1990) Size-structured mortality in a threespine stickleback (*Gastrosteus aculeatus*) – cutthroat trout (*Oncorhynchus clarki*) community. Can J Fish Aquat Sci 47:1194–1205

Reimchen TE (1992) Injuries on stickleback from attacks by a toothed predator (*Oncorhynchus*) and implications for the evolution of lateral plates. Evolution 46:1224–1230

Reimchen TE (1994) Predators and morphological evolution in threespine stickleback. In: Bell MA, Forster SA (eds) The evolutionary biology of the threespine stickleback 1st edn. Oxford University Press, pp 240–276

Reimchen TE, Bergstrom CA (2009) The ecology of asymmetry in stickleback defense structures. Evolution 63:115–126

Reimchen TE, Ingram T, Hansen SC (2008) Assessing niche differences of sex, armour and asymmetry phenotypes using stable isotope analyses in Haida Gwaii sticklebacks. Behaviour 145:561–577

Reimchen TE, Nosil P (2001b) Lateral plate asymmetry, diet and parasitism in threespine stickleback. J Evol Biol 14:632–645

Reimchen TE, Nosil P (2004) Variable predation regimes predict the evolution of sexual dimorphism in a population of threespine stickleback. Evolution 58:1274–1281

Reimchen TE, Nosil P (2001c) Ecological causes of sex-biased parasitism in threespine stickleback. Biol J Linn Soc 73:51–63

Reimchen TE, Nosil P (2006) Replicated ecological landscapes and the evolution of morphological diversity among *Gasterosteus* populations from an archipelago on the west coast of Canada. Can J Zool 84:643–654

Reimchen TE, Steeves D, Bergstrom CA (2016) Sex matters for defence and trophic traits of threespine stickleback. Evol Ecol Res 17:459–485

Reist JD, Bodaly RA, Fudge RJP, et al (1987) External scarring of whitefish, *Coregonus nasus* and *C. clupeaformis* complex, from the western Northwest Territories, Canada. Can J Zool 65:1230–1239

Revelle W (2020) psych: procedures for psychological, psychometric, and personality research. Northwestern University, Evanston, Illinois

Ridgway SH (2002) Asymmetry and symmetry in brain waves from dolphin left and right hemispheres: some observations after anesthesia, during quiescent hanging behavior, and during visual obstruction. Brain Behav Evol 60:265–274

Rivera G, Neely CMD (2020) Patterns of fluctuating asymmetry in the limbs of freshwater turtles: are more functionally important limbs more symmetrical? Evolution 74:660–670

Roche DG, Amcoff M, Morgan R, et al (2020) Behavioural lateralization in a detour test is not repeatable in fishes. Anim Behav167:55–64

Rogers LJ (2000) Evolution of hemispheric specialization: advantages and disadvantages. Brain Lang 73:236–253

Rogers LJ (2010) Relevance of brain and behavioural lateralization to animal welfare. Appl Anim Behav Sci 127:1–11

Rogers LJ (2002) Lateralization in vertebrates: its early evolution, general pattern, and development. Adv Study Behav 31:107–161

Rogers LJ (1990) Light input and the reversal of functional lateralization in the chicken brain. Behav Brain Res 38:211–221

Rogers LJ, Andrew R (2002) Comparative vertebrate lateralization. Cambridge University Press

Rogers LJ, Rigosi E, Frasnelli E, Vallortigara G (2013) A right antenna for social behaviour in honeybees. Sci Rep 3:2045

Rogers LJ, Zucca P, Vallortigara G (2004) Advantages of having a lateralized brain. Proc R Soc B-Biol Sci 271:S420–S422

Rott P of PH, Press OU (2003) Developmental instability: causes and consequences. Oxford University Press

Rouse G, Pickles J (1991) Paired development of hair cells in neuromasts of the teleost lateral line. Proc R Soc B-Biol Sci 246:123–128

Roux N, Duran E, Lanyon RG, et al (2016) Brain lateralization involved in visual recognition of conspecifics in coral reef fish at recruitment. Anim Behav 117:3–8

Rubio AO, French CM, Catenazzi A (2020) Morphological correlates of invasion in Florida cane toad (*Rhinella marina*) populations: shortening of legs and reduction in leg asymmetry as populations become established. Acta Oecol 109:103652

Rudolfsen T, Watkinson DA, Poesch M (2018) Morphological divergence of the threatened Rocky Mountain sculpin (*Cottus* sp.) is driven by biogeography and flow regime: Implications for mitigating altered flow regime to freshwater fishes. Aquat Conserv 28:78–86

Scharnweber K, Watanabe K, Syväranta J, et al (2013) Effects of predation pressure and resource use on morphological divergence in omnivorous prey fish. BMC Evol Biol 13:132

Schilthuizen M, Davison A (2005) The convoluted evolution of snail chirality. Naturwissenschaften 92:504–515

Schwalbe MAB, Bassett DK, Webb JF (2012) Feeding in the dark: lateral-line-mediated prey detection in the peacock cichlid *Aulonocara stuartgranti*. J Exp Biol 215:2060–2071

Schwarz JS, Reichenbach T, Hudspeth AJ (2011) A hydrodynamic sensory antenna used by killifish for nocturnal hunting. J Exp Biol 214:1857–1866

Schwassmann HO, Kruger L (1965) Organization of the visual projection upon the optic tectum of some freshwater fish. J Comp Neurol 124:113–126

Seligmann H (1998) Evidence that minor directional asymmetry is functional in lizard hindlimbs. J Zool 245:205–208

Sherratt E, Serb JM, Adams DC (2017) Rates of morphological evolution, asymmetry and morphological integration of shell shape in scallops. BMC Evol Biol 17:248

Shields BA, Underhill JC (1993) Phenotypic plasticity of a transplanted population of dwarf cisco, *Coregonus artedii*. Environ Biol Fish 37:9–23

Soule M (1967) Phenetics of natural populations. II. Asymmetry and evolution in a lizard. Am Nat 101:141–160

Sovrano VA, Bertolucci C, Frigato E, et al (2016) Influence of exposure in ovo to different light wavelengths on the lateralization of social response in zebrafish larvae. Physiol Behav 157:258–264

Sovrano VA, Bisazza A, Vallortigara G (2001) Lateralization of response to social stimuli in fishes: a comparison between different methods and species. Physiol Behav 74:237–244

Sovrano VA, Rainoldi C, Bisazza A, Vallortigara G (1999) Roots of brain specializations: preferential left-eye use during mirror-image inspection in six species of teleost fish. Behav Brain Res 106:175–180

Spiller L, Grierson PF, Davies PM, et al (2017) Functional diversity of the lateral line system among populations of a native Australian freshwater fish. J Exp Biol 220:2265–2276

Spoljaric MA, Reimchen TE (2007) 10 000 years later: evolution of body shape in Haida Gwaii three-spined stickleback. J Fish Biol 70:1484–1503

Stewart WJ, McHenry MJ (2010) Sensing the strike of a predator fish depends on the specific gravity of a prey fish. J Exp Biol 213:3769–3777

Stewart WJ, Nair A, Jiang H, McHenry MJ (2014) Prey fish escape by sensing the bow wave of a predator. J Exp Biol 217:4328–4336

Stoffel MA, Nakagawa S, Schielzeth H (2017) rptR: repeatability estimation and variance decomposition by generalized linear mixed-effects models. Methods Ecol Evol 8:1639–1644

Suli A, Watson GM, Rubel EW, Raible DW (2012) Rheotaxis in larval zebrafish Is mediated by lateral line mechanosensory hair cells. PLoS ONE 7:e29727

Swaddle JP, Witter MS, Cuthill IC, et al (1996) Plumage condition affects flight performance in common starlings: Implications for developmental homeostasis, abrasion and moult. J Avian Biol 27:103–111

Takeuchi Y, Hori M (2008) Behavioural laterality in the shrimp-eating cichlid fish *Neolamprologus fasciatus* in Lake Tanganyika. Anim Behav 75:1359–1366

Taylor WR (1967) An enzyme method of clearing and staining small vertebrates. Proc US Natl Mus 122:1–17

Thoday JM (1953) Components of fitness. In: Symposia of the society for experimental biology, vol 7. Academic Press, New York, p 1931

Torres-Dowdall J, Rometsch S, Aguilera G, et al (2020) Asymmetry in genitalia is in sync with lateralized mating behavior but not with the lateralization of other behaviors. Curr Zool 66:71–81

Trokovic N, Herczeg G, Ab Ghani NI, et al (2012) High levels of fluctuating asymmetry in isolated stickleback populations. BMC Evol Biol 12:115

Trokovic N, Herczeg G, McCAIRNS RJS, et al (2011) Intraspecific divergence in the lateral line system in the nine-spined stickleback (*Pungitius pungitius*). J Evol Biol 24:1546–1558

Vallortigara G (2000) Comparative neuropsychology of the dual brain: a stroll through animals' left and right perceptual worlds. Brain Lang 73:189–219

Vallortigara G, Rogers LJ (2005) Survival with an asymmetrical brain: advantages and disadvantages of cerebral lateralization. Behav Brain Sci 28:575-

Vallortigara G, Rogers LJ, Bisazza A (1999) Possible evolutionary origins of cognitive brain lateralization. Brain Res Rev 30:164–175

Velando A, Costa MM, Kim S-Y (2017) Sex-specific phenotypes and metabolism-related gene expression in juvenile sticklebacks. Behav Ecol 28:1553–1563

Wada H, Ghysen A, Satou C, et al (2010) Dermal morphogenesis controls lateral line patterning during postembryonic development of teleost fish. Dev Biol 340:583–594

Waddington CH (1942) Canalization of Development and the Inheritance of Acquired Characters. Nature 150:563–565

Wark AR, Mills MG, Dang L-H, et al (2012) Genetic architecture of variation in the lateral line sensory system of threespine sticklebacks. G3-Genes Genom Genet 2:1047–1056

Wark AR, Peichel CL (2010) Lateral line diversity among ecologically divergent threespine stickleback populations. J Exp Biol 213:108–117

Warren JM (1980) Handedness and laterality in humans and other animals. Psychobiology 8:351–359

Webb JF (1989) Gross morphology and evolution of the mechanoreceptive lateral-line system in teleost fishes. Brain Behav Evol 33:34–53

Werner YL, Seifan T (2006) Eye size in geckos: asymmetry, allometry, sexual dimorphism, and behavioral correlates. J Morphol 267:1486–1500

Westin L (1998) The spawning migration of European silver eel (*Anguilla anguilla* L.) with particular reference to stocked eel in the Baltic. Fish Res 38:257–270

Wilson ADM, Godin J-GJ (2009) Boldness and behavioral syndromes in the bluegill sunfish, *Lepomis macrochirus*. Behav Ecol 20:231–237

Wilson ADM, Stevens ED (2005) Consistency in context-specific measures of shyness and boldness in rainbow trout, *Oncorhynchus mykiss*. Ethology 111:849–862

Wiper ML (2017) Evolutionary and mechanistic drivers of laterality: A review and new synthesis. Laterality 22:740–770

Wolfrath B (1993) Observations on the behaviour of the European fiddler crab *Uca tangeri*. Mar Ecol Prog Ser 100:111–118

Wootton RJ (1976) The Biology of the Sticklebacks. Academic Press

Wu J, Jiao H, Simmons NB, et al (2018) Testing the sensory trade-off hypothesis in New World bats. Proc R Soc B-Biol Sci 285:20181523

Wund MA, Baker JA, Golub JL, Foster SA (2015) The evolution of antipredator behaviour following relaxed and reversed selection in Alaskan threespine stickleback fish. Anim Behav 106:181-189

York CA, Bartol IK (2014) Lateral line analogue aids vision in successful predator evasion for the brief squid, *Lolliguncula brevis*. J Exp Biol 217:2437–2439

Yoshizawa M, Gorički Š, Soares D, Jeffery WR (2010) Evolution of a behavioral shift mediated by superficial neuromasts helps cavefish find food in darkness. Curr Biol 20:1631–1636

Yoshizawa M, Robinson BG, Duboué ER, et al (2015) Distinct genetic architecture underlies the emergence of sleep loss and prey-seeking behavior in the Mexican cavefish. BMC Biol 13:15

Zucchini W (2000) An introduction to model selection. J Math Psychol 44:41–61